Concrete Resistivity Impact on the Design of Impressed Current Cathodic Protection Systems

Author:
Cheytani, Martin

Publication Date:
2021

DOI:
https://doi.org/10.26190/unsworks/2046

Concrete Resistivity Impact on the Design of Impressed Current Cathodic Protection Systems

Martin Cheytani

Doctor of Philosophy

School of Material Science and Engineering

Faculty of Science

University of New South Wales

Australia

September 2021

Thesis/Dissertation Sheet

Surname/Family Name	: Cheytani
Given Name/s	: Martin
Abbreviation for degree as give in the University calendar	: PhD
Faculty	: Materials Science and Engineering
School	: Science
Thesis Title	: Concrete Resistivity Impact on the Design of Impressed Current Cathodic Protection Systems

Abstract 350 words maximum: (PLEASE TYPE)

The impact of concrete resistivity on the design of cathodic protection systems has been noted in all global concrete cathodic protection standards as a significant issue for design consideration. However, none of the standards include specific, relevant guidelines related to the consideration of resistivity data in the design of cathodic protection systems.

The research work in this thesis includes various experiments related to the measurement of concrete resistivity in atmospheric conditions, long-term concrete resistivity development over time, and the assessment of concrete resistivity on the design of cathodic protection systems. Six experiments were conducted as part of this thesis. Experiment 1 involved the development of concrete material compositions to achieve a wide range of concrete resistivity levels, representative of a full range of real-world concrete resistivity conditions. With the use of admixtures, nine compositions were trialed achieving concrete sample resistivities from a low of 1.6kΩcm to a high of 2000kΩcm within a short period of 57 days. Compositions were limited to widely available admixtures allowing them to be easily recreated for concrete resistivity experiments in this thesis and in future works.

Experiment 2 explored the effect of water saturation on concrete resistivity measurements. The AASHTO Standard [1] adopted for the measurement of concrete requires water saturation as a method to minimise contact surface resistance between the Wenner probe equipment and the concrete surface. Although the Standard [1] was designed for chloride permeability testing, it has been widely adopted for all concrete resistivity testing, particularly in laboratory settings to achieve sufficient electrolytic contact between the Wenner Probe and concrete. The purpose of Experiment 2 was to assess if there is an impact on resistivity measurements of atmospherically exposed concrete when water saturated. Experiment 2 identified that water saturation resulted in a significant decrease in resistivity measurements and identifies the need for a new methodology for testing concrete located in atmospheric conditions, without the need for water saturation.
Experiment 3 involves the development of a new concrete resistivity testing methodology for concrete in atmospheric conditions, without the need for surface wetting or water saturation (a solution to the issue identified in Experiment 2). This experiment presents a new method minimising the impact of concrete surface variability by establishing an alternative, reliable electrolytic contact between the Wenner equipment probes and concrete. Based on the results in this experiment, a 15mm probe depth was identified to provide the most consistent resistivity measurements of concrete in varied exposure conditions. Through experimental laboratory testing, resistivity measurements were found to decrease by up to 8% between surface and probe measurements. The output from this experiment can contribute to the development of guidelines and additions of the current Standard for the measurement of concrete resistivity via the Wenner probe in atmospheric conditions.
Experiment 4 assesses the level of concrete resistivity increase over time for four commonly used repair mortars used in conjunction with cathodic protection. The testing was conducted over a period of 564 days under saturated and outdoor atmospheric exposure conditions. The experiment indicated that concrete resistivity continues to increase with time under both saturated and atmospheric outdoor conditions. The conclusion from this experiment is that the use of repair mortar based on published short term resistivity data (28 days) and under saturated conditions is misleading. The suitability of polymer-modified repair mortars in conjunction with cathodic protection must be verified based on long-term test data under atmospheric outdoor conditions. Testing in accordance with the methodology trialed in Experiment 3 provides a solution which can be adopted by the industry to test concrete in representative atmospheric conditions.

Experiments 5 and 6 involved the assessment of the impact of anode-to-rebar spacing and concrete resistivity on the current output of impressed current cathodic protection systems. A trend line representing this correlation was developed based on two laboratory testing programs over 63 days (Experiment 5) and 564 days (Experiment 6). The trend line was verified using data extracted from an operating impressed current cathodic protection system (Experiment 7). The experiments indicate a significant impact of anode-to-rebar spacing at different levels of concrete resistivity on the current output of impressed current cathodic protection systems. The developed trend line generated from this work is the first reported research data correlating concrete resistivity, anode-to-rebar spacing and current output for impressed current cathodic protection systems. This trend line can be considered as an effective tool for the design of impressed current cathodic protection systems.
This research presents the first major work on the topic of concrete resistivity and its relationship with impressed current cathodic protection through laboratory trials supported by data from a real operational structure with an operating impressed current cathodic protection system. The results from this thesis can contribute to the improvement of existing concrete resistivity testing Standards and provide invaluable data to the international cathodic protection design Standards.

INCLUSION OF PUBLICATIONS STATEMENT

UNSW is supportive of candidates publishing their research results during their candidature as detailed in the UNSW Thesis Examination Procedure.

Publications can be used in their thesis in lieu of a Chapter if:

- The candidate contributed greater than 50% of the content in the publication and is the "primary author", ie. the candidate was responsible primarily for the planning, execution and preparation of the work for publication
- The candidate has approval to include the publication in their thesis in lieu of a Chapter from their supervisor and Postgraduate Coordinator.
- The publication is not subject to any obligations or contractual agreements with a third party that would constrain its inclusion in the thesis

Please indicate whether this thesis contains published material or not:

☐ This thesis contains no publications, either published or submitted for publication
(if this box is checked, you may delete all the material on page 2)

☒ Some of the work described in this thesis has been published and it has been documented in the relevant Chapters with acknowledgement
(if this box is checked, you may delete all the material on page 2)

☐ This thesis has publications (either published or submitted for publication) incorporated into it in lieu of a chapter and the details are presented below

CANDIDATE'S DECLARATION

I declare that:

- I have complied with the UNSW Thesis Examination Procedure
- where I have used a publication in lieu of a Chapter, the listed publication(s) below meet(s) the requirements to be included in the thesis.

Candidate's Name	Signature	Date (dd/mm/yy)
Martin Cheytani		**03/03/22**

ORIGINALITY STATEMENT

'I hereby declare that this submission is my own work and to the best of my knowledge it contains no materials previously published or written by another person, or substantial proportions of material which have been accepted for the award of any other degree or diploma at UNSW or any other educational institution, except where due acknowledgement is made in the thesis. Any contribution made to the research by others, with whom I have worked at UNSW or elsewhere, is explicitly acknowledged in the thesis. I also declare that the intellectual content of this thesis is the product of my own work, except to the extent that assistance from others in the project's design and conception or in style, presentation and linguistic expression is acknowledged.'

Signed ……..

Date ……..

COPYRIGHT STATEMENT

Signed …….....

Date …….....

AUTHENTICITY STATEMENT

‘I certify that the Library deposit digital copy is a direct equivalent of the final officially approved version of my thesis.’

Signed …….....

Date …….....

Preface & Acknowledgements

This thesis is in fulfilment of the requirements for the degree of Doctor of Philosophy in the School of Material Science and Engineering, University of New South Wales.

I would like to extend my gratitude to my thesis supervisor, Professor Sammy Lap Ip Chan for his ongoing guidance and support, and A/Prof Ranyu Yang for providing laboratory facilities.

I would like to acknowledge the support of Remedial Technology Pty Ltd, Parchem Construction Supplies Pty Ltd and the NSW branch of the Australian Corrosion Association (ACA) for their support.

I would also like to acknowledge the Commonwealth's financial support through the Australian Government Research Training Program Scholarship.

Abstract

The impact of concrete resistivity on the design of cathodic protection systems has been noted in all global concrete cathodic protection standards as a significant issue for design consideration. However, none of the standards include specific, relevant guidelines related to the consideration of resistivity data in the design of cathodic protection systems.

The research work in this thesis includes various experiments related to the measurement of concrete resistivity in atmospheric conditions, long-term concrete resistivity development over time, and the assessment of concrete resistivity on the design of cathodic protection systems. Six experiments were conducted as part of this thesis.

Experiment 1 involved the development of concrete material compositions to achieve a wide range of concrete resistivity levels, representative of a full range of real-world concrete resistivity conditions. With the use of admixtures, nine compositions were trialed achieving concrete sample resistivities from a low of 1.6kΩcm to a high of 2000kΩcm within a short period of 57 days. Compositions were limited to widely available admixtures allowing them to be easily recreated for concrete resistivity experiments in this thesis and in future works.

Experiment 2 explored the effect of water saturation on concrete resistivity measurements. The AASHTO Standard [1] adopted for the measurement of concrete requires water saturation as a method to minimise contact surface resistance between the Wenner probe equipment and the concrete surface. Although the Standard [1] was designed for chloride permeability testing, it has been widely adopted for all concrete resistivity testing, particularly in laboratory settings to achieve sufficient electrolytic contact between the Wenner Probe and concrete. The purpose of Experiment 2 was to assess if there is an impact on resistivity measurements of atmospherically exposed concrete when water saturated. Experiment 2 identified that water saturation resulted in a significant decrease in resistivity measurements and identifies the need for a new methodology for testing concrete located in atmospheric conditions, without the need for water saturation.

Experiment 3 involves the development of a new concrete resistivity testing methodology for concrete in atmospheric conditions, without the need for surface wetting or water saturation (a solution to the issue identified in Experiment 2). This experiment presents a new method minimising the impact of concrete surface variability by establishing an alternative, reliable

electrolytic contact between the Wenner equipment probes and concrete. Based on the results in this experiment, a 15mm probe depth was identified to provide the most consistent resistivity measurements of concrete in varied exposure conditions. Through experimental laboratory testing, resistivity measurements were found to decrease by up to 8% between surface and probe measurements. The output from this experiment can contribute to the development of guidelines and additions of the current Standard for the measurement of concrete resistivity via the Wenner probe in atmospheric conditions.

Experiment 4 assesses the level of concrete resistivity increase over time for four commonly used repair mortars used in conjunction with cathodic protection. The testing was conducted over a period of 564 days under saturated and outdoor atmospheric exposure conditions. The experiment indicated that concrete resistivity continues to increase with time under both saturated and atmospheric outdoor conditions. The conclusion from this experiment is that the use of repair mortar based on published short term resistivity data (28 days) and under saturated conditions is misleading. The suitability of polymer-modified repair mortars in conjunction with cathodic protection must be verified based on long-term test data under atmospheric outdoor conditions. Testing in accordance with the methodology trialed in Experiment 3 provides a solution which can be adopted by the industry to test concrete in representative atmospheric conditions.

Experiments 5 and 6 involved the assessment of the impact of anode-to-rebar spacing and concrete resistivity on the current output of impressed current cathodic protection systems. A trend line representing this correlation was developed based on two laboratory testing programs over 63 days (Experiment 5) and 564 days (Experiment 6). The trend line was verified using data extracted from an operating impressed current cathodic protection system (Experiment 7). The experiments indicate a significant impact of anode-to-rebar spacing at different levels of concrete resistivity on the current output of impressed current cathodic protection systems. The developed trend line generated from this work is the first reported research data correlating concrete resistivity, anode-to-rebar spacing and current output for impressed current cathodic protection systems. This trend line can be considered as an effective tool for the design of impressed current cathodic protection systems.

This research presents the first major work on the topic of concrete resistivity and its relationship with impressed current cathodic protection through laboratory trials supported by data from a real operational structure with an operating impressed current cathodic protection

system. The results from this thesis can contribute to the improvement of existing concrete resistivity testing Standards and provide invaluable data to the international cathodic protection design Standards.

Abbreviations

ICCP	Impressed Current Cathodic Protection
CP	Cathodic Protection
MMO	Mixed Metal Oxide
mA	Milliampere
V	Volts
DC	Direct Current
m	Metre
mm	Millimetre
AS	Australian Standard
W/W	Weight by Weight
W/C	Water to Cement
FP	Four-Point Wenner probe
RC	Reinforced Concrete
SS	Stainless Steel
TDS	Technical Data Sheet

Table of Contents

List of Tables

List of Figures

1 Introduction

1.1 Background

Cathodic Protection (CP) is an electrochemical technique used for the corrosion protection and prevention for structures suffering from chloride-induced corrosion. There are Australian [2] and International Standards [3] [4] which cover all aspects related to the design, material selection, commissioning and monitoring of cathodic protection systems.

Cathodic protection can be applied either by impressing an external current, or by galvanic means. For galvanic anode cathodic protection, the anode - commonly zinc - is connected to the reinforcement and the potential difference between the zinc and the steel causes a small protection current to flow from the zinc to the embedded rebar in concrete. Galvanic anode systems have limited current output capacity and are normally used in conjunction with the repair work, or where it is not practical to use impressed current cathodic protection systems. Galvanic anodes will not work effectively in high resistivity concrete due to the limited driving voltage developed between the anode and the rebar which makes resistivity values more relevant than for impressed current systems.

For impressed current cathodic protection (ICCP) systems, based on the current applicable Australian Standard for the design of cathodic protection systems in concrete [2], various factors must be considered during the design process. These factors include: the exposure condition of the protected element; the extent of concrete deterioration; reinforcement continuity; concrete cover; assessment of the corrosion activity of embedded reinforcement; concrete carbonation; level of chloride contamination in the concrete; steel density; and concrete resistivity.

For ICCP systems, the input data from the site testing can provide the required information for the design process. This includes the system's current density, type of anodes, spacing of anodes and system zoning. However, the resistivity data of the original concrete cannot be incorporated into the design of impressed current systems in any profound way due to the lack of any relevant guidelines in the applicable Standards [2] [3] [4].

The research work in this thesis includes various experiments related to the development of an innovative method for concrete resistivity testing for atmospheric concrete structures and the development of a design trend line that incorporates resistivity data and anode-to-rebar spacing for the design of cathodic protection systems.

1.2 Objectives and Scope

This section describes the research plan, objectives, and scope of this thesis.

This thesis incorporates laboratory work in conjunction with data obtained from a marine structure with an operating ICCP system. Further detail on the experimental procedure will be discussed in subsequent corresponding chapters.

This thesis is divided into six chapters.

Chapter 1 - The present chapter presents a brief background and introduction to cathodic protection as well as providing the objectives, scope, and structure of each chapter.

Chapter 2 - This chapter presents the literature review which includes an overview of corrosion in concrete structures, the main application of electrochemical protection systems to combat corrosion, and the relationship between concrete resistivity and electrochemical protection systems. The literature review highlights areas of limited knowledge and the lack of data related to the design and performance of electrochemical protection systems in varying concrete resistivities.

Chapter 3 - This chapter is divided into four experiments:

Experiment 1: The resistivity of concrete can range from kΩcm to MΩcm based on compositions, age, contaminants, and environmental exposure. In practice, every concrete structure has a unique variation of these variables. As there are many variables which contribute to resistivity, the objective of Experiment 1 is to develop concrete compositions which would result in a sweep of resistivities

(representative of a full range of real-world conditions), all within a short period of time (months) where variables can be controlled, suitable for laboratory testing. Variations in admixtures are trialed and tested to achieve different levels of resistivity.

The scope is limited to achieving different resistivity values with the use of admixtures. Research into the direct effects of the admixtures, pore network structures or any other grout characteristics (compressive/tensile strength, durability, creep, shrinkage, etc.) is outside the scope of this research. The purpose is to obtain varied resistivities within a short time range (months).

Experiment 2: Involves research into the impact of water saturation on Wenner probe resistivity measurements. The current resistivity Standard [1] for the measurement of concrete requires the saturation of concrete in order to measure resistivity. The purpose of the water saturation is to minimise contact surface resistance between Wenner probe equipment and the concrete surface. Although the Standard [1] was designed for chloride permeability testing, it has been widely adopted for all concrete resistivity testing, particularly in laboratory settings. The purpose of Experiment 2 is to assess if water saturation of concrete will impact on resistivity measurements of atmospherically exposed concrete. It is anticipated that the water saturation will lead to a significant decrease in resistivity, signifying an issue with the current common methodologies used for the measurement of resistivity for samples in atmospheric conditions.

Experiment 3: Trials a new method of measuring concrete resistivity of concrete located in atmospheric conditions, without the need for surface wetting or water saturation (a solution to the issue identified in Experiment 2). The aim of this experiment is to test a new method utilising externally embedded probes as an alternative to water saturation or surface wetting and identify the impact on resistivity measurement between surface and probe measurements.

Experiment 4: Involves the comparison between resistivity data of four different (commercially available) repair mortars over a period of 564 days,

with samples exposed to saturated and outdoor conditions. The objective is to assess if the long-term resistivity increases past the commonly stated 28-day resistivity values provided by grout manufacturers. It is predicted that resistivity will continue to increase past the 28-day period, and that testing in saturated conditions (as per the current testing Standard [1]) will yield unrepresentative results (as identified in Experiment 2).

Chapter 4 - This chapter is divided into two experimental sections:

Experiment 5: The design of impressed current cathodic protection systems are governed by international Standards [2], [3] and [4]. These Standards note concrete resistivity as a design consideration, but due to the lack of research on this topic, they present limited data. The lack of data on the impact of resistivity on ICCP design has led to the installation of ICCP systems to real structures, which on commissioning exhibit high limiting voltages, greatly reducing the effectiveness of the system. As the concrete acts as the electrolyte in an ICCP system, this section experiments using different concrete resistivities (designed in Experiment 1), to identify at what resistivity the ICCP system will reach its 8-volt limit. Anode-to-rebar spacing of 30mm and 60mm is also undertaken to identify if anode-to-rebar spacing can be adjusted as a solution to achieve ICCP performance at higher concrete resistivities. Testing was limited to plotting the initial 60 minutes of the ICCP system being switched ON.

Experiment 6: Further continuing the work in Experiment 5, Experiment 6 examines the effect of concrete resistivity on the ongoing application of ICCP and the effect of anode placement. The objective of which is to plot the full increase of voltage of newly cast concrete and continue to measure the current output density of each test sample through a spectrum of low kΩcm to high MΩcm concrete resistivities. This data can provide a graphical representation of the current density output, developing a trend line representing anode-to-rebar spacing, concrete resistivity and current output.

Chapter 5 - Chapter 5 involves the extrapolation of data from a real reinforced concrete structure with an operating impressed current cathodic protection system. The purpose of this chapter is to identify if the laboratory data from Chapter 4 is consistent with that of a real reinforced concrete structure with an operating ICCP system.

Chapter 6 - Chapter 6 presents the thesis conclusions and provides recommendations for future research.

2 Literature Review

This chapter provides an overview of corrosion in concrete structures, the main application of electrochemical protection systems to combat corrosion, and the relationship between concrete resistivity and electrochemical protection systems. This chapter contains three main sections:

1. Introduction into the main causes of corrosion and mechanisms of corrosion of reinforced concrete structures.
2. Factors which are considered in the design of electrochemical systems, corrosion potential, current density design, steel density and resistivity.
3. The measurement of concrete resistivity, methods, what influences concrete resistivity, the importance of concrete resistivity in corrosion prevention and protection, and the relationship with electrochemical protection systems.

2.1 Corrosion in Concrete

Corrosion of steel reinforcement in concrete is one of the major problems impacting on the integrity and serviceability of structures. Reinforcing steel in new, good-quality concrete does not corrode even if sufficient moisture and oxygen are present. New concrete generally has a high alkaline pH of above 13, which is attributed to high levels of calcium hydroxide. The interaction between high levels of hydroxyl ions (OH^-), and the steel reinforcement form an insoluble ferric oxide film around the reinforcement, causing the steel to passivate and create a protective oxide layer. This oxide layer provides protection to the steel reinforcement by preventing metal atoms from dissolving however, this passive layer cannot always be maintained. Chloride and carbonation ingress to the level of steel reinforcement as a result of poor-quality concrete, concrete cracking and insufficient concrete cover-to-reinforcement can lead to a decrease in concrete alkalinity and a breakdown of the protective oxide layer.

The two main causes of corrosion of steel reinforcement are carbonation and chloride contamination. In the case of carbonation, rectification methods include patch repair, the application of anti-carbonation coating and the use of realkalisation. For chloride-contaminated structures, electrochemical treatments are normally considered in conjunction with the repair work. Impressed current cathodic protection, galvanic anode protection or chloride extraction

(desalination) are the common methods used in conjunction with the repair work for the corrosion protection of chloride-contaminated structures.

Impressed current cathodic protection (ICCP) is one of the main established and implemented electrochemical protection systems. ICCP is regarded as the most effective electrochemical method used for structures in high chloride environments. The application of ICCP requires a permanent power supply and ongoing monitoring of the system over the life of the structure. ICCP systems are generally applied for major rehabilitation projects, typically for marine structures such as wharves and bridges.

Galvanic cathodic protection is currently an area of substantial growth. It is becoming increasingly attractive because of its simplicity, low monitoring, and maintenance requirements. Galvanic anodes consist of highly active metals (zinc) which have a more negative electrochemical potential than steel, and this protects the reinforcing steel from corrosion. Once sacrificial anodes are installed in a structure, they can provide a certain level of corrosion protection. With galvanic anodes, there is no need for ongoing monitoring or the use of a power supply unit. For this reason, galvanic anodes are favoured and have been widely used in many applications in recent years. Galvanic anode systems have limited current output capacity and service life and are normally applied in conjunction with the repair work for incipient anode prevention or where the current density requirement is very low [5].

2.1.1 Corrosion Process and Mechanism

Corrosion of concrete involves an electrochemical process in which both flow of electrical currents and chemical reactions occurs. The process of corrosion initiates when anodic and cathodic zones occur simultaneously on the same metal surface [6]. Chloride ingress and carbonation contamination are the two most common causes of the degradation of the steel reinforcement's protective oxide layer. Regardless of the cause of corrosion, once the alkalinity of the concrete at the level of steel reinforcement decreases to a level beyond the steel passivation threshold, the electrochemical process of steel corrosion will begin.

Carbonation is the exposure of carbon dioxide (CO_2) to the concrete. Depending on the permeability of the concrete and level of hydration, carbon dioxide penetrates and dissolves into the concrete pores. The mixture of carbon dioxide into the calcium hydroxide ($Ca(OH)_2$) rich concrete reacts to form calcium carbonate:

$$Ca(OH)_2 + CO_2 \rightarrow CaCO_3 + H_2O$$

Consumption of $Ca(OH)_2$ decreases the pH of the concrete to as low as 8.5, which is well below the necessary alkalinity required to keep the steel passivated. The decrease in pH causes the deterioration of the oxide layer, enabling the corrosion process.

The second type of concrete contamination is through chloride ingress. The diffusion of chloride ions into the concrete through the concrete cover or through cracks that form in the concrete is the primary mechanism of chloride contamination of concrete structures. In Australia, many structures are built in coastal locations which are exposed to airborne chlorides or are in direct proximity to seawater. The quality of concrete, porosity, concrete cover-to-reinforcement, and shrinkage cracking of the concrete are the primary enablers of chloride ingress. When the chloride reaches the steel reinforcement the breakdown of the protective oxide layer occurs, and corrosion initiation starts.

The process of steel corrosion in concrete begins with the variance in steel potential in different locations of one continuous steel element. The variance in steel potential is caused by the macrocell mechanisms of the concrete causing a breakdown of the passive layer, which leads to the creation of the anodic and cathodic areas.

Where the oxide layer is damaged, steel generates positively charged ions and releases electrons. The reaction is shown by:

$$\mathrm{Fe} \rightarrow \mathrm{Fe}^{2+} + 2\mathrm{e}^{-}$$

This area known as the anodic area becomes the host of the oxidation process, where electrons are released from the anode and flow to the cathode:

$$\mathrm{O}_2 + 2\mathrm{H}_2\mathrm{O} + 4\mathrm{e}^{-} \rightarrow 4\mathrm{OH}^{-}$$

At the cathode, electrons react with an external source of water and oxygen, producing hydroxyl ions. The hydroxyl ions at the cathode then react and produce ferrous hydroxide at the anode, which when exposed to oxygen and is oxidised, produce hydrated ferric oxide (rust).

2.1.2 Corrosion Mechanisms

The first step in understanding electrochemical corrosion is to identify and understand the mechanisms. The corrosion rate of macrocell mechanisms can be determined by the following formula:

$$Corrosion\ \ Rate = k \cdot I_c \cdot \frac{S_C}{S_a}$$

Where *Corrosion Rate* is in mm/y; I_c is A/m^2; S_C and S_a are the cathodic and anodic surface area in m^2; k is the constant equivalence (carbon steel k = 2.7) [7]. The surface area ratio must incorporate the extent of influence within the electrolyte, which can be characterised as throwing power. Throwing power is a computer modelled theory which refers to the ability of current generated at the anode to reach distant cathodic zones, incorporating resistivity, geometry and overvoltage. In general, it is expected that driving voltage will decrease with increasing resistivity. The geometric theory is depicted in the following expression:

$$L_{max} \cong k\ \frac{\Delta V}{p \cdot i_c}$$

Where, L_{max} is the throwing power; ΔV is the driving voltage; p is the resistivity in Ωm [7]. Driving voltage ΔV can be given by the following equation:

$$\Delta V = (E_{eq,C} - n_c) - \left(E_{eq,A} - n_A\right) = IR_{el}$$

Where, $E_{eq,C}$ and $E_{eq,A}$ are the equilibrium potential of the cathodic and anodic processes, $n_c\ and\ n_A$ is the overvoltage. IR_{el} is the resulting IR drop in the electrolyte [6].

2.1.3 Corrosion Consequences

The process of electrochemical reactions culminates in the production of iron oxide (rust) at the anode. The formation of iron oxide is many times the volume of the original steel, causing an expansive internal pressure within the concrete structure. The build-up of this internal pressure leads to the eventual degradation of the structure, causing spalling, cracking, loss of section, a decrease in structural strength, and eventual collapse if no protection or prevention measures are taken. For this reason, corrosion of reinforcements in concrete has a major

impact on the life and health of structures in highly corrosive environments. The aim of incorporating corrosion protection systems within the repair work is to minimise the impact of corrosion and maintain the serviceability of the structure with minimal maintenance cost.

2.2 Corrosion Prevention & Protection Measures

For new structures, corrosion prevention measures may include; modifying the concrete mix to decrease concrete permeability; adjusting steel depth to provide adequate concrete cover; changes in construction designs to minimise the exposure of some key structural elements to chloride ingress; coating application to limit chloride ingress and carbon dioxide into the concrete; use of corrosion resistant reinforcement; use of inhibitors to fresh concrete, and the application of impressed current cathodic prevention systems.

For existing structures, common remediation methods for structures with carbonation-induced corrosion includes conventional patch repair, coating application and realkalisation. For structures with chloride induced corrosion, the common methods include impressed current cathodic protection, galvanic anode protection and chloride extraction (desalination). In recent years, hybrid anode corrosion protection systems have been used for various applications for chloride contaminated structures. The hybrid system consists of a temporary impressed current followed by permanent galvanic application. The concept of this system is that during the initial impressed current phase, corrosion pits are realkalised and this returns the embedded rebar to a passive state. Following the short-term application of the impressed current phase, the passivity of the steel is maintained by the galvanic anode system.

2.2.1 Structure Condition Assessment

Before any repair work is carried out, an investigation is required to assess the causes and extent of existing defects. The aim of the investigation is to provide information related to the causes and extent of damage, and the impact of damage on the structural integrity and serviceability of the structure. For the corrosion assessment, a typical material and electrochemical investigation is performed.

This investigation involves a combination of in situ testing and laboratory analysis. The main components of a typical investigation are visual inspection, cover-to-reinforcement

measurement, delamination testing, chloride testing, carbonation testing, half-cell potential mapping, continuity testing, compressive strength testing and resistivity testing. Other investigation methods such as gamma radiology, infrared thermography, ground penetrating radar, corrosion rate measurement and ultrasonic pulse velocity can be used to obtain more detailed information related to the condition of the structure.

Based on the investigation results, the repair methodology can be selected. In the case an electrochemical repair system is selected in conjunction with concrete repair, the relevant data from the investigation can be used for the system design.

2.2.2 Selection of Electrochemical Protection systems

Cathodic protection is the most commonly used method for the corrosion protection of reinforced concrete chloride contaminated structures. The data from the investigation includes continuity of embedded rebar, level of corrosion activity, level of chloride contamination, the exposure condition of the elements of the structure, and concrete resistivity. Based on this data, the estimated current density which is required to achieve corrosion protection in accordance with the applicable Standards can be determined. Selection of the electrochemical system can be carried out based on the level of corrosion, system design life, cost, and maintenance consideration. Impressed current cathodic protection systems, galvanic or hybrid anode systems can be considered for the corrosion protection in conjunction with the repair work.

2.2.3 Impressed Current Systems

Impressed current cathodic protection (ICCP) for reinforced concrete structures is a proven technology which can provide long term corrosion protection for structures suffering from chloride-induced corrosion. ICCP technology for steel in concrete has now reached maturity after more than 40 years of global application. This technology is considered a reliable technique for the long-term corrosion protection of structures suffering from chloride-induced corrosion.

Figure 2.1 displays the main components of an ICCP system in concrete.

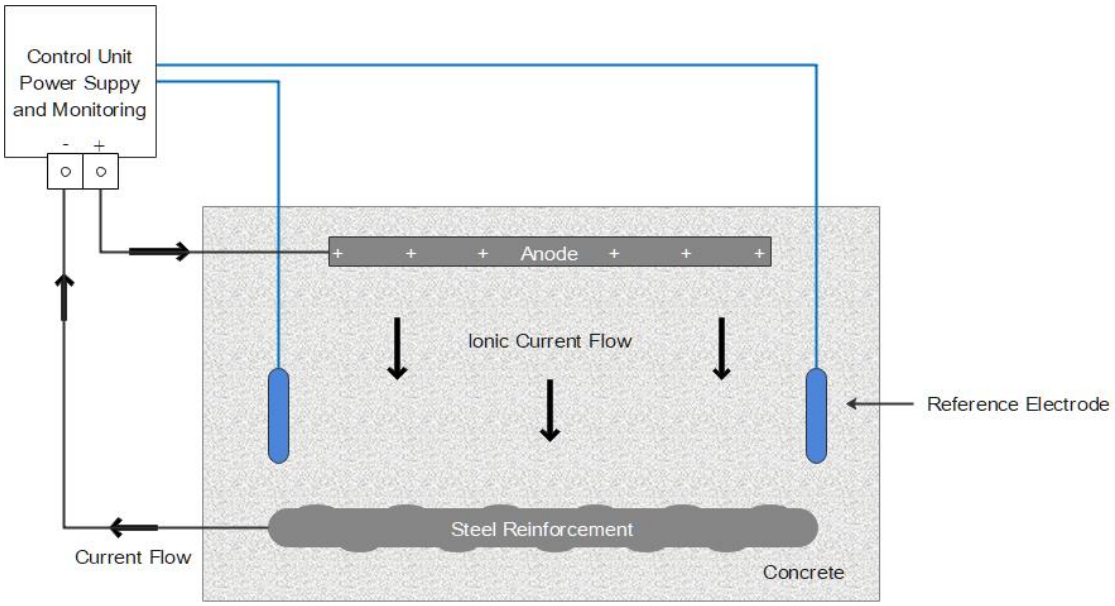

Figure 2.1 - Impressed current cathodic protection system schematic

The principle of cathodic protection is to move all the embedded rebar within a structure into a cathodic phase by moving the anodic reaction to an external anode normally embedded into the concrete cover, or in drilled holes in the concrete. This is achieved by driving current between the anode and the embedded reinforcement through the electrolytic concrete.

Cathodic protection promotes the development of alkalinity at the steel surface and the migration of chloride ions from the rebar toward the anode. The increase of alkalinity allows for the regeneration of the protective passive oxide layer at the steel surface and the passivation of the steel.

There are many types of concrete impressed current anodes [3]. The anode types can be divided into surface applied, encapsulated, and immersed buried anodes. The most common anodes used for concrete structures are activated Mixed Metal Oxide Titanium expanded ribbon, mesh or discrete anodes. Activated titanium anodes comprising a substrate of titanium, niobium or tantalum, and an electrocatalytic coating containing oxides of platinum group metals, such as platinum, iridium or ruthenium, with oxides of titanium, zirconium and tantalum [2]. These anodes are embedded into the cementitious grout in chases cut in the concrete cover or installed into holes drilled into the concrete.

To determine the performance of cathodic protection systems, reference electrodes are installed at representative locations in the elements. In addition to the anodes, the components of a typical cathodic protection system include reference electrodes, reference return connections, titanium conductor strips, anode connections, rebar connections, junction boxes, DC cables and transformer rectifier/control system.

2.2.3.1 Limiting Voltage

The commonly used mixed metal oxide (MMO) titanium ribbon, mesh or discrete anodes are connected by uncoated titanium conductor strips. The uncoated titanium conductor strips may be at risk of corroding by pitting in chloride environments if operated in excess of approximately 8-volt metal/electrolyte potential [3].

The MMO titanium mesh or ribbon anodes are normally spot-welded to the uncoated titanium conductor bar and the spot weld connection is normally embedded into the concrete. The anode connection is normally spot-welded to the conductor bar and the anode connection cables are terminated into the junction boxes and the transformer rectifier unit. Uncoated titanium bars are used as they allow for a simple and secure spot-welded connection to the anodes, compatibility between materials, and because of titanium's low electrical resistance (0.04 – 0.11 Ohm/m) [8].

The Australian Standards states AS 2832.5-2008 Cathodic Protection of Metals, Part 5: Steel in concrete structures [2];

"Voltage applied to titanium strips or wires (sometimes referred to as conductor bars) used to conduct current in the anode systems shall be limited so as to avoid any overvoltage which can result in premature anode circuit failure."

Normally, ICCP systems operate at low voltages in wet/low resistivity concrete elements. For high resistivity concrete, the circuit voltage increases, and the limiting 8-volt metal/electrolyte potential impacts on the amount of cathodic protection current.

2.2.4 Galvanic Protection

There are two ways of providing cathodic protection current to embedded reinforcement in concrete - using impressed current and/or galvanic anodes. Galvanic anodes are well proven in

buried/submerged steel and reinforced concrete element applications, particularly in marine environments where moisture and salts maintain the activity of the anodes. For concrete in atmospheric conditions, the high resistivity of the concrete and low driving voltage of galvanic anodes limits the use of this technology. This limitation is mostly applicable for structures with high corrosion activity and where it is required to design a cathodic protection system that meets the applicable Standards for cathodic protection [2] [4] [3]. Regardless of this limitation, galvanic cathodic protection is becoming attractive because of the low maintenance cost associated with galvanic anode systems.

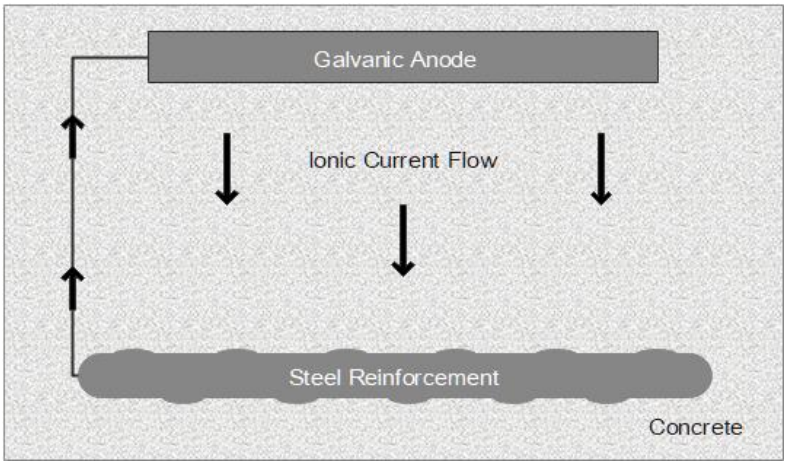

Figure 2.2 - Galvanic anode cathodic protection system schematic

Figure 2.2 displays the main components of a galvanic anode system in concrete. A galvanic anode system is based on an electrochemical reaction between dissimilar metals where one metal preferentially corrodes over another. Which metal corrodes preferentially is based on the electrochemical series of metal potentials. When two dissimilar metals are connected, the lower potential metal will become the anode E_A, and the higher potential metal, E_C, will become the cathode. The maximum driving voltage between the two metals is expressed in the following formula [7]:

$$\Delta V = E_C - E_A$$

The selection of metals is determined on the driving voltage ΔV, surface corrosion mechanics of the metal in addition to the feasibility of the metal. In general, galvanic anodes are made from aluminium, magnesium or zinc with the selection based on the environmental factors, varying

from soil to salt and brackish water. Galvanic anode systems are widely used for the protection of steel and reinforced concrete elements located in water and soil. For concrete structures, zinc anodes are commonly used.

Galvanic anodes are generally used on structures which exhibit early signs of corrosion, as their level of protection is limited to the potential differences between dissimilar metals (ΔV). This limits the usability of sacrificial anode systems, especially for structures exposed to harsh marine environments. In addition to this, galvanic anodes must generally be used in low resistivity concrete and may require a large number of galvanic anodes to meet the design requirements. Galvanic anode systems have a limited design life of 10 - 20 years, and full replacement is required after expiration.

2.3 Electrochemical System Design Considerations

The aim of any electrochemical system is to control corrosion by making the steel in the reinforced concrete structures the cathode. All electrochemical protection techniques require current to flow between the anode and cathode, which in this case would entail the flow of electrons through the concrete. The performance of any electrochemical system is based on sufficient electron flow between the anode and cathode. For electrochemical protection systems, this is referred to as current density, or current output per unit surface area. In this case, milliamperes of current output per m^2 of steel surface (mA/m^2).

2.3.1 Current Density Output

Current density output is one of the main factors which is considered in the design and implementation of a cathodic protection (CP) system. The selection of a suitable current density output is critical in CP design [8]. Experimental research on the topic is limited. Technical Report No. 73 [9] specifies, the effective corrosion protection can be achieved by applying protective current in the range of 0.2-20mA/m^2 of steel surface area, depending on conditions. For structures exposed to high chloride environments (marine structures, wharves, coastal bridges), design currents in the range of 10 – 20mA/m^2 may be required. For structures in light-to-moderate chloride contamination, design currents as low as 5mA/m^2 may be sufficient. Structures located in higher ambient temperatures generally require higher current densities.

For the purposes of cathodic prevention, current densities in the order of 0.2 – 2mA/m^2 may be sufficient to prevent corrosion and to ensure steel passivity [9].

Much of the current density data is based on practical guides developed through experience. One source [8] is displayed in Table 2.1.

Table 2.1 - Practical guide of CP current density in different exposure conditions [8]

Environment surrounding steel reinforcement	Current density mA per m^2 of reinforcement
Alkaline, no corrosion occurring, low oxygen supply	0.1
Alkaline, no corrosion occurring, exposed structure	1 – 3
Alkaline, chloride present, dry, good quality concrete, high cover, light corrosion observed on rebar	3 – 7
Chloride present, wet, poor quality concrete medium-low cover, widespread pitting and general corrosion on steel	8 – 20
High chloride levels, wet fluctuating environment, high oxygen level, hot, severe corrosion on steel, low cover	30 – 50

Due to the inhomogeneous nature of concrete, including the environmental and physical variables associated with concrete structures, an accurate and effective method of defining the required current density is by undertaking CP trials [8]. Standards quote similar recommendations and ranges, lacking further details. Australian Standard [2] states:

"Typically, applied initial current ranges from 5 to 20 mA/m2 for cathodic protection of active steel and from 2 to 10 mA/m2 for cathodic protection of new structures."
"Typical cathodic prevention current densities range between 2 mA/m2 and 10 mA/m2 compared with 5 mA/m2 to 20 mA/m2 for cathodic protection for uncoated steel in concrete."
"The cathodic protection of uncoated steel in water-saturated buried or submerged concrete will typically require steel current densities in the range 0.1 to 5 mA/m2 owing to the low rate of oxygen diffusion through the water-saturated pore structure in the concrete."

Limited research is available on this topic as shown in the available information presented. Reports [9], Standards [2] and literature based on industry experience [8] provide a range of current density values. Current density output is based on multiple factors, including the

environmental exposure of the concrete, concrete characteristics (admixtures), design, and anode placement.

2.3.2 Reinforcement Location and Depth

For the design of electrochemical protection systems, the reinforcement size, spacing and concrete cover thickness must be determined.

In conjunction with the construction/as-built drawings of the structure, the surface area of the embedded rebar is required for the current density calculation.

The spacing and diameter of the embedded rebar is essential to determine the anode layout and the type of anode to be used in the design of a CP system. For structures with multiple layers of embedded rebar and congested reinforcement, discrete anodes drilled in holes may not be a viable solution. In this case, the entire process of positioning the discrete anodes at the required spacing from the rebar becomes extremely destructive.

Determining the exact concrete cover to the first layer of reinforcement is essential when titanium ribbon anodes are considered. The positioning of the ribbon anode within the concrete cover must be at a suitable distance from the rebar and with sufficient cover. Consideration of durability and current distribution is essential. The use of ribbon anodes may not be suitable for concrete elements with low concrete cover. A minimum anode-to-reinforcement length of 15mm should be maintained for all forms of this type of anode [1].

The presence of rebar affects electrical resistivity measurements due to its high electrical conductance in comparison to the surrounding concrete. For this reason, it is essential to determine the rebar layout, as reinforcing bars should not be directly beneath the resistivity meter probes and should not run parallel to the probe when measuring concrete resistivity [10].

One of the major considerations of concrete cover-to-embedded rebar on the current output of CP systems is the anode-to-rebar spacing. In theory, based on Ohm's law, placement of the anode at a closer spacing to the rebar will decrease the circuit's resistance.

The resistivity of concrete indicates the ease with which an electrical charge is transported in the concrete and is a measure of the "transport" of current through the concrete. On this basis, the impact of anode-to-rebar spacing will be assessed in this research work. The assumption for

high resistivity concrete is that the anode-to-rebar spacing will have an impact on the current output of the CP system.

2.3.3 Concrete Resistivity and Reinforcement Corrosion

The depassivation of steel causes the initiation of steel reinforcement corrosion. The corrosion rate will determine the speed of reinforced concrete deterioration. The speed of corrosion is dependent on many parameters including oxygen availability, ratio of anodic/cathodic areas, relative humidity and concrete electrical resistivity [11]. When oxygen is available to supply anodic current in locations such as splash zones, cathodic control no longer exists [12]. In exposure conditions with high-frequency saturation or tidal exposure, the corrosion rate can be limited by controlling the flow of ionic current through concrete or concrete resistivity [12]. Research into the correlation between corrosion probability and corrosion rate to concrete electrical resistivity has been attempted [12] [13] [14]. Studies conducted suggest corrosion of reinforcement and concrete resistivity have an inverse relationship, where increasing resistivity correlates to decreasing corrosion rates. An anodic control theory exists which suggests that the corrosion rate of reinforced concrete is under anodic control with the anodic reactions being limited by mortar resistivity [13]. It was found that rebar was likely to achieve an active state of corrosion when resistivity less than 10 kΩcm, and likely to present passive behaviour when concrete resistivity is higher than 30 kΩcm [13]. A number of researchers and commercial Wenner probe instrument manuals (Proceq [10] and Giatec [15]) provided general guidelines regarding the relationship between corrosion rates and concrete resistivity measurements. This is summarised in Table 2.2.

Table 2.2 - Corrosion risk of steel reinforcement at concrete resistivities [10] [15] [16]

Corrosion Risk	kΩcm
High	<10
Moderate	10-50
Low	50-100
Negligible	>100

Although research has been conducted on the relationship between concrete resistivity and reinforcement corrosion, knowledge is still lacking in the literature to understand which mechanism dominates the corrosion process and how resistivity measurements are impacted [12]. It is important to note that field data from investigations on the relationship between concrete resistivity and reinforcement corrosion is limited [12]. In practice, corrosion of concrete structures is evident not only in locations with low resistivity values, but as in many cases, corrosion of steel reinforcement has been found to occur in structures with higher resistivity values. Much of the research which exists on this topic [12] is limited to the study of the corrosion process in the short to medium-term (years). More research is required on reinforced concrete structures decades after construction and with long term exposure to different environments.

Another aspect which must be assessed is the non-standardised resistivity measurement methods which have been used in concrete resistivity research.

2.4 Concrete Resistivity

Resistivity is the physical property of a material to resist the conduction of electricity or transfer of ions subject to an electrical field and is measured in ohm-cm. Material with a high resistivity is a poor conductor of electricity and vice versa [17]. The resistivity of concrete is dependent on the concrete's microstructure such as capillary pore size distribution and interconnection. A finer pore network with less connectivity leads to lower permeability, translating into higher resistivity [18]. If the microstructure of the concrete consists of large pores and interconnection, permeability increases alongside resistivity.

Electrical resistivity measurements in porous material such as concrete is described in the following equation [19]:

$$p^T = P_o \cdot \left(\frac{1}{\emptyset\beta}\right)$$

Where P^T is the total resistivity, P_o is the resistivity of the pore solution, a function of the ions composition and concentration in the solution, $\emptyset$ is the porosity of the system accessible to

fluids, and β is the connectivity of the powers in the system [20]. Figure 2.3 displays a visual representation of the pore solution, porosity and connectivity.

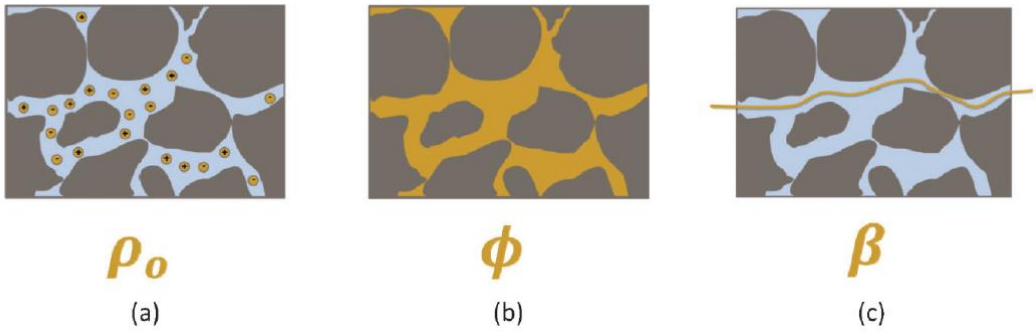

Figure 2.3 - Parameters to describe electrical measurement of porous materials, (a) resistivity of pore solution, (b) porosity, (c) connectivity, sourced from [20]

The electrical resistivity measurements in the porous material equation is invalidated by steel reinforcement and does not address the effects of aggregates. The effects of the chemical characteristics of concrete including concrete additives, water-to-cement ratio (w/c), exposure to environmental factors such as carbonation and chloride ingress. Other factors such as saturation, temperature and humidity are discussed below.

2.4.1 Concrete Resistivity Measurement

Resistivity is a material property affected by the topics previously discussed in this section. The measurement of electrical resistivity (p) is a ratio between impressed voltage (V) and measured current (I) multiplied by a cell constant. The following equation is used as a basis to calculate resistivity:

$$p = k \cdot R = k \cdot \left(\frac{V}{I}\right)$$

Where p is the electrical resistivity, k is the geometrical factor and R is the concrete resistance. The geometrical factor k will be discussed in the following sections.

Concrete resistivity measurement can be performed in several destructive and non-destructive methods. The two main non-destructive methods of testing concrete resistivity include bulk electrical testing and four-point Wenner probe testing. Choosing which method to use is dependent on what is most suitable for the type of specimen being tested with the four-point Wenner probe method generally being the choice for laboratories and on-site resistivity testing because of its quick measurement and portable design. This review focuses on the four-point Wenner probe methods, with a brief description of the bulk electrical resistivity method.

2.4.2 Bulk Electrical Resistivity Test

The bulk electrical resistivity method also known as the Uniaxial method, involves the placement of two parallel electrodes with a conductive medium (usually a moist sponge or conductive gel) acting as an electrical contact between the electrodes and the concrete specimens. This method determines the electrical conductivity by measuring the current passing through all the phases of a test specimen (cement, sand, aggregate and any additives).

In the laboratory environment this method can be simple and reliable, however this method may not be well suited to on-site testing as it does require access to two sides of the specimen, which in most cases will require the removal of concrete in the form of cores for testing of existing structures [18]. This testing method cannot be used for specimens embedded with steel (reinforcement) as the steel will result in lower resistivity due to its conductivity yielding unrepresentative results.

The geometrical factor (k) in bulk resistivity testing can be obtained from the following equation:

$$k = \frac{A}{L}$$

Where A is the cross-sectional area perpendicular to the anode and L is the height of the specimen [12].

Consideration of the resistance caused by the conductive medium has been proposed in the following equation [21]:

$$R = R_{measured} - R_{top\ sponge} - R_{bottom\ \text{sponge}}$$

A diagram of the setup of bulk electrical resistivity testing is presented in Figure 2.4.

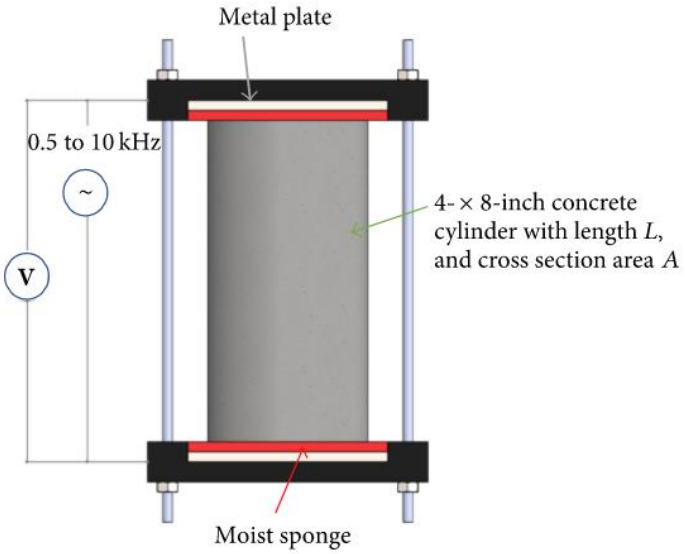

Figure 2.4 - Bulk electrical resistivity testing [14]

2.4.3 Four-Point Wenner Probe

The four-point Wenner probe method is the most widely used technique for onsite concrete resistivity testing as it is non-destructive, portable, fast and simple to use. The four-point (FP) probe consists of four equally spaced linear electrodes with a distance a (m) between each probe. The probes are placed in contact along the concrete's surface. The two external electrodes impress AC current (I), while the two middle electrodes measure electrical voltage potential (V). If (*P*) is the difference in potential (V) between the two inner probes, and (I) is the current (A) between the external probes of a semi-infinite body, the resistivity of the body material is given by:

$$p = 2\pi\, \alpha \left(\frac{P}{I}\right)$$

Experimental research papers have been published examining how specimen geometry, probe spacing, rebar layout and surface contact can affect FP probe resistivity results.

2.4.4 Specimen Geometry and Correction Factor

As the FP method is generally used for large concrete elements, it is assumed that the calculation is based on a semi-infinite geometrical figure. The geometrical factor is presented in the following equation:

$$k = \gamma\alpha$$

Where α is the distance between the electrodes and γ is the dimensionless geometry factor, which in the case for a semi-infinite concrete slab is γ = 2π [18]. However, for smaller samples such as for laboratory testing, current can be restricted as shown in Figure 2.5, and therefore the geometry of the specimen must be considered. Experimental findings [22] have recommended that FP contact spacing is less than or equal to one-quarter of the concrete section thickness. In addition, testing should be a minimum of twice the probe spacing from the edge of a concrete specimen.

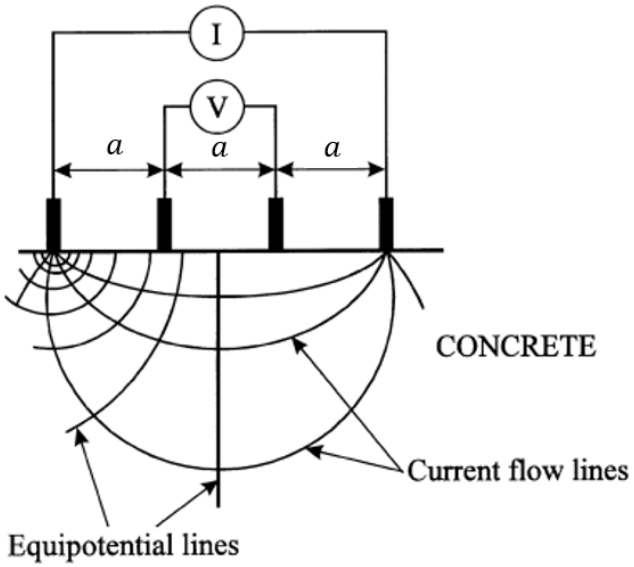

Figure 2.5 - Four-point Wenner probe current flow [23]

Experimental work conducted [23] explored the effect of Wenner probe electrode spacing and the correction coefficient (*k)* of cylindrical specimens. The research found that for accurate resistivity of concrete to be obtained, the correction coefficient, (*k)* must be used. Without the

use of the correction value, cylindrical specimen readings varied with specimen size although probe spacing remained the same. The correction coefficient, (*k)* can be determined by the ratio of the specimen size to the probe spacing. The geometric correction factor *(k)* is calculated using the following formula [24]:

$$k \cong \frac{2\pi}{1.09 - \frac{0.527}{\frac{d}{a}} + \frac{7.34}{(\frac{d}{a})^2}}$$

Where d is the diameter of the cylinder (mm), a is the probe spacing (mm).

2.4.5 Probe Spacing

AASHTO T358-19 [1] specified that each probe shall be spaced 38mm apart, with an AC frequency of 13Hz. However, probe spacing can be varied (20 to 70mm) to conduct readings over larger areas providing more representative results as concrete is nonhomogeneous. The inconsistency of concrete homogeneity especially regarding aggregate distribution, may affect resistivity readings [12]. Experimental findings [22] recommend probe contact spacing of at least 1.5 times the size of the maximum aggregate size.

2.4.6 Rebar Consideration

Another aspect which must be considered is the steel reinforcement layout as the conductivity of steel reinforcement can distort resistivity results. Researchers have been exploring the effect of steel reinforcement on FP measurements [22] [25] [26]. When carrying out resistivity measurements using the FP method, it is recommended that an electromagnetic cover-meter is used to non-destructively map out rebar locations to ensure that measurements are taken away from underlying rebar [22]. In circumstances where proximity to the rebar is unavoidable, contact spacing ≤ 2/3 of concrete cover is recommended [22]. Paper [25] writes that FP measurements should not be performed parallel to the rebar notably where the concrete cover to the rebar is less than 30mm, although in practice, the influence of rebar can be avoided by changing orientation and testing several points [25]. A numerical investigation [26] was carried out on the effect of rebar mesh spacing and rebar cover on Wenner probe readings. It was found that a 30% increase in accuracy can be achieved by selecting the appropriate location and

orientation. The most suitable orientation in minimising rebar interference is to place the probe parallel to the top rebar midway between both top and bottom bars [26]. Figure 2.6 configuration #9 has been previously suggested to be the most suitable FP measuring technique. Paper [26] concluded that configuration # 4 gave the most accurate resistivity results for rebar spacing ≤ 200mm. However, these numerical study results have not been validated by experimental research [12].

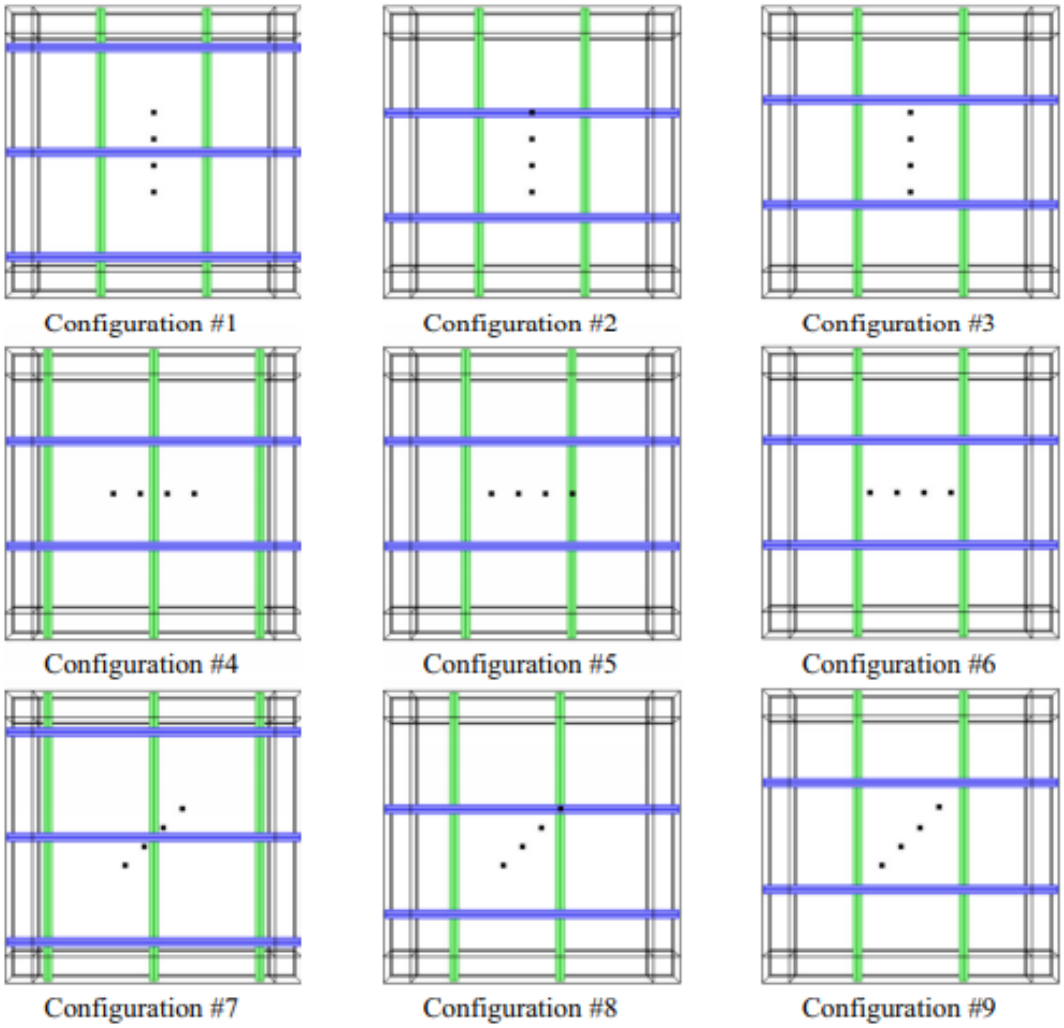

Figure 2.6 - Configurations tested in [27]

Commercial Wenner Probe manufacturers [10] recommend that reinforcement bars should not run parallel to the probe. Figure 2.7 (a) shows the optimum orientation when the probe span is less than the rebar grid. If the rebar grid spacing is smaller than the probe length, Figure 2.7 (b) is recommended.

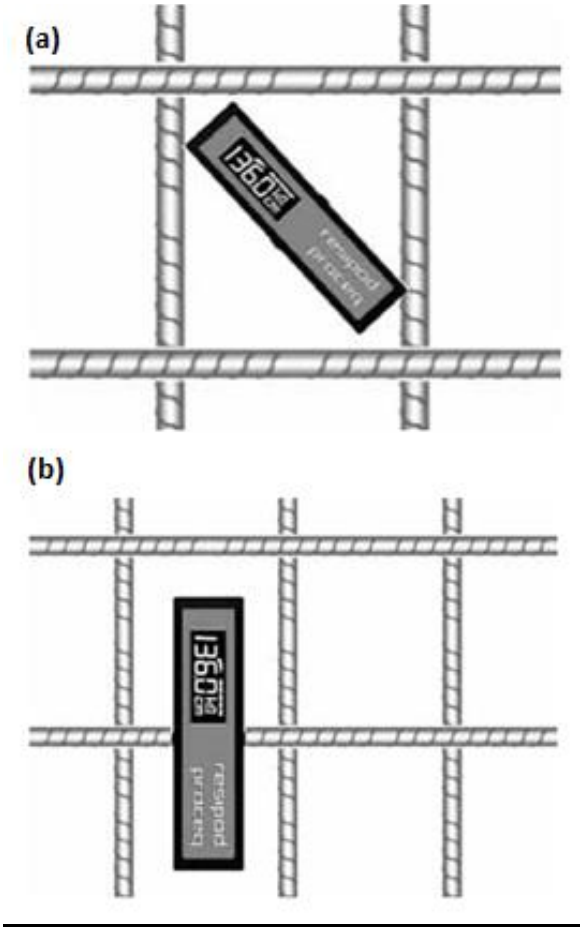

Figure 2.7 – Configurations recommend by commercial Wenner probe manufacturers [28]

2.4.7 Surface Contact

Concrete resistivity testing requires sufficient contact between the measurement device and the concrete specimens' surface. Accurate resistivity measurements are highly dependent on this contact [14]. Research into how this contact can be achieved without the addition of water or gels is limited. In addition, concrete resistivity is highly dependent on environmental factors such as temperature, humidity and moisture content [10] [15]. In many cases for Wenner probe testing to achieve the necessary contact required for resistivity testing, surface alterations must be made primarily in the form of water saturation.

2.4.8 Cement

Cement is the primary component in making mortar (fine sand with cement) and concrete (sand, cement and aggregate). Cement acts as a binder which sets, hardens, and adheres materials

together. Manufacturing cement involves the controlled chemical combination of silicon, calcium, iron, aluminium, and other ingredients [29]. Many types of cement exist, but Portland cement is the most commonly used globally. Portland cement is primarily made of limestone (calcium carbonate) and the addition of a selection of other smaller quantities of materials such as chalk, marl, and shell which is combined with blast furnace slag, slate, shale, clay, silica sand and iron ore. The mixture is then heated to approximately 1,450 degrees Celsius forming a rock-like substance which is then ground to a fine powder [29].

The electrical conduction of cement begins during the hydration process when cement is mixed with water. The hydration process causes a reaction between cement and water, releasing conductive ions into the pore solution. These ions are primarily positively and negatively charged: potassium (K^+), sodium (Na^+), calcium (Ca^{2+}), hydroxide (OH^-) and sulfate (SO_4^{2-}). [19] The exact composition of these ions is dependent on the chemical composition and concentrations of the water-to-cement (w/c) ratio.

2.4.9 Effect of Water-to-Cement (W/C) Ratio

The porosity of concrete is highly dependent on the water-to-cement (w/c) ratio. Generally, the higher the w/c ratio (increase of water to cement), the higher the percentage of porosity, leading to a lower level of concrete resistivity. In hardened concrete, ionic movement flows through the fluid contained in the pores, therefore resistivity is controlled by the volume of interconnected pores. Experimental studies have confirmed that concrete's electrical conductivity will increase as w/c increases [12] [30]. Experiments [31] have been conducted in which various w/c ratios (0.45, 0.55 and 0.65) were cast and tested. It was found that although there was a minor difference in resistivity between 0.55 and 0.65 w/c ratios, there was a significant difference between the 0.45 specimen. Another study [23] found that there was an approximately 15-20% decrease in electrical resistivity between specimens with a w/c of 0.4 to 0.6 w/c ratio.

2.4.10 Aggregate Size and Type

In general, the resistivity of concrete can be dependent on the mining locality and size of the aggregate. Experimental research [32] conducted found that an increase of aggregate content resulted in higher levels of electrical resistivity. It was also found that mixtures containing larger aggregates (16-32mm) had higher resistivities compared to specimens with smaller particle sizes

(0-0.4mm). Experimentation was also conducted on how different types of aggregates can affect concrete resistivities. Concrete specimens produced with crushed limestone aggregates were higher than those with the gravel aggregates for the same aggregate volume concentrations [32]. This is due to the differing characteristics of the two aggregates, with gravel having a rounded smooth surface texture acting as a poor bonding surface, while limestone aggregates have a high tortuosity (irregular particle shape with a rough surface), allowing for greater cement bonding increasing resistivity [12].

2.4.11 Chemical Admixtures

As reinforced concrete structures continue to be built, there is a push to build structures faster, to a higher quality, with less financial cost and with increased durability. This leads to the development of new materials which can be modified to suit increasing requirements. Although this can be representative of all RC structures, it is most relevant in harsh environments, especially in major infrastructure in and around the marine environment.

The addition of chemical admixtures into the basic concrete mix of water, sand, cement, and aggregate, is one method used to enhance performance characteristics. Chemical admixtures can have a direct effect on concrete resistivity. Some types of additives include [33]:

- Water reducing admixtures – reducing the required water content (5-10% reduction), allowing for higher strength concrete to be produced with less water increasing the cement content of the mixture.
- Superplasticizers – further reducing the water content by 12% to 30%. Allows concrete to flow, increasing workability and requiring no vibration or compaction during the curing process.
- Retarding admixtures - used to slow the setting rate of concrete, counteracting the accelerating effect of hot weather on the concrete setting. Retarding admixtures keep the concrete workable for longer periods and provide adequate time for the concrete to cure.
- Accelerating admixtures – the opposite of retarding admixtures, accelerating admixtures increase the rate of early strength development and curing, speeding up the process. Areas which this can be used for curing in cold weather, or around marine environments, where curing times are limited.

- Air entraining agents – the addition of air bubbles in the concrete to reduce damage during free-thaw cycles.
- Corrosion-inhibiting admixtures – used to slow the corrosion process, primarily chloride ion penetration to the steel surface. Mainly used in marine structures, roads, and bridges where direct or airborne chloride may be present.
- Shrinking reducers – admixtures which reduce shrinkage cracking in structures where cracking may cause durability problems such as around chloride environments.
- Pigments – used to aesthetically modify the colour of concrete
- Bonding agents – the addition of a polymer which can increase bonding strength between new and old concrete (mainly used in repair works).

2.4.12 Mineral Admixtures

In addition to chemical admixtures, mineral admixtures and blended cements can be used. These include:

- Fly ash – a by-product of coal combustion in power stations. Improves concrete's workability, reduces water demand, controls bleeding, and lowers the heat of hydration. Increases long term strength and can improve resistance to chemical attacks such as chloride ingress by reducing permeability. There are two grades of fly ash – Normal Grade (typically used in conventional concrete applications) which is used as a 20-30% cement replacement in concrete. Special Grade fly ash increases concrete density, increases strength, is highly durable and reduces permeability [34].
- Ground granulated black furnace slag (GGBFS) – produced by quenching molten iron slag from a blast furnace into water producing a granular product which is grounded into a fine powder. GGBFS is used in aggressive environments around groundwater, adverse environmental conditions, and concrete which requires a lower heat of hydration [35].
- Silica fume – silica fume increases mechanical properties of concrete, increasing strength and permeability, as well as benefits in elasticity, drying shrinkage, steel-to-concrete bonding and resistance to steel corrosion (due to its low permeability) [27].
- Carbon nanofibers – carbon nanofibers can enhance the concrete's mechanical properties. Mechanical benefits include increased compressive strength, tensile properties (higher Young's modulus) and improved fatigue resistance [28].

2.4.13 Effect of Curing Conditions

Concrete resistivity is highly dependent on the composition, curing methodology and exposure time of the concrete [36]. A numerical study [37] based on NIST-developed Virtual Cement and Concrete Testing Laboratory (VCCTL) model was used to simulate a mortar with a w/c of 0.42 exposed to three curing conditions:

(A) Sealed during curing and testing - found to have the highest resistivity
(B) Sealed during curing and saturated during testing - found to have the lowest resistivity
(C) Saturated during curing and testing.

While the pore structure and degree of hydration of both samples (a) and (b) was the same, the difference can be explained by the moisture content of the samples [24] [37]. Curing methods can influence the moisture content of concrete, affecting concrete resistivity. In addition, proper concrete curing can prevent the formation of cracking in the concrete. This can be demonstrated in experimental paper [38] where three different types of curing were carried out:

(1) Uncontrolled curing (UC): specimens were air-cured at uncontrolled temperatures and relative humidity until the test age.
(2) Controlled curing (CC): specimens were immersed in 20 ± 2 °C water for 7 days and then air-cured in a room at 20 ± 1 °C and 50 ± 5% relative humidity until the test age.
(3) Wet curing (WC): specimens were immersed in 20 ± 2 °C water until the test age.

It was found that uncontrolled concrete curing led to the shortest corrosion cracking time when compared with controlled cured and wet cured samples. Experimental data in paper [38] found that a better curing procedure resulted in samples with higher electrical resistivity. It was also found that samples which had been cured under uncontrolled curing (UC) conditions had a lower strength and corrosion resistance compared to controlled (CC) and wet curing (WC) conditions. Figure 2.8 from paper [38] shows the time to failure of samples under different curing conditions. The figure shows that UC samples failed quicker than those which were CC and WC.

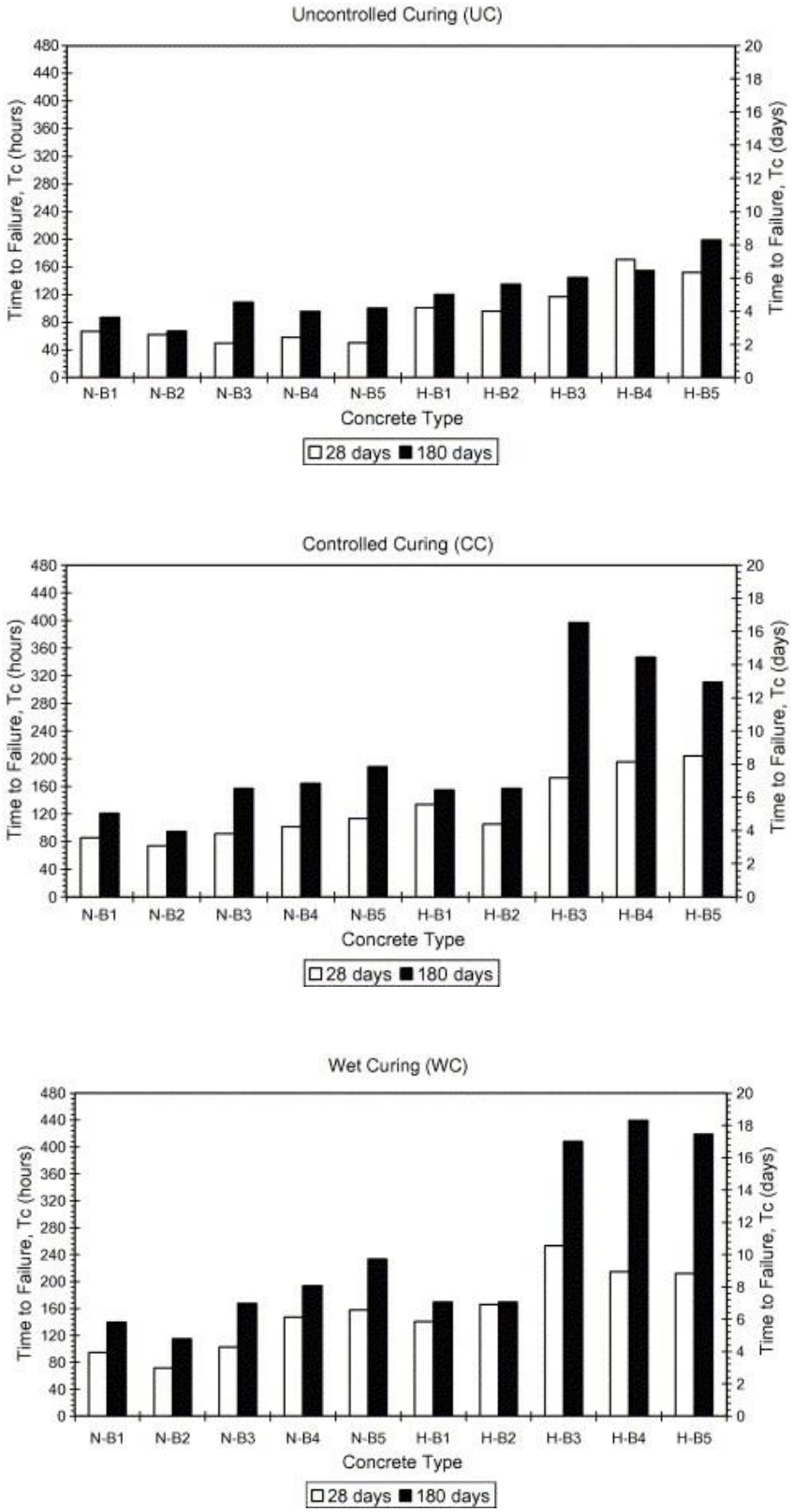

Figure 2.8 - Comparison of time to failure for samples cured under different conditions [24]

2.4.14 Moisture Content

As a large portion of concrete ICCP systems are located in structures around the marine environment, the degree of liquid saturation into the concrete pore network will affect resistivity [18]. Electrical conductivity increases with an increased moisture content due to an increase in ion mobility [39]. Moisture content is dependent on the level of direct liquid pore saturation as a result of moisture replenishment through weather exposure (rainfall and tidal fluctuations in marine environments), relative humidity [40], and temperature variations.

2.4.15 Temperature

The effect of temperature variations on concrete resistivity have a significant effect on electrical resistivity. Experiments have confirmed based on the Arrhenius law, that an increase of temperature will increase ion mobility in moisture exposed situations, decreasing the level of resistivity [39]. Temperature fluctuations cause changes in ion (Na^+, K^+, Ca^{2+}, SO_4^{2-} and OH^-) mobility and ion-ion and ion-solid interactions, as well as ion concentration [12] [41]. However as shown in Figure 2.9, in a dry environment an increase in temperature will result in the reduction of moisture content, consequently leading to an increased resistivity.

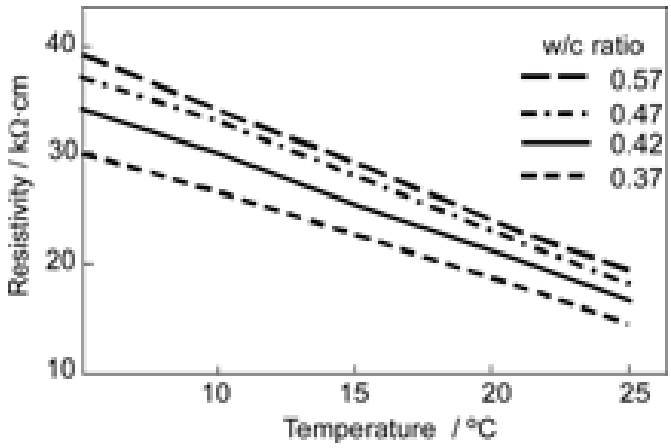

Figure 2.9 - Temperature and w/c influences on resistivity, at RH = 75% [30]

2.4.16 Relative Humidity

A relationship between ambient humidity and concrete moisture content can be determined experimentally; and is related to concrete pore structure [41]. Figure 2.10 shows the interrelation between relative humidity, moisture content and capillary pore radius.

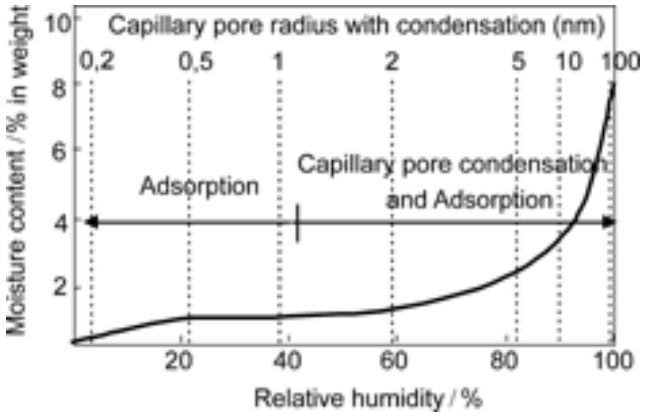

Figure 2.10 - Isotherm of water adsorption in concrete [30]

2.4.17 Environmental Contaminates

Environmental contaminants, primarily chloride and carbonation, can greatly affect concrete resistivity. An experimental paper on the effect of moisture, chloride, and sulphate contamination on electrical resistivity [42] identified that electrical resistivity decreased with increased chloride concentrations and increased sulphate concentrations. Laboratory testing of carbonated concrete samples found carbonation contamination to increase concrete resistivity [43]. Carbonation was found to increase electrical resistivity due to the concrete pore refinement caused by the advance of carbonation depth. Carbonation penetration caused concrete pore density to increase (calcium carbonate) and decrease the electrical conductivity [43]. An increase of resistivity with carbonation has also been supported in other research papers [44] [45].

2.5 Standards and Reports

This section explores the current Standards and Reports on the topics of concrete resistivity measurement, and the impact of concrete resistivity on cathodic protection systems.

2.5.1 Measurement of Concrete Resistivity

The study and research on concrete resistivity has been primarily used for the evaluation of concrete characteristics such as concrete durability, permeability, and chloride ion diffusivity [46] [47]. The measurement of concrete resistivity can be an indicator of the corrosion resistance of embedded steel in reinforced concrete structures [18] [48]. Most of the research on concrete resistivity has been conducted in laboratory environments. There are two main concrete resistivity standards for the measurement of concrete resistivity - The American Association of State Highway and Transportation Officials (AASHTO) designation: T358-19 [1] for four-point Wenner probe testing, and ASTM C1876 – 19 [49] for bulk electrical resistivity testing of concrete. Both these standards present a replicable and standardised method of testing concrete resistivity in laboratory conditions.

Resistivity testing of existing concrete structures is predominantly carried out using the four-point Wenner probe method due to its non-destructive nature. Bulk resistivity testing requires destructive core extractions.

AASHTO designation: T358-19 [1] requires water saturation of the test samples. The purpose of water saturation is to eliminate the relative humidity variable. 100% relative humidity is typically used in the study of concrete permeability and chloride ion diffusivity research, with resistivity Standards intended for this purpose. However, for resistivity measurements of existing concrete structures to be representative, the resistivity measurements of existing concrete structures must be carried out in a comparable environment to that of the structure, as environmental exposure is one of the main variables of concrete resistivity.

When measuring the concrete resistivity of existing structures onsite using the four-point Wenner probe method, measurements in atmospheric locations have been found to be heavily scattered with high standard deviations. Concrete resistivity testing requires sufficient contact between the measurement device and concrete sample's surface. Accurate resistivity measurements are highly dependent on this contact [22]. Research into how this contact can be achieved without the addition of water or gels is limited. In addition, concrete resistivity is highly dependent on environmental factors such as temperature, humidity and moisture content [41] [42]. In many cases for Wenner probe testing to achieve the necessary contact required for resistivity testing, surface alterations must be made primarily in the form of water saturation.

A test method statement by Main Roads Western Australia [50], details a method of concrete resistivity testing using embedded steel probe pins. However, no research has been conducted into the effect of using such steel pins in concrete resistivity measurements. The use of steel pins may be a solution to provide the necessary contact between a four-point Wenner probe and a concrete sample's surface without the application of any wet sponges or gels, removing the variables associated with these external applications.

2.5.2 Cathodic Protection and Concrete Resistivity

There are three widely used Standards for the design of cathodic protection applications. These include the European International Standard ISO 12696 – 2016 [3] , NACE (US) Standard SP0290 – 2007 [4] and the Australian Standard AS2832.5 – 2008 (R2018) [2]. These standards provide the basis for the design requirements for impressed current cathodic protection, and in many cases are referred to in the design of galvanic anode system designs (as a separate standard for galvanic anode cathodic protection for concrete structures does not exist).

The three standards all refer to concrete resistivity as an important factor requiring consideration in the design of cathodic protection systems. The NACE (US) Standard SP0290 – 2007 [4], provides minimal information on the topic of concrete resistivity, noting that concrete resistivity data is one set of information which is useful in selecting and designing an impressed current cathodic protection system. No further information is provided.

The European International Standard ISO 12696 – 2016 [3] states:

"The impact of variations in concrete resistivity on the cathodic protection system shall be considered. There is no firm guidance on limits of electrical resistivity with respect to cathodic protection, but the designer shall consider whether full protection can be achieved where required for the ranges and absolute values of concrete resistivity found on the structure."

"NOTE Typically, these repair materials will have an electrical resistivity within the range approximately half to twice that of the parent concrete when measured under the same conditions as the parent concrete. However, the electrical resistivity of the parent concrete will be that of an aged material (age > 20 years), whereas the electrical resistivity of the repair material will reflect the properties at a relatively young age; it is anticipated that there will be a

significant ageing effect over time. Also, measurements made in the laboratory on prisms will not represent the conditions of the structure."

The European International Standard ISO 12696 – 2016 [3] identifies three main points:

1. There is no firm guidance on limits of electrical resistivity
2. Electrical resistivity of an aged concrete is different from that of new concrete,
3. The measurement of laboratory prisms do not represent conditions of a real structure

The Australian Standard AS2832.5 – 2008 (R2018) [2] states:

"Electrical resistivity surveys shall be carried out on representative areas of concrete to provide information for the design of the cathodic protection system. Core samples may also be obtained from the structure to evaluate volumetric concrete resistivity."

For repair applications, *"overlay application may be combined with concrete repair. In such cases, the long-term electrical resistivity of concrete repair materials shall be within the range 50% to 150% of the parent concrete electrical resistivity. The resistivity of anode overlays may exceed 200% of parent concrete electrical resistivity subject to it being a maximum of 1000 Ω.m* (100 kΩcm) *at ambient conditions and subject to the anode within the overlay being able to pass its design current at the design voltage."*

It is important to note that the global cathodic protection Standards [2] [3] [4] do not provide any information related to the impact of concrete resistivity on the circuit voltage output of a cathodic protection system. In addition, the Standards do not provide technical information regarding the possible impact of the performance of cathodic protection in different concrete resistivities. Although the international Standards governing ICCP design and installation do not provide much detail regarding concrete resistivity, there is one report which does address the topic. Technical Report No. 73 [9] notes:

"For Impressed current cathodic protection systems, the laboratory-tested resistivity (vacuum saturated and tested in compliance with RILEM TC 154) should not exceed 150 kΩcm or should be within 50 - 200% of the resistivity of the parent concrete."

The relationship between vacuum-saturated concrete and atmospherically located concrete is not noted. Testing is required in atmospheric conditions. Reports of concrete resistivity note that laboratory testing of concrete in controlled conditions such as 100% vacuum saturated, are difficult to compare with those made in the field on actual structures [51]. Technical Report No. 73 [9] states:

"For galvanic anodes the repair material resistivity should not exceed 15 kΩcm."

No information is provided on how this value has been calculated.

"Impressed current systems are more adaptable to site conditions and by their very nature they have a higher driving voltage capability to assist current distribution in high-resistivity media such as concrete." [9]

Further research is required to identify the relationship between impressed current driving voltage and current density output.

"For anode overlay materials, the resistivity of the material must allow ionic current to flow: typically, maximum workable resistivity of anode overlays is 50 kΩcm (minimum conductivity of 20μS/cm)." [9]

"Polymer modified cement-based materials with resistivities as high as 133 kohm.cm (laboratory tested) have been successfully used in both repairs and as cementitious overlays to impressed current cathodic protection systems on concrete that was actively corroding and therefore low resistivity (5-10 kohm.cm)."

No detail on the exposure conditions of the test sample are noted.

Technical Report No. 73 [9] provides the most detail regarding concrete resistivity and design recommendations for cathodic protection systems. The Report identifies that there is a need for further research on this topic, with concrete resistivity continually appearing as a design consideration which must be assessed during the design of electrochemical protection systems. Although it does state certain limits of 15 kΩcm for galvanic anodes systems and 150 kΩcm for impressed current systems, detailed information primarily on current density output of anodes

at different resistivities is non-existent. Resistivity measurement results are shown to be affected by the presence of reinforcement, the moisture content, and the temperature of the concrete, with all factors changing with time, structure location and concrete cover. No further information regarding the impact of these variables is discussed.

Research conducted by the Strategic Highway Research Program National Research Council Washington, DC in 1993 [17];

"Using the Wenner Four-Electrode Method, field tests are conducted to determine the resistivity. 89 Measurements are made in concrete after locating the reinforcement steel and positioning the probe as far as possible from the reinforcement. Measurements should not be made directly over reinforcing steel. Materials with resistivities which remain in excess of 50,000 ohm-cm are not considered compatible with cathodic protection.

These sources together with the noted international Standards, provide an indication of the importance of concrete resistivity in the design of electrochemical cathodic protection systems. Although there are some recommendations on resistivity values in which galvanic anode and ICCP will operate, more research is required to increase knowledge on the impact of concrete resistivity on the performance of electrochemical protection systems.

2.6 Conclusion

The literature explores the process and causes of corrosion in reinforced concrete structures, the main types of electrochemical protection systems which are used to combat corrosion and identifies areas requiring further research. There are two main areas discussed below, which were identified as requiring further research.

2.6.1 Measurement of Concrete Resistivity for Reinforced Concrete Structures

This chapter identifies the use of concrete resistivity measurements, the main methods of measuring concrete resistivity, and the variables which affect concrete resistivity. Concrete resistivity is a tool which has been used in the analysis of concrete properties, primarily in controlled laboratory environments. In addition to assessing concrete properties, much research has been carried out in regard to what affects concrete resistivity such as chemical compositions,

humidity, water-to-cement ratio, curing conditions, and contaminations. For the purposes of laboratory testing, variables for the assessment of concrete resistivity have been minimised. This is most evident in the current AASHTO [1] and ASTM [49] resistivity measurement Standards, in which testing is carried out on water-saturated concrete samples.

When identifying all variables which contribute to concrete resistivity values, it is evident that for resistivity values to be representative of real reinforced concrete structures, resistivity measurement of the concrete structure must be carried out in its same environmental exposure conditions, encompassing all the variables discussed in this Chapter. A new resistivity testing methodology incorporating embedded probes with current four-point Wenner probe methods was identified [50]. This method can remove the surface saturation required for four-point Wenner probe testing and allow for resistivity measurements, removing the variations caused by surface wetting. Further research to assess the effect of probes versus surface resistivity measurements is one area which requires research. If repeatable trends can be identified using embedded probes, a new, quick standardised test method for atmospherically exposed concrete can be formed.

Wherever concrete resistivity values are quoted in these Standards [2] [3] [4] and Technical Reports [9], the quoted resistivity values are not related to the age of the concrete or repair mortar when the resistivity is measured. While it can be assumed that resistivity of aged concrete is relatively stable and can vary only due to environmental conditions within certain limits, this assumption is not applicable for new repair mortars.

There is no research into the long-term change (increase) of resistivity values under saturated or atmospheric conditions for repair mortars. The resistivity data of repair mortars has become relevant in recent years when used in conjunction with galvanic anodes and ICCP systems. For this reason, manufacturers of repair mortars are now including resistivity data in the repair mortars technical data sheets [52] [53]. The resistivity data is normally quoted at 7 days, 28 days and 56 days [52] [53]. The resistivity data supplied by the manufacturer however is conducted in saturated conditions. The rate of resistivity increase is not determined, and it is unknown when the resistivity stabilises. An experiment into the increase of concrete resistivity under saturated and atmospheric conditions is presented in Chapter 3.

2.6.2 Relationship Between Cathodic Protection Current Density Output and Concrete Resistivity

This literature review identifies that the topic of concrete resistivity is increasingly noted in literature and Standards related to concrete rehabilitation and cathodic protection design. Although the importance of concrete resistivity is being observed in Standards and papers, concrete resistivity information is quite limited when it comes to the design of electrochemical protection systems. The current literature identifies that there is a relationship between concrete resistivity and electrochemical protection system performance, but no direct research into this area has been conducted especially regarding the relationship between current density output and concrete resistivity. The ionic current flow through the concrete (as shown in Figure 2.1 and

Figure 2.2 is a vital aspect to the design and implementation of electrochemical protection systems, particularly regarding performance. Resistivity is understood to play a vital role in anodic output current, but experimental research on this topic is extremely limited. Research into identifying the limiting concrete resistivity factor for the performance of impressed current and galvanic anode systems is required. Research work into various aspects on the impact of concrete resistivity into the performance of impressed current cathodic protection systems is included in chapters 4 and 5.

3 Concrete Compositions for Laboratory Resistivity Research and the Development of a Resistivity Testing Methodology for Atmospherically Exposed Concrete

This chapter describes the methodology for creating concrete with varying resistivity for use in this laboratory research, the identification of an issue with the current methods of measuring concrete resistivity, the development of a more reliable and replicable method of concrete resistivity measurement without the use of water saturations, and a data comparison over time between four different polymer modified repair mortars under saturated and outdoor conditions.

3.1 Research Background

The literature review identified concrete resistivity as a topic highly researched and developed for the laboratory study of concrete permeability and chloride ion diffusivity [46] [47], and the effects of singular environmental changes such as temperature and humidity on resistivity. For this type of testing, variables have been limited most notably in the current procedures and standards of resistivity testing. The current concrete resistivity Standards [1] [49] require the water saturation of samples in order to allow for replicable, consistent measurements. In practice, the majority of concrete structures are not located in such saturated conditions. This becomes problematic for the measurement of concrete structures, repair mortars and concrete mixes which are exposed to atmospheric outdoor conditions. Resistivity data based on the current measurement Standards will therefore not be applicable for these conditions. Research on the measurement of concrete resistivity in these atmospheric, dry, and outdoor conditions is lacking.

A method for concrete resistivity testing which can provide a quick, reliable, consistent method of concrete resistivity testing for samples in atmospheric dry conditions is required - a method which can be carried out with laboratory accuracy, but also practical for on-site testing.

Resistivity of concrete repair mortars and concrete mixtures are currently being tested in saturated conditions to the current Standards. Testing of these repair mortars and concrete mixtures commonly used in concrete remediation and in conjunction with electrochemical protection systems in comparable environmental conditions is required. With the development of a new method of resistivity testing without the saturation, trends in concrete repair mortars and mixtures can be researched to better understand the actual performance of concrete in practice.

3.2 Sample Design

The literature review identified variables which contribute to the changes of concrete resistivity. The purpose of these experiments is to assess concrete samples with varying resistivities. To carry out a replicable and methodical approach, certain variables were kept consistent for the laboratory testing samples.

A series of concrete samples were used in the design considerations to decrease variables as follows:

- All samples used for concrete resistivity measurements were cast with no steel reinforcement. For samples in which electrochemical testing is carried out, a cylindrical concrete sample consisting of the same composition was cast with no steel and used for resistivity measurements. Samples were mixed in the same batch to ensure concrete mixture uniformity between electrochemical test samples and concrete resistivity measurement samples. The purpose of this was to remove the variable associated with steel reinforcement conductivity on the resistivity test results.

- No aggregate was used in any of the tested concrete samples. As stated in the literature review, the resistivity of concrete can be dependent on the mining locality, aggregate type, and size [32]. Furthermore, the impact of aggregate on resistivity within small concrete sample sizes can be unpredictable and greatly affect concrete resistivity measurements [12]. Therefore, resistivity variations of all samples in this research work were carried out by varying only the admixture compositions. Admixtures such as fly ash, and ground slag are available and display consistent compositions worldwide allowing for the experimental procedures with the same compositions to be recreated.

A common curing method was employed for all laboratory testing. As stated in the literature review, concrete resistivity is highly dependent on the composition [12] [30], curing methodology and exposure time of concrete [23] [31] [36]. To address this issue and remove the curing variable, a standard curing period of 24 hours was adopted for all experiments. The 24-hour duration was selected as to allow for the initial curing of the concrete. Following the 24-hour curing period, the samples were removed from their formwork. The time prior to testing is detailed in each experimental section and is dependent on the purpose and design of each experiment.

As stated in the literature review, the degree of liquid saturation into the concrete pore network will affect resistivity [18] [24] [37]. To address this issue unless otherwise specified, test samples were stored and tested in dry laboratory conditions. There are three reasons for carrying out testing of the samples in dry conditions:

1. For samples to be in a comparative environment to that of atmospherically exposed concrete. As identified in the literature review, the majority of concrete structures are located in atmospheric conditions, and not in saturated conditions.

2. The literature review stated that an increase in moisture content results in a decrease in concrete resistivity [39]. In the aim of limiting variables, resistivity values of concrete samples were adjusted with the use of widely available admixtures. Attaining high concrete resistivity values in saturated conditions would require the addition of epoxy-based materials which is uncommon and adds an additional variable.

3. Due to the inhomogeneous nature of concrete, the saturation of test samples in water may cause substantial variations in the performance of the ICCP current as water penetration through parts of the samples can result in current dumping [54]. Testing samples with ICCP installed in saturation conditions adds a variable which cannot be controlled, and therefore, all testing which involves impressing current for cathodic protection testing purposes in this thesis is carried out in dry conditions.

3.3 Wenner probe equipment details

A Proceq four-point Wenner probe (50mm probe spacing model) was used for all resistivity testing in this thesis. The Proceq Resipod is extensively utilised onsite and in laboratory research [55] [56] [57] [58] [59]. Figure 3.1 displays an image of the Proceq Resipod. The Proceq Resipod measurement principle is displayed in Figure 3.2.

Figure 3.1 - Proceq Resipod four-point Wenner probe array

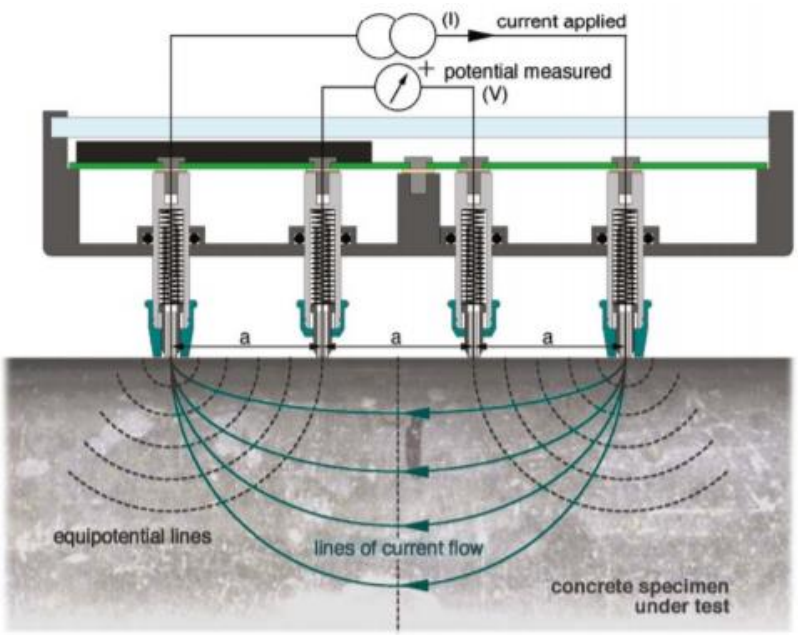

Figure 3.2 - Wenner Probe measurement principal

Based on the manufacturer's details:

Resipod is a fully integrated 4-point Wenner probe, designed to measure the electrical resistivity of concrete in a completely non-destructive test. It is the most accurate instrument available, extremely fast, and stable and packaged in a robust, waterproof housing designed to operate in a demanding site environment. [10]

The technical data of the Proceq Resipod is detailed below in Figure 3.1.

Table 3.1 - Proceq Resipod Wenner probe equipment technical data

Probe spacing (a)	50mm
Range	0.1 – 2000 kΩcm
Resolution (nominal current 200µA)	±0.2 kΩcm or ±1% (whichever is greater)
Resolution (nominal current 50µA)	±0.3 kΩcm or ±2% (whichever is greater)
Resolution (nominal current <50µA)	±2 kΩcm or ±5% (whichever is greater)
Frequency	40 Hz
Operating temperature	0° to 50°C

Testing of the Resipod was carried out in accordance with the manufacturer's operation manual [10] progressively throughout each experiment (with the use of the manufacturer's test strip) to confirm that the unit's accuracy was within the equipment manufacturers stated range.

3.4 Experiment Sections

This chapter is divided into four experimental sections:

Section 1: Involves the development and resistivity testing of different concrete compositions for the purposes of laboratory resistivity experimentation with the aim of creating samples with variable resistivities, with minimal admixtures and within certain timeframes.

Section 2: Involves experimental research on the impact of water saturation of Wenner probe resistivity measurements on resistivity values and the standard deviation of measurements.

Section 3: Identifies and tests a new method of measuring concrete resistivity of concrete located in atmospheric conditions, without the need for surface wetting or water saturation.

Section 4: Involves the comparison between resistivity data of four different repair mortars over a period of 564 days, with samples exposed to saturated and outdoor conditions.

3.5 Experiment 1 – Development of Concrete Mixtures For Resistivity Testing

The aim of experiment 1 was to create concrete samples with varied resistivity, identify a trend in resistivity of the different mixtures over time, and verify the applicability of atmospheric concrete resistivity testing using the four-point Wenner probe method. Variations in mixture compositions were used to achieve the variation in resistivity, keeping all other variables such as temperature, relative humidity, and curing conditions consistent.

3.5.1 Materials and Method

Nine concrete samples A, D, D1, F, F1, G, G1, H and H1. These samples were created with different compositions for the purpose of creating samples that increase in resistivity at different speeds, allowing for future testing to be carried out at various resistivity ranges at a given point in time. These samples were comprised of the following materials and mixture composites as detailed in Table 3.2 and Table 3.3.

Table 3.2 - Material list

Material List:	General Purpose Cement – Sourced from Cement Australia
	Ground Granulated Blast Furnace Slag – Sourced from Cement Australia
	Fly Ash – Sourced from Cement Australia
	Sibelco Silica Sand
	Silica Fume
	Denka Sigma 2000

Table 3.3 - Experiment 1 mixture by weight %

Mixture Composite		Material Composition by weight %						
		GP Cement	Ground Slag	Fly Ash	Silica Sand	Silica Fume	Denka Sigma	Water
Sample Set 1	A	41%			41%			18%
	D	25%	16%		41%			18%
	F	14%	27%		41%			18%
	G	14%	32%		31%	5%		18%
	H	14%	37%		26%		5%	18%
Sample Set 2	D1	25%		16%	41%			18%
	F1	14%		27%	41%			18%
	G1	14%		32%	31%	5%		18%
	H1	14%		37%	26%		5%	18%

Each sample was cast in a PVC container with dimensions W88 x D300 x H90mm. All samples were left to cure under normal atmospheric conditions for 24 hours. Samples were then removed from the containers. Samples were stored and tested at a temperature of 23 ± 1 ^{o}C and relative humidity of 55 ± 10%. No correction factor was used for this experiment. Surface resistivity measurements were conducted using a Proceq four-point Wenner probe (50mm probe spacing). Sample surface wetting was carried out as per the manufacturer recommendations:

"A good connection between the instrument and the concrete surface is the most important factor for obtaining a reliable measurement. Dip the contacts in water several times before making a measurement – use a shallow container so you can press against its bottom – this will fill the reservoirs. Press the Resipod firmly down until the outer two rubber caps rest on the surface to be tested." [10]

A single reading was measured during each monitoring period for each sample after the reading stabilised for a minimum of 10 seconds.

The design and testing location is displayed in Figure 3.3.

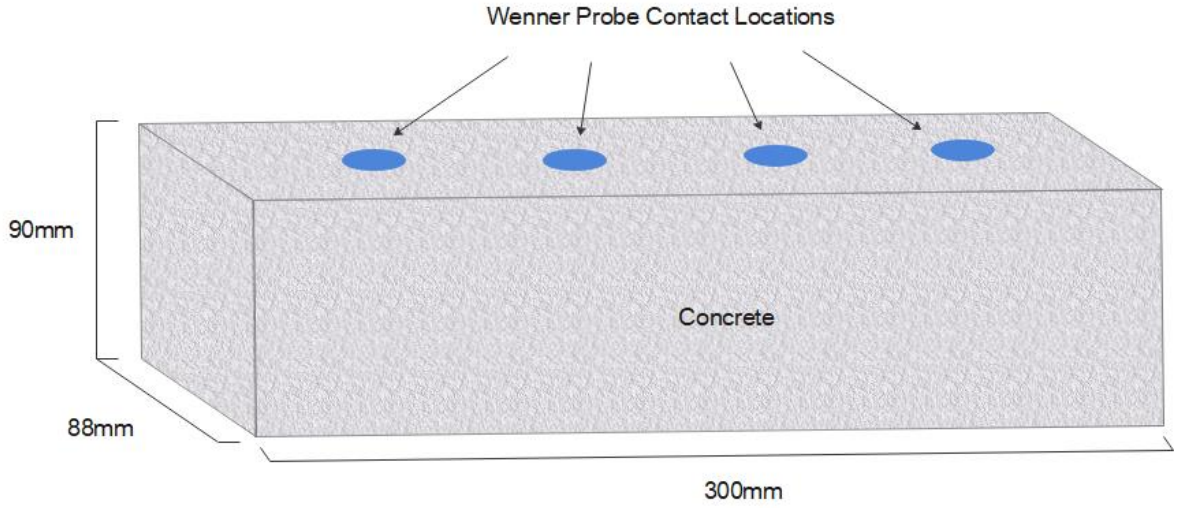

Figure 3.3 - Experiment 1 - Sample design and testing locations

3.5.2 Results

The results from Experiment 1 are detailed in

Table 3.4. 246 resistivity measurements were carried out over a period of 139 days for the samples in Set 1, and 90 days for the samples in Set 2. The samples in Set 1 and the samples in Set 2 were cast at different times (due to the availability of fly ash and laboratory access) resulting in gaps in the data displayed in

Table 3.4. Set 2 was limited to 90 days due to the fact that 3 of the 4 samples (Samples F1, G1 and H1) reached the maximum resistivity measurement of the Proceq equipment (>2000 kΩcm). The fast increase in concrete resistivity is believed to be due to the incorporation of fly ash. Additional data from Sample D1 past the 90-day period did not merit an experimental extension.

Table 3.4 – Resistivity data of various mixture compositions for laboratory concrete resistivity testing

Experiment 1 Data (kΩcm)									
Days	Samples								
	A	D	F	G	H	D1	F1	G1	H1
1	3	2	2	2	2	1.7	1.4	1.4	1.6
2	5	4	4	4	6	3.6	2.5	2.2	2.1
3	6	6	7	7	10	4.1	2.7	2.5	2.4
4	7	6	9	11	16	6.4	5.1	5.4	6.9
5	8	8	12	14	18				
6	8	9	13	19	24				
7	10	11	17	22	28	10	13.7	19.8	26
9						13.5	25.4	36.3	47
10						15.7	31.5	43.8	59.8
21						46	131	225	284
22						52.1	148.8	230	349
25	19	37	65	84	106	63.4	191.4	297	442
28	21	45	79	105	121	73.5	251	366	541
30	22	46	80	109	145	76.9	270	405	580
31	24	47	81	118	144				
33	25	51	88	126	144				
34	26	55	96	130	146				
35	26	55	98	133	148				
36	26	56	101	131	160				
37	26	57	102	141	177	115	389	567	619
43						125.5	490	748	1065
46						135.4	570	892	1307
47	31	66	118	152	194				
48	35	75	134	164	194				
49	35	76	136	170	194	157.1	757	1140	1551
51	34	77	136	177	195				
52	34	78	135	192	201				
54	35	83	143	207	207				
55	36	88	150	205	210				
56	35	84	147	203	212				
57	35	81	145	203	236	187.7	960	1420	2000
63	37	86	146	203	260	195.5	999	1525	2000
64	40	92	148	203	260				
70	40.9	87.7	142.8	219	268				
73	41.8	87.6	144	224	274				
77	45.6	101	161.8	238	281				
84	50.5	105.6	171.1	286	329				
90	45.6	105.7	171.6	268	299	382	2000	2000	2000
108	60.4	132.9	218	338	396				
139	95.3	186.9	320	445	484				

3.5.3 Discussion

The data from

Table 3.4 has been plotted in Figure 3.4 and Figure 3.5. The graphs show an increase in resistivity of all samples over time. The data shows that concrete resistivity values are greatly varied by altering concrete composition with different mixture compositions and admixtures.

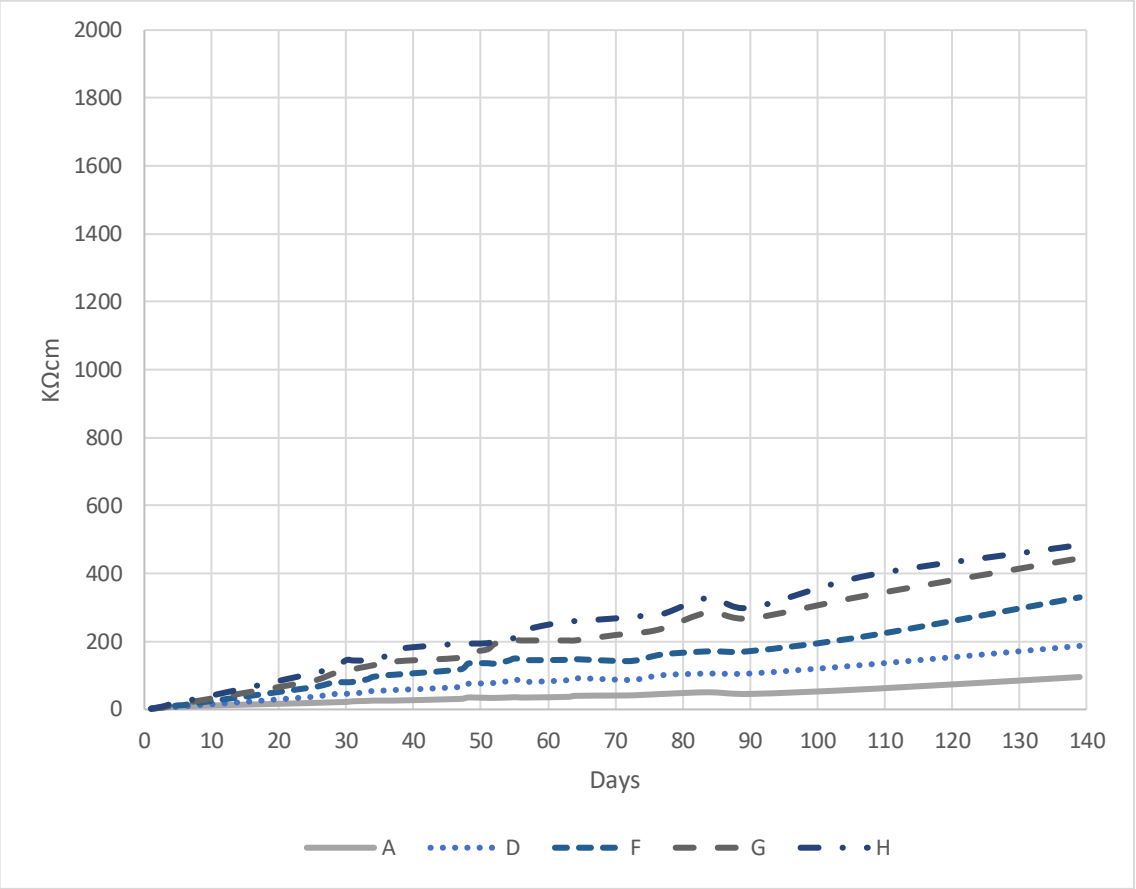

Figure 3.4 - Set 1 Ground slag admixture trends

Figure 3.4 shows resistivity value's range for samples A, D and F from 95 kΩcm to 440 kΩcm, by increasing the percentage of ground slag. With the addition of Silica Fume and Denka Sigma, resistivity values increased to 445 kΩcm and 484 kΩcm in Sample G and H at 139 days. The resistivity data within the first two to three days show consistent readings due to the highly saturated pore structure. With the drying out of the concrete, the variation of resistivity values begins to increase. The data in Figure 3.4 shows a linear resistivity increase for the entire test

duration of 139 days, with no indication of resistivity stabilisation. Resistivity values between samples indicate that the testing mixtures can be used to achieve varied resistivity values for the purpose of concrete resistivity testing.

The mixtures in samples A, D, F, G, and H can be utilised for resistivity testing which require a limited resistivity range for an extended duration, for example between 30 kΩcm and 40 kΩcm. Sample A can be tested from day 47 through to day 64, for a duration of 17 days.

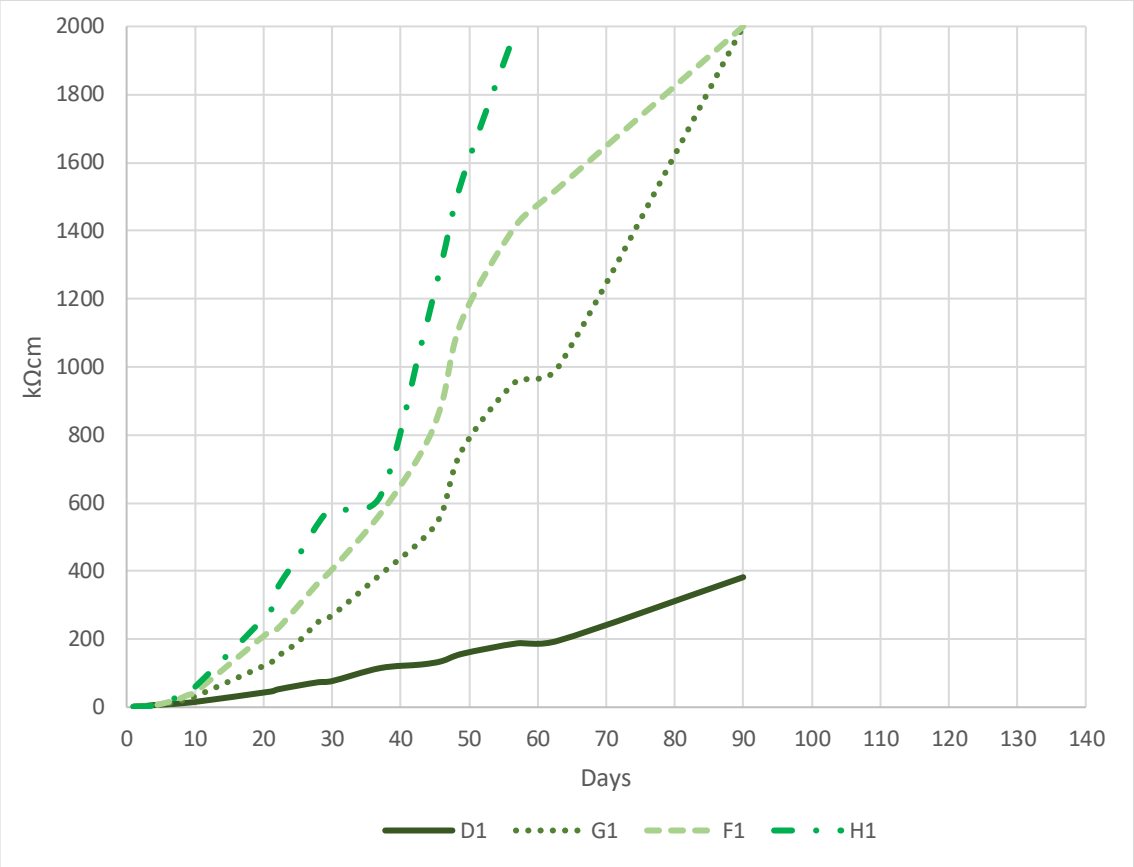

Figure 3.5 - Set 2 Fly ash admixture trends

Figure 3.5 shows the resistivity data gathered over a period of 90 days for samples D1, G1, F1, and H1. The increase in resistivity over this period is substantially greater when compared to the sample in set 1. The substitution of fly ash for ground slag was found to substantially increase resistivity values within a shorter timeframe. Samples G1, F1, and H1 exhibited exponential increases in resistivity values, while sample D1 exhibited a linear increase in resistivity, similar to that of sample H from sample set 1.

This data indicated that if shorter timeframes for resistivity testing or high resistivity values over 500 kΩcm are required, fly ash in the mixture ratios as detailed in Table 3 can be used.

A comparison of results between the samples in Set 1 and 2 from Experiment 1 at Day 63 is displayed in Figure 3.6. The varied concentration of quantities of GP cement, ground slag, fly ash silica sand, silica Fume, and Denka Sigma were shown to considerably vary the resistivity properties of the samples.

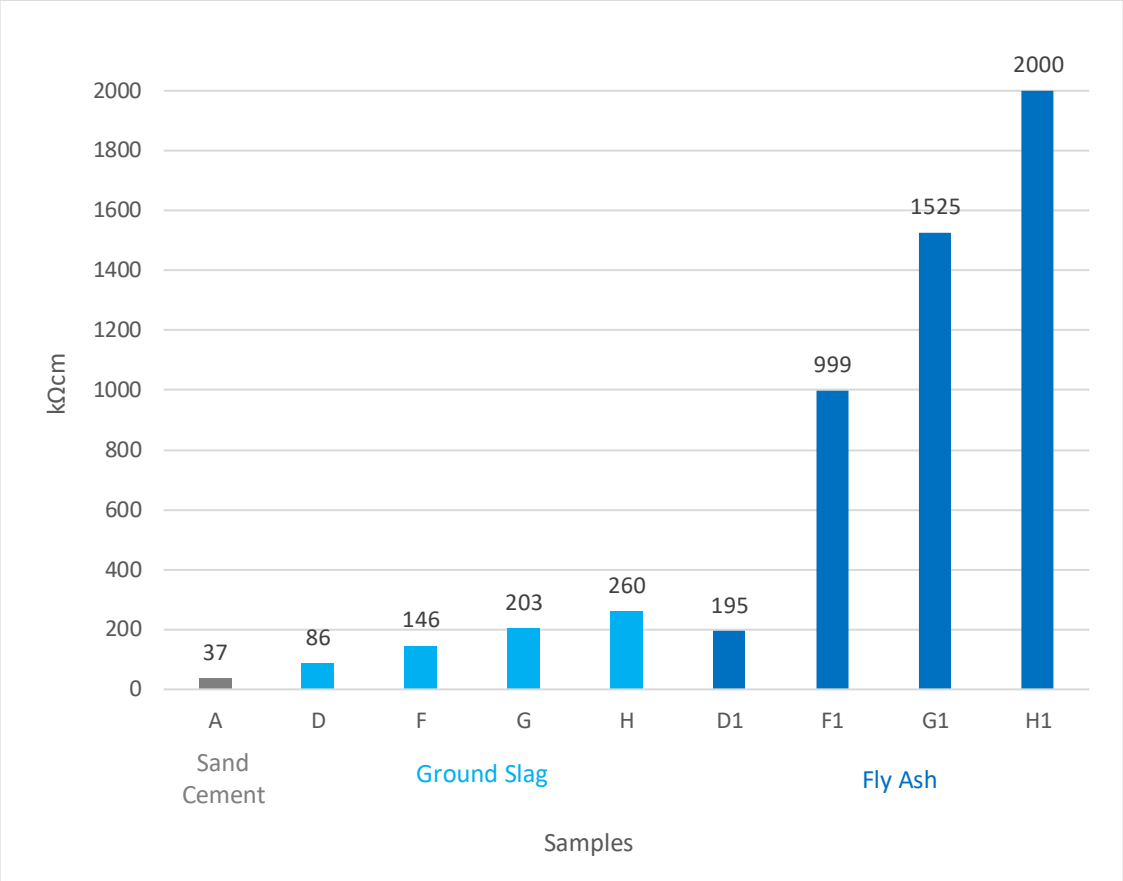

Figure 3.6 - Resistivity data of mixture composites at day 63

Sample A which comprised of a basic concrete mix of sand, cement and water, measured the lowest resistivity value from the samples tested. Sample A measured a resistivity of 37 kΩcm. The addition of ground slag increased the resistivity by 132.43% in sample D, and 294.59% in sample F. The increase in ground slag with the addition of silica fume increased the sample's resistivity by 448.64%. The addition of Denka Sigma increased the sample resistivity by 602.70%. The substitution of ground slag to fly ash, increased the resistivity between samples D and D1

by 127.32%, between samples F and F1, 584.24%, between samples G and G1, 651.23%, and between H and H1, ≥669.23%.

Experiment 1 identified an issue with the stability and replicability of resistivity measurements of concrete in atmospheric conditions. Resistivity measurement consistency was found to decrease with increased resistivity. Surface wetting of the concrete probes was required to carry out surface measurements, and a trend between the amount of surface wetting and a drop in resistivity values was observed. As stated in the literature review, electrical conductivity increases with an increased moisture content due to an increase in ion mobility [39], with the moisture content dependent on the level of direct liquid pore saturation [40]. This phenomenon was observed in this experiment but in the case of resistivity testing, no research has been conducted on the impact of surface wetting, (liquid content or duration of exposure) on the resultant change of resistivity.

3.5.4 Conclusion

Experiment 1 provided information on the development of concrete mixtures for the purpose of laboratory concrete resistivity testing of exposed samples under atmospheric conditions. By varying the materials and compositions, the increase of resistivity can be controlled, allowing for the creation of samples with concrete resistivity between 37 kΩcm and 2000 kΩcm within a period of 63 days. The data gathered in this experiment provides a mixture composition guide to design concrete mixtures for use in laboratory resistivity experiments. Note, no geometric correction factor was applied in this experiment (Proceq flat setting used). Raw resistivity values may vary when compared with samples of different dimensions. Note, no geometric correction factor was applied in this experiment (Proceq flat setting used). Raw resistivity values may vary when compared with samples of different dimensions. Due to the small dimensional size of the test samples in Experiment 1, the impact of resistivity measurement variations caused by sample size edge effects is unknown. In order to remove the impact of any edge effects, a new larger and standardised sample design would be required for subsequent experiments.

The following results were identified from this experimental work:

- The use of fly ash over ground slag in the composition of the samples was found to substantially increase concrete resistivity.

- At 63 days from casting, the resistivity value was measured at 37 kΩcm for a basic concrete mix of sand, cement, and water. The addition of ground slag increased the resistivity by 132.43% in sample D and 294.59% in sample F.

- The addition of Silica fume increased the resistivity by 448.64% in sample F, and the addition of Denka Sigma increased the resistivity by 602.70%.

- The substitution of ground slag in place of fly ash increased the resistivity between samples D and D1 by 127.32%, between samples F and F1 by 584.24%, between samples G and G1 by 651.23%, and between samples H and H1 by more than 669.23%.

This experiment identified two areas requiring further research.

1. A consistent sample specification regarding dimension size and shape is required to provide a consistent and replicable method of concrete resistivity measurements and uniformity between experiments. A re-design of future samples in this research was developed in accordance with AASHTO T 358-19 [1]. This experimental re-design is described in Experiment 2.

2. The second involves the method of resistivity measurement. As noted in the results sections, variations in concrete resistivity readings were found to increase with increasing resistivity, with an increased duration required before a resistivity measurement would stabilise. Based on observations, four-point resistivity measurement variations increased over time after casting, and with increasing sample resistivity. For measurements carried out near the casting date of ≤10 days, resistivity measurements were found to be quick to stabilise and replicable. This is due to the high amount of moisture from the initial casting of the samples. With higher resistivities and the subsequent dry atmospheric exposure (23 ± 1 ^{o}C and relative humidity of 55 ± 10%) of the samples, additional surface water application was necessary to be able to measure resistivity values. At higher resistivities, especially in samples F1, G1, and H1, the application of water on the surface was essential in measuring resistivity, and the amount of water and time after surface wetting was found to greatly affect resistivity values. A study into the effect of surface water saturation is carried out in Experiment 2.

3.6 Experiment 2 – Effect of Water Saturation on Wenner Probe Resistivity Measurements

Four-point Wenner probe testing is the most commonly used method of measuring concrete resistivity due to its simplistic and non-destructive nature. There are two different methods of measuring concrete resistivity using a four-point Wenner probe. In the laboratory, measurements are made on concrete cylinders either cast in the laboratory or extracted as cores from a concrete structure. The samples are tested at 100% saturated conditions in the laboratory. This method of testing is in accordance with AASHTO designation: T358-19 [1]. The purpose of saturating the samples is to obtain good contact between the concrete sample surface and the resistivity test equipment. The second method of testing is conducted non-destructively onsite. For the field testing, the resistivity meter probes are directly placed on the concrete surface. As the majority of concrete is located in atmospheric conditions, surface wetting of the concrete is required as recommended by the manufacturer to achieve adequate contact between the concrete and contact probes. The resistivity data in this case can be affected by the presence of reinforcement, temperature, and the moisture content of the concrete. No guidelines or research exist regarding the amount of water required or its impact on resistivity measurements.

Experiment 1 identified that reliable and stable resistivity measurements can be obtained in the laboratory atmospheric conditions without surface saturation of the concrete within approximately 10 days from the casting date. This is due to sufficient moisture during casting of the concrete enabling sufficient probe-to-concrete surface contact. As the concrete surface dries out, wetting the surface is required and in this case, it is observed in Experiment 1 that the amount of water used for the wetting process alters the results significantly.

The aim of experiment 2 was to identify the effect of water saturation on Wenner probe concrete resistivity measurements. Experiment 2 includes an analysis of the standard deviation between measurements prior to and after water saturation.

3.6.1 Materials and Method

Five test sample composition mixtures were created: A, D1, F1, G1, and H1. These samples comprise of the following materials and mixture composite as detailed in Table 3.2 and Table 3.5.

Table 3.5 - Experiment 2 sample mixture by weight %

Material Composition by weight %							
Mixture Composite	Sample	GP Cement	Fly Ash	Silica Sand	Silica Fume	Denka Sigma	Water
A	1	41%	-	41%	-	-	18%
D1	2	25%	16%	41%	-	-	18%
F1	3	14%	27%	41%	-	-	18%
G1	4	14%	32%	31%	5%	-	18%
H1	5	14%	37%	26%	-	5%	18%

Each test sample was mixed in a single batch using a paddle mixing rotary tool for a duration of 10 minutes. Each mixture composition was cast into a 100mm diameter x 250mm length PVC cylinder. The base of the cylinder was capped off using a 100mm PVC cap during casting. All samples were left to cure for 24 hours, removed from their PVC casts, and stored in a laboratory at room temperature. During casting and for the duration of storage, all samples were kept at a temperature of 23 ± 1°C and a humidity of 55 ± 10%. As identified in the conclusion of Experiment 1, the use of rectangular samples may have resulted in possible unknown edge effects and geometric variations in Wenner probe measurements. Wenner probe measurements are geometrically dependent and a comparison between the raw resistivity values obtained in Experiment 1 cannot be directly compared to the obtained values in the subsequent experiments without geometric corrections. As this was identified as an issue in Experiment 1 a redesign of the sample dimensions was carried out in order to standardise the samples and remove the need for any geometric corrections between future experiments. Samples were therefore designed in accordance to AASHTO T358-19 [1], but with alterations to sample length (due to the use of a 50mm probe in place of the 38mm probe specified in AASHTO T358-19 [1]). Spacing configuration of probes was adjusted for. The design of the sample is displayed in Figure 3.7.

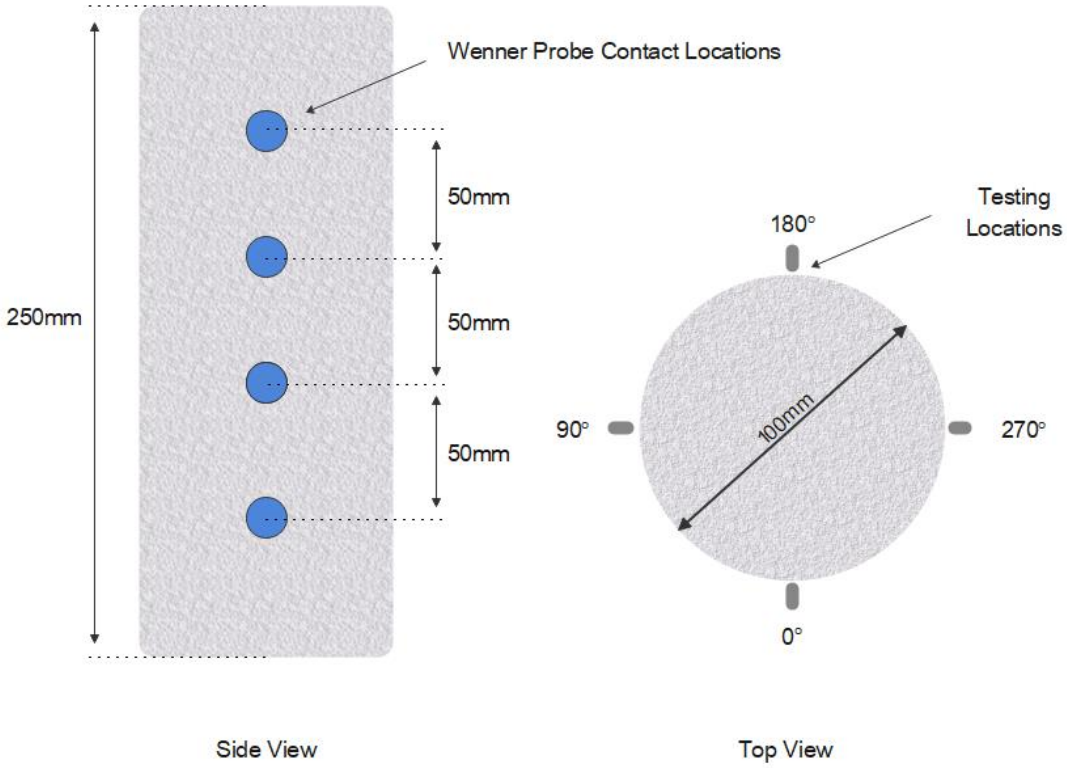

Figure 3.7 - Experiment 2 - Concrete sample for resistivity measurements

Sample testing was carried out as per AASHTO T358-19 [1], with eight surface resistivity measurements carried out for each sample. The first measurement sessions were carried out when the samples were dry, at a temperature of 23 ± 1°C and a humidity of 55 ± 10%. After testing in dry atmospheric conditions, the samples were saturated in water for 5 minutes with resistivity measurements carried out at 1 minute, 30 minutes and 60 minutes after saturation.

For the testing in dry atmospheric conditions, the probes of the resistivity equipment were dipped in a shallow container of water several times before making a measurement in accordance with the Wenner Probe manufacturer recommendations.

3.6.2 Results

Figure 3.8, Figure 3.9, Figure 3.10, and Figure 3.11 display the resistivity measurements and standard deviations of each sample in the different exposure conditions.

ID	Mean Value	Total	Std. Deviation
1	10.2 kΩcm	8	0.32
2	40.3 kΩcm	8	5.94
3	149.4 kΩcm	8	35.01
4	260.1 kΩcm	8	60.48
5	423.8 kΩcm	8	97.24

Figure 3.8 - Resistivity data and standard deviation of samples in dry conditions

ID	Mean Value	Total	Std. Deviation
1	9.9 kΩcm	8	0.30
2	30.4 kΩcm	8	2.08
3	79.2 kΩcm	8	3.25
4	125.5 kΩcm	8	5.11
5	126.7 kΩcm	8	5.71

Figure 3.9 - Resistivity data and standard deviation of samples 1 minute after saturation

ID	Mean Value	Total	Std. Deviation
1	10.1 kΩcm	8	0.34
2	27.8 kΩcm	8	0.61
3	73.9 kΩcm	8	3.27
4	125.0 kΩcm	8	5.81
5	169.8 kΩcm	8	8.34

Figure 3.10 - Resistivity data and standard deviation of samples 30 minutes after saturation

ID	Mean Value	Total	Std. Deviation
1	10.4 kΩcm	8	0.34
2	28.3 kΩcm	8	0.55
3	74.7 kΩcm	8	4.27
4	124.7 kΩcm	8	6.07
5	178.6 kΩcm	8	5.87

Figure 3.11 - Resistivity data and standard deviation of samples 60 minutes after saturation

3.6.3 Discussion

There are two trends which can be identified in this data.

Figure 3.12 shows a drop in resistivity measurements of the samples after 5 minutes of water saturation. It is noted that the higher the resistivity, the larger the resistivity drop after saturation. The testing at 1 minute after saturation indicates a 70.10% decrease in resistivity for sample 5 (highest resistivity dry value), while for sample 1 (lowest resistivity dry value) the decrease of resistivity was only 2.94%.

Figure 3.12 displays the polynomial trendline of samples 1 to 5. This trendline shows an initial drop in resistivity values for the 1-minute testing. Following this initial drop, a slow increase in resistivity values is observed.

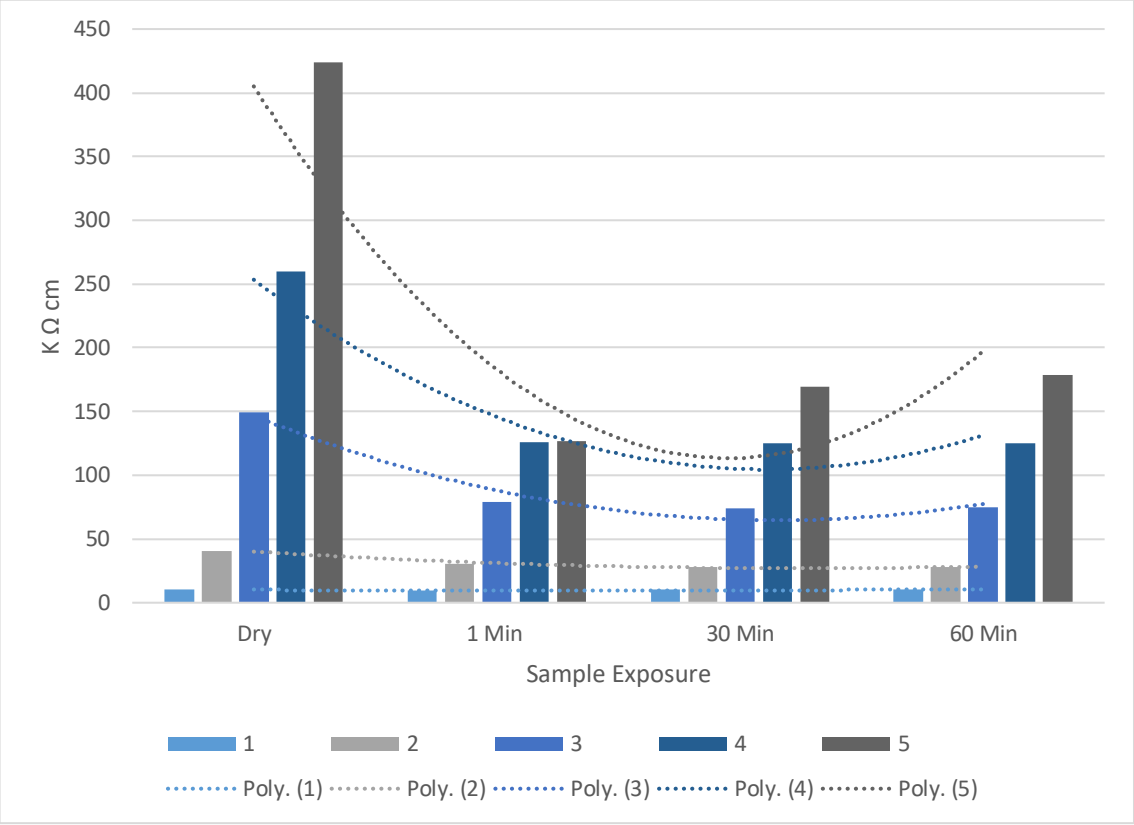

Figure 3.12 - Resistivity values of concrete samples before and after water saturation

Figure 3.13 shows both the standard deviation of each sample and the polynomial trend between the measurement intervals. Measurements carried out in the dry conditions prior to saturation show that for samples 3, 4, and 5 (with initial high resistivity values) have considerably higher standard deviation values than samples 1 and 2 (with initial low resistivity value). This test indicates a clear correlation between resistivity value and standard deviation. The higher the resistivity, the higher the impact of saturation.

Figure 3.13 indicates that resistivity measurement is greatly reduced by the saturation of the test samples. Sample 1 displayed a smaller standard deviation while in sample 5 the standard deviation is high. The resistivity decreases from 97.24 to 5.87 (93.96%) between dry and 60-minute measurements.

The polynomial lines between

Figure 3.12 and Figure 3.13 show that there is a direct correlation between concrete resistivity and standard deviation. In both Figures, resistivity and standard deviation drops substantially between dry and the 1-minute measurement, but then starts to decrease at 30- and 60-minute measurements.

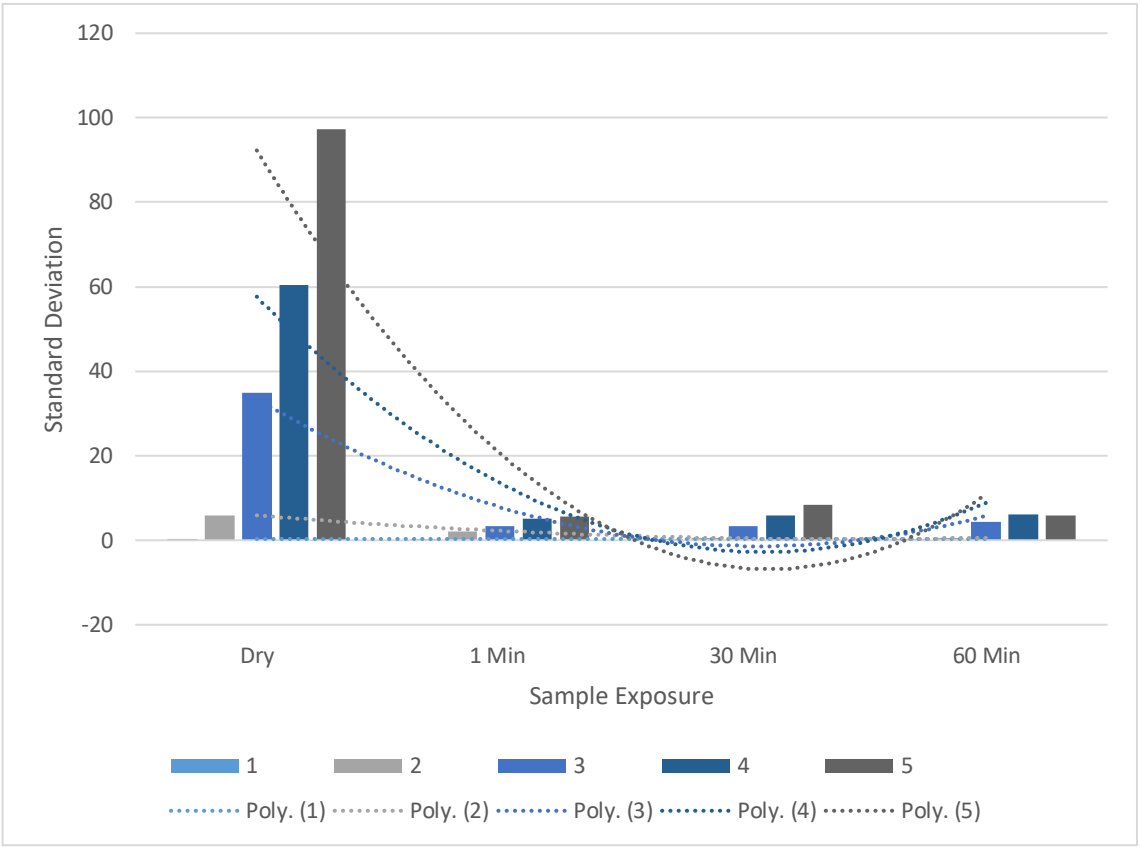

Figure 3.13 - Standard deviation of concrete samples before and after water saturation

3.6.4 Conclusion

The aim of Experiment 2 was to identify the effect of water saturation on Wenner probe concrete resistivity measurements by measuring resistivity prior to and after water saturation. Experiment 2 identified that surface wetting/temporary water saturation had a substantial impact on the resistivity values and measurement consistency.

A significant drop in resistivity value was identified after the water saturation of the dry concrete sample. The drop was significant (70.1%) for the sample with a high initial resistivity value of 420 kΩcm and was relatively minor (2.94%) for the sample with a low initial resistivity value of 10 kΩcm.

The standard deviation was smaller for the saturated samples, and larger for the dry samples. This is indicative of concrete in atmospheric conditions where there is a large variation in resistivity data, the stability and repeatability of measurements cannot be achieved.

The only current Standard for the measurement of concrete resistivity using the four-point Wenner probe is AASHTO T358-19 [1]. This standard is based on testing under saturated conditions only. Water saturation decreased standard deviation as shown in Figure 3.13, however water saturation as shown in

Figure 3.12 greatly alters resistivity values. Therefore, to test samples located in dry atmospheric conditions, an alternative method of testing must be developed in order to obtain accurate resistivity readings and eliminate the effect of water saturation on the resistivity measurements.

3.7 Experiment 3 – New Method of Concrete Resistivity Measurement for Concrete in Atmospheric Conditions

Based on the findings in experiments 1 and 2, the aim of experiment 3 was to test a new method of concrete resistivity measurements. As discussed in the literature review, AASHTO T358-19 [1] is the most recent Standard for concrete resistivity testing by four-point Wenner probe detailing the method of concrete resistivity measurement for water-saturated concrete. Currently, there is no international standard for concrete resistivity measurements for non-saturated concrete samples. Resistivity testing requires contact with the concrete sample's surface. Accurate

resistivity measurements are highly dependent on this contact. Research into how this contact can be achieved without the addition of water or gels is limited. In many cases for Wenner probe testing to achieve the necessary contact required for resistivity testing, sample surface alterations must be made primarily in the form of water saturation.

A test method statement by Main Roads Western Australia [50], details a method of concrete resistivity testing using embedded steel probe pins. However, no research has been conducted into the effect of the use of steel pins on concrete resistivity measurements. The use of steel pins may be a solution to provide the necessary contact between a four-point Wenner probe and a concrete sample's surface without the application of any wet sponges or gels, removing the variables associated with these external applications. The use of embedded steel pins and their effect on resistivity is explored in this experiment.

3.7.1 Materials and Methods

For this work, the comparison of resistivity measurements was performed between surface measurements and embedded steel probes at depths of 10 – 35mm at 5mm intervals.

Eight cylindrical concrete samples labelled 1 to 8 were used. Samples 1, 2 and 5 comprised of polymer modified repair mortars. The compositions of the remaining concrete mixtures are presented in Table 1. The samples were exposed to different environments: saturated/dry, tested at different time periods from curing, and comprise of different concrete mixtures to compare a broad range of environmental exposure conditions and resistivity values. The samples exposure conditions are detailed in the following sections:

3.7.2.1 Resistivity Surface and Probe Measurements of Water-Saturated Concrete.

3.7.2.2 Resistivity Surface and Probe Measurements of Concrete in Laboratory Dry Conditions.

3.7.2.3 Resistivity Surface and Probe Measurements of Newly Cast Concrete in Laboratory Dry Conditions.

3.7.2.4 Resistivity Surface and Probe Measurements of Concrete Before and After Water Immersion.

Table 3.6 - Sample compositions (gravimetric %) and exposure conditions

Samples	Exposure Condition	GP Cement	Silica Sand	Ground Slag	Fly Ash	NaCl	Water
1	Saturated condition, long Term	Polymer modified Concrete Repair Mortar (L)					
2		Polymer modified Concrete Repair Mortar (S)					
3	Laboratory dry condition, long term	41.0%	41.0%				18.0%
4		25.0%	16.0%	41.0%			18.0.%
5		Polymer modified Concrete Repair Mortar (L)					
6	Laboratory dry condition, short term	25.0%	16.0%	41.0%			18.0%
7	Combined dry/saturated condition, short term	14.0%	41.0%		27.0%		18.0%
8		13.8%	40.8%		26.8%	0.6%	18.0%

Samples 1, 2 and 3 were prepared in accordance with manufacturer technical specifications. Each test sample was mixed using a paddle mixing rotary tool for a duration of 10 minutes. The samples were cast into ø100 x 250mm cylinders, with samples being cured for 24 hours in their PVC casts. In order to eliminate variables which may impact on the accuracy of the resistivity results, no aggregate or rebars were used for the concrete samples.

For the temporary embedment of internal probes prior to testing each sample, four 3mm holes spaced 50mm apart were drilled into each concrete sample. Four 316 stainless steel marine CSK Phillips self-taping screw A4 6-gauge x 50mm were screwed initially to the test depth of 15mm. After the resistivity measurement at 15mm, the screws were progressively drilled at 5mm increments for further measurements, to the final depth of 35mm. A four-point Wenner probe array with 50mm spacing was used for the testing. The experimental setup for the measurement of concrete resistivity with the use of embedded probes is displayed in . Embedded probe depths of 15 - 30mm were used in Sections 3.7.2.1 and 3.7.2.2 and 10 - 30mm in Sections 3.7.2.3 and 3.7.2.4. The Wenner probe tips were placed in direct metal to metal contact with the 316 stainless-steel screws. Measurements were conducted using a commercial device for concrete resistivity measurement (Proceq four-point Wenner probe - 50mm probe spacing).

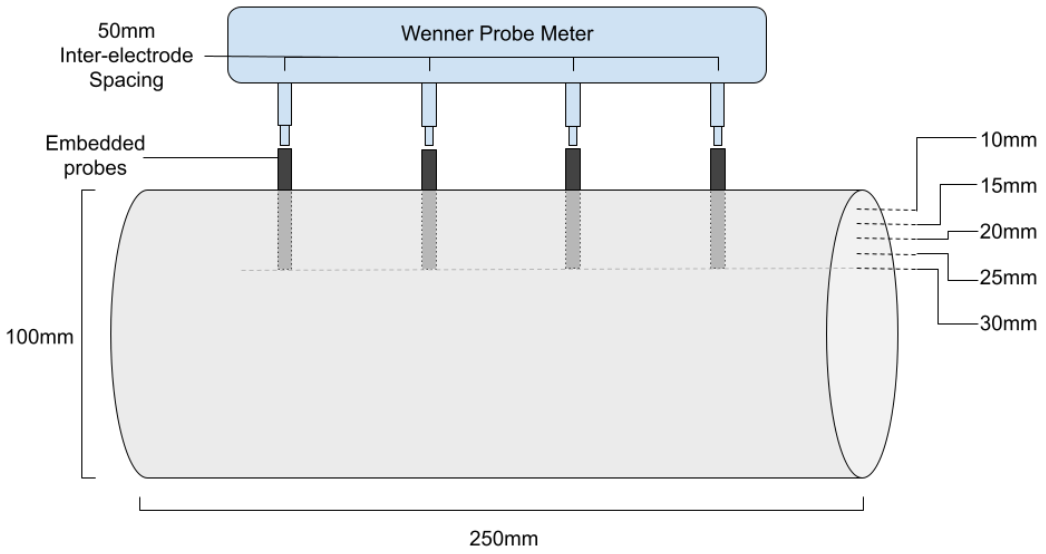

Figure 3.14 - Schematic of resistivity probe measurement. Figure showing 30mm probe depth

3.7.2 Results and Discussion

3.7.2.1 Resistivity Surface and Probe Measurements of Water-Saturated Concrete

Samples 1 and 2 were used to confirm the correlation between surface resistivity in saturated conditions (as per AASHTO T358-19 Standard) and the resistivity measured at depth using embedded stainless-steel probes.

The electrical resistivities of Samples 1 and 2 were measured in accordance to AASHTO T358-19 [1]. The samples were immersed in water for a duration of 6 months prior to testing. To perform the testing, the samples were removed from the water and the surface was cleaned with a wet sponge. Eight surface point measurements were carried out and averaged as per AASHTO T358-19 [1]. Drilling was then carried out by a 3mm masonry drill bit. Four screws were screwed into the holes, and the first readings were measured at 15mm screw depth. The screws were then progressively drilled and tested at depths of up to 30mm. The results from Samples 1 and 2 are presented in Table 3.7.

Table 3.7 - Comparison between AASHTO T358-19 surface resistivity measurements and probe resistivity measurements of saturated samples

	Sample 1		Sample 2	
Depth	kΩcm	% Change	kΩcm	% Change
Surface	68.8	-	55.5	-
15mm	65.5	4.79%	51.7	6.84%
20mm	64.8	5.81%	51.4	7.38%
25mm	63.9	7.12%	50.8	8.46%
30mm	62.9	8.57%	50.3	9.36%

The results show a consistent decrease in resistivity with increased probe depth. Samples 1 and 2 displayed a resistivity measurement decrease of 4.79% (from 68.8 kΩcm to 65.5 kΩcm) and 6.84% (from 55.5 kΩcm to 51.7 kΩcm) between the surface measurement (tested in accordance with AASHTO T358-19) and 15mm probe depth. The data shows that the largest change in resistivity for both Samples 1 and 2 were between the surface and 15mm probe depth measurement. For both samples, an average decrease of approximately 1% was identified between probe depth measurements.

To validate the proposed embedded probe method a comparison of results must be made with a current universally adopted Standard, in this case AASHTO T358-19 **[1]**. The data of Samples 1 and 2 plotted in Figure 4 verifies a relationship between the existing AASHTO T358-19 **[1]** Standard (surface measurement) and the new proposed method (probe measurements). Figure 3.15 displays consistent, decreasing measurements all within a range of less than 10% between surface measurements and probe measurements. If similar results are identified when testing concrete in atmospheric conditions, verification of this trend may lead to the development of an adjustment factor between the AASHTO Standard and the proposed probe method.

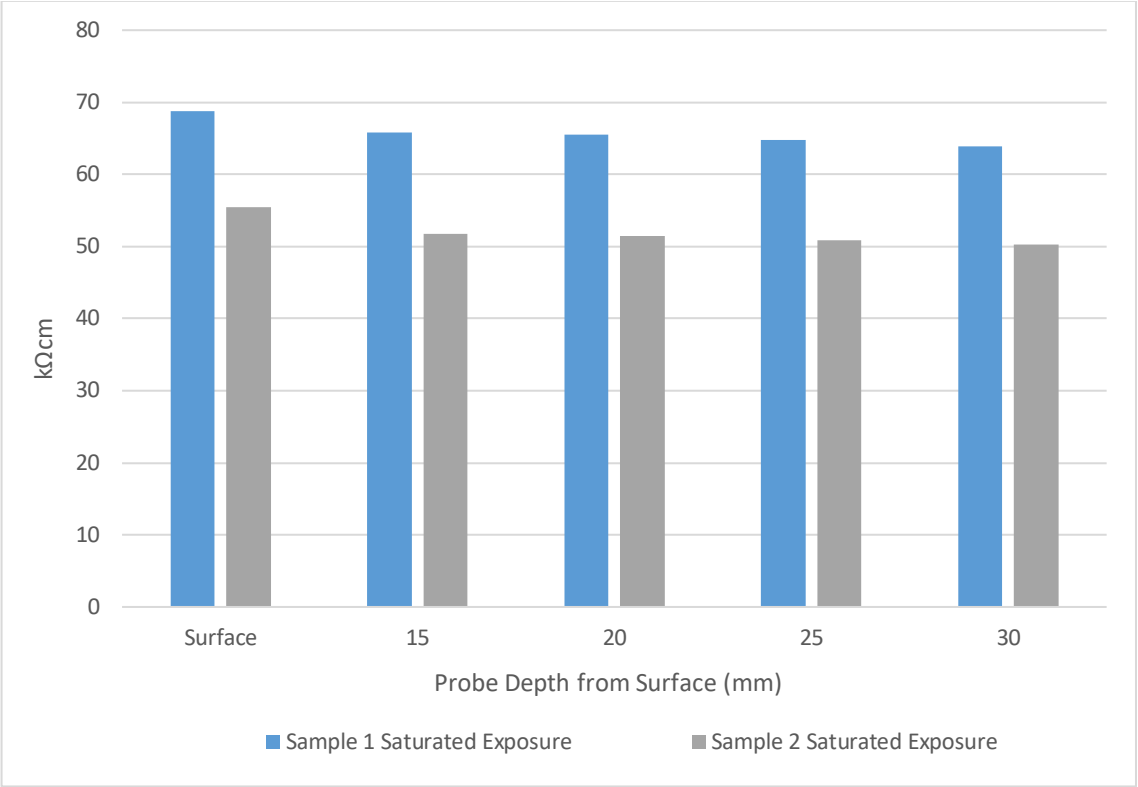

Figure 3.15 - Trend line of surface and probe depth resistivity measurements of saturated concrete samples 1 and 2

3.7.2.2 Resistivity Surface and Probe Measurements of Concrete in Laboratory Dry Conditions

Samples 3, 4 and 5 were used to study the resistivity values between dry surface measurements and embedded probes at depths between 15mm and 30mm. The mixture compositions for these samples were designed to obtain samples with varied resistivities, with Sample 3 being low resistivity, and Samples 4 and 5 being high resistivity. These samples were cast and stored in dry laboratory conditions at a temperature of 23±1°C and humidity of 55±10% and tested six months after casting.

A comparison of resistivity data between surface measurements for samples in dry laboratory conditions and measurements using embedded probes at depths between 15mm and 30mm was carried out. The surface measurement was performed using the recommended procedure for the testing equipment [10] which included localised wetting of the concrete surface by water discharged from the equipment probe at the probe/concrete contact. The test results are presented in Table 3.8.

Table 3.8 - Resistivity embedded probe measurement of dry concrete samples after 6 months from casting (concrete surface too dry for surface measurements)

	Sample 3	Sample 4	Sample 5
Depth	kΩcm	kΩcm	kΩcm
Surface	>Limit	>Limit	>Limit
15mm	42.8	340	311
20mm	43.1	334	313
25mm	42.3	327	309
30mm	41.6	314	304

Surface resistivity measurement for the three samples could not be performed, indicating a surface resistivity value greater than the Wenner probe equipment limit of 2000 kΩcm. This data suggests that the surface of concrete samples exposed to dry laboratory conditions are unsuitable for concrete resistivity measurements beyond the recommended procedure [10] of the testing equipment (using localised concrete surface wetting at the probe contact location). It was also found that the external surface of a concrete sample kept in dry laboratory conditions for a six-month duration was not representative of the sample's internal resistivity.

Resistivity measurement using embedded probes were performed at 15 - 30mm depths and the data is presented in Table 3.8. The 8 resistivity measurements at each probe depth were stable, consistent, and repeatable. The resistivity data indicates a percentage change of 1.40%, 2.54% and 1.13% respectively for Samples 3, 4 and 5 for each 5mm increment with an average resistivity change of 1.69%. The percentage change was not impacted by the resistivity magnitude (resistivity of Samples 4 and 5 was higher in comparison to Sample 3). The resistivity trend of the samples is displayed in Figure 3.16.

Figure 3.16 plots the probe resistivity data from Samples 3, 4 and 5. The embedded probe measurements show consistent and trends with Samples 1 and 2. This suggests that the use of internal probe measurements can be considered as a suitable and reliable alternative to surface saturation, with consistent probe measurement trends observed in both water-saturated and dry laboratory exposed concrete.

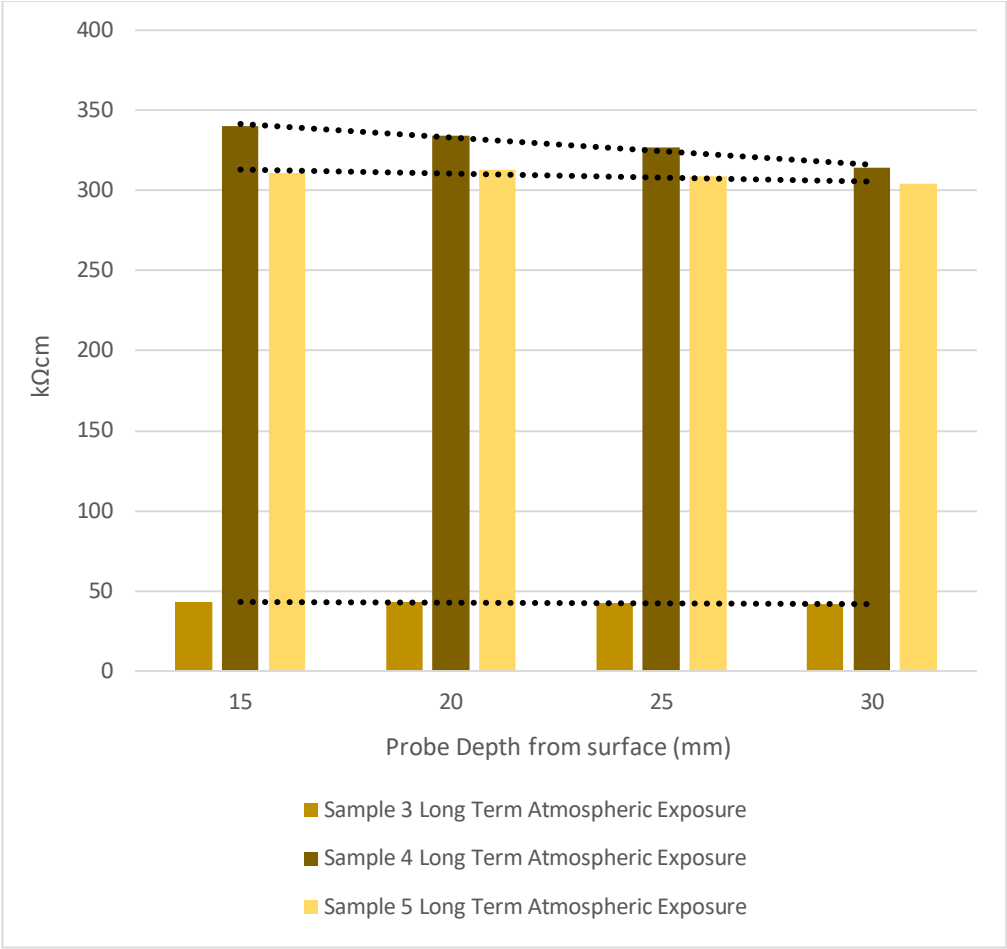

Figure 3.16 - Trend line of surface and probe depth resistivity measurements of dry concrete Sample 3 (low resistivity), Samples 4 and 5 (high resistivity)

3.7.2.3 Resistivity Surface and Probe Measurements of Newly Cast Concrete in Laboratory Dry Conditions

Sample 6 was used to compare surface resistivity testing and embedded probe resistivity testing while the moisture content of the concrete was still high after a relatively short duration from casting (14 and 30 days).

Sample 6's mixture was designed to obtain rapid resistivity increase over a short period of time (with the addition of fly ash in the composition). The sample was stored and tested in dry laboratory conditions at a temperature of 23±1°C and a humidity of 55±10%. The resistivity test was performed at 14 days and 30 days from the date of casting. The data gathered is presented in Table 3.9.

Table 3.9 - Resistivity measurement of dry sample at 14 and 30 days after casting

	Sample 6 (14 Days)		Sample 6 (30 Days)	
Depth	kΩcm	% Change	kΩcm	% Change
Surface	66.3	-	342.4	-
10mm	66.2	0.15	325	5.08
15mm	64	3.46	314	8.29
20mm	62.4	5.88	300	12.38
25mm	57.5	13.27	290	15.30
30mm	56.7	14.47	288	15.88

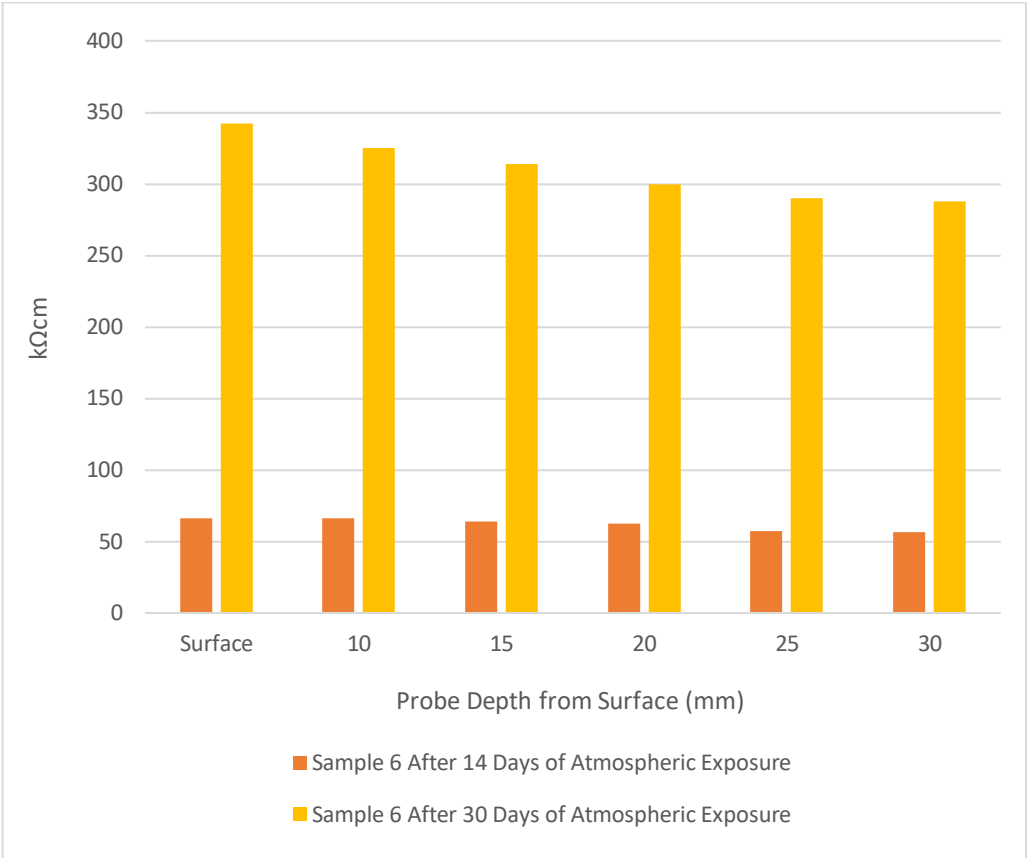

Figure 3.17 - Trend line of surface and probe depth resistivity measurements comparing the effect of dry laboratory exposure duration (14 and 30 days) on resistivity measurements

Surface resistivity measurements of Sample 6 were performed without the use of any surface saturation. This was due to the available surface moisture from the sample casting after both 14 and 30 days. As the surface resistivity of Samples 3, 4 and 5 could not be measured after six months of exposure to dry conditions, the data suggests that the drying out of the concrete surface may be the contributing factor. This is further supported by the increase in resistivity readings for Sample 6 between the surface and the 10mm probe depth reading of 0.15% (from 66.3 kΩcm and 66.2 kΩcm) at 14 days, and 5.08% (from 342.4 kΩcm and 325 kΩcm) at 30 days.

Figure 3.17 plots the surface and probe depth resistivity measurements of Sample 6. Embedded probe measurements showed similar trends to saturated and dry concrete samples as tested in Samples 1 to 5, with the results consistent and replicable.

Based on this experiment, resistivity testing could be carried out without the addition of surface wetting or saturation up to 30 days from casting. Within this period, the level of surface moisture can be assumed to be sufficient to establish electrolytic contact. In practice, varied exposure conditions will impact on the level of surface moisture, affecting this 30-day timeframe.

3.7.2.4 Resistivity Surface and Probe Measurements of Concrete Before and After Water Immersion

Samples 7 and 8 were used to evaluate the impact of water immersion on the resistivity value between surface measurements and measurements using embedded probes in the concrete. Two sample mixtures (samples 7 and 8) were designed to provide different resistivities. Samples 7 and 8 were cast and stored in dry laboratory conditions for six months at a temperature of 23±1^{o}C and a humidity of 55±10%.

Surface and probe resistivity measurements were carried out in dry laboratory conditions. Immediately following the dry surface and probe depth measurements, 7 and 8 were immersed in water with surface resistivity measurements carried out at 1, 2, 3, 24, 48 and 72 hours from water immersion. The data gathered from Samples 7 and 8 is presented in Table 3.10.

Table 3.10 - Resistivity measurements of dry concrete samples before and after water immersion

		Sample 7		Sample 8	
		kΩcm	% Change	kΩcm	% Change
Surface Readings	Dry	50.6	-	121.1	-
	Saturated 1h	46.4	8.30%	21.8	81.99%
	Saturated 2h	37.5	25.88%	8.0	93.39%
	Saturated 3h	25.7	49.20%	5.6	95.37%
	Saturated 24h	11.3	77.66%	3.8	96.86%
	Saturated 48h	9.8	80.63%	4.0	96.69%
	Saturated 72h	9.2	81.81%	4.3	96.44%
Probe Depth (In Dry Conditions)	10mm	47.5	6.12%	111.1	8.25%
	15mm	48.8	3.55%	111.5	7.92%
	20mm	49.5	2.17%	111.6	7.84%
	25mm	49	3.16%	110	9.16%
	30mm	47.7	5.73%	108.5	10.40%

The results from Samples 7 and 8 can be divided into two groups: Group one before immersion and Group two after immersion. Group one results indicate that the resistivity test measurements at surface dry conditions and using probe depth between 10mm and 30mm is consistent with the testing of the previous experiments. The percentage change is lower for the sample with low resistivity (3.55% at 15mm depth for Sample 7) and relatively higher for the sample with relatively higher resistivity (7.92% at 15mm depth).

For the resistivity readings following immersion (Group two), the data shows a large drop in resistivity between dry and saturated conditions with a decrease in resistivity of over 80% for both Samples 7 and 8 after 72 hours of immersion.

Sample 7 indicated a surface resistivity of 50.6 kΩcm, the immersion impact ranged between 8.3% (from 50.6 kΩcm and 46.4 kΩcm) after 1-hour of immersion to 81.81% (from 121.1 kΩcm and 21.8 kΩcm) after 72 hours of immersion.

For Sample 8 which indicated a surface resistivity of 121.1 kΩcm, the immersion impact ranged between 81.99% after 1-hour of immersion to 96.44% after 72 hours of immersion.

Samples 7 and 8 indicated that immersion of the concrete substantially alters the measured concrete resistivity. The current procedure for testing atmospheric concrete based on the AASHTO T358-19 [1] by extracting cores and testing concrete resistivity of these cores under

saturated conditions will result in highly inaccurate and non-representative resistivity data for concrete in atmospheric conditions.

Samples 7 and 8 confirm the need for a methodology which can provide the required electrolytic contact between the Wenner Probe and concrete without water saturation or surface wetting.

3.7.2.5 Depth of Probe Measurement Percentage Change

Figure 3.18 displays the resistivity measurement data from Samples 1, 2, 6, 7 and 8 (samples where surface resistivity measurements could be performed). The chart displays the surface percentage decrease for these samples at the recorded probe intervals of 10, 15, 20, 25, 30 and 35mm probe depths. The figure shows that all measurements at 10 – 15mm probe depths are within 9% of surface measurements, with a 16% range between 10 – 30mm probe depths. The resulting trend is similar in all the samples tested, regardless of the admixtures or sample exposure conditions. The data shows that the range of variation between surface and embedded probes is consistent with samples tested in saturated and dry conditions.

Figure 3.18 identifies that the smallest variation of measurements between the samples was recorded at 15mm probe depths, suggesting that a 15mm probe depth is most consistent when comparing probe depth resistivity measurements to sample surface resistivity readings in all tested conditions and all tested concrete compositions. The data presented in Figure 4.17 can be used to develop an adjustment factor between surface measurements and measurements at probe depth.

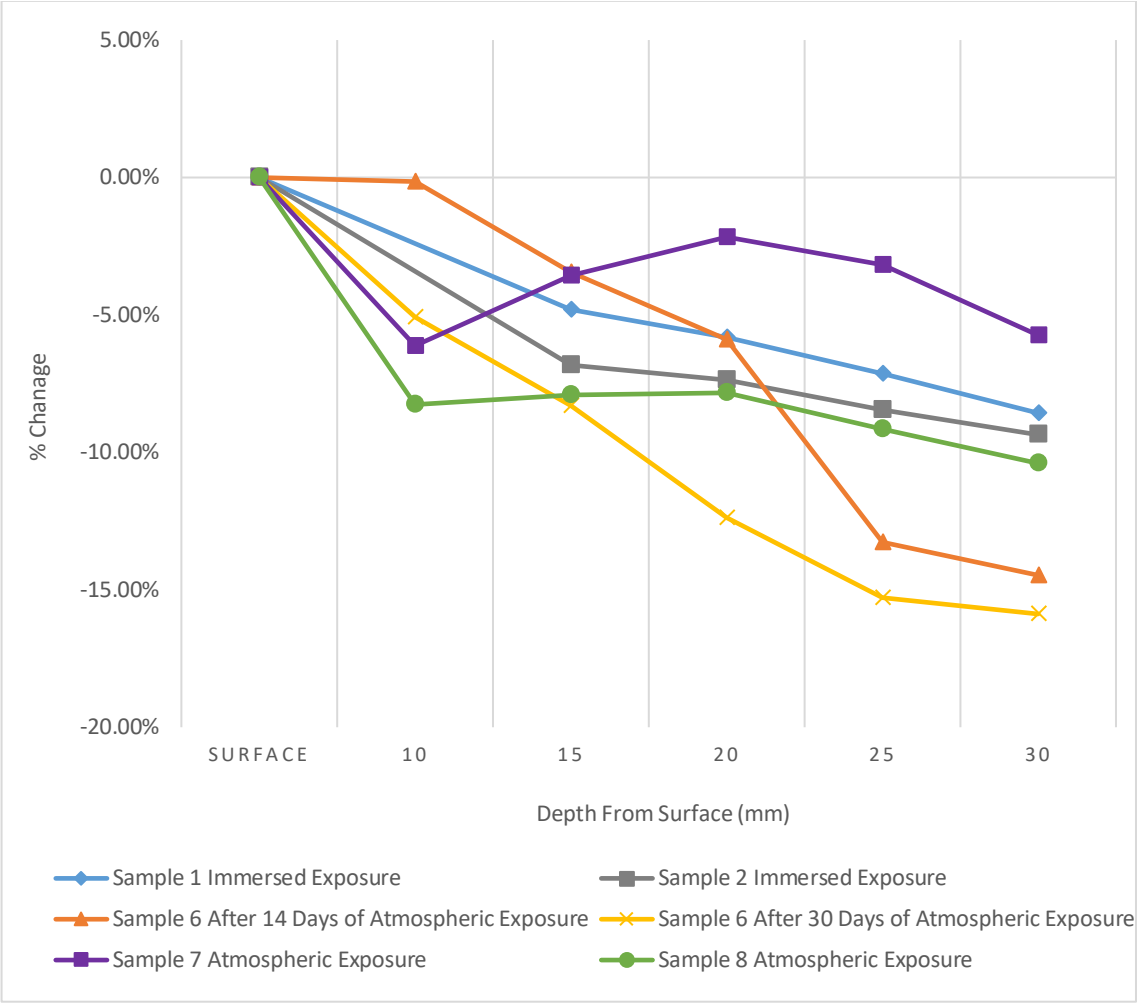

Figure 3.18 - Percentage change from surface resistivity measurement and measurements at probe depths between 10 and 30mm

3.7.2.6 Applications

The AASHTO T358-19 [1] Standard was developed to indicate the concrete's ability to resist chloride ion penetration and has become a universally adopted method for Wenner probe concrete resistivity testing. This is due to the increasing adoption of the Four Point Wenner probe equipment as it is quick and simplistic, particularly with the development of new generation handheld Wenner Probe equipment [10].

In the field, a lack of an established method for testing concrete in atmospheric conditions has led to the adoption of the AASHTO T358-19 [1] Standard by concrete material manufacturers, as resistivity testing must be in accordance with a Standard. Due to this, concrete manufacturers

commonly test in accordance with AASHTO T358-19 [1], conducting concrete resistivity testing in saturated conditions. As presented in Table 3.10 of this paper, water saturation will yield unrepresentative results, making current accepted practices with testing to the Standard problematic particularly for products being designed to be used in atmospheric conditions. In practice, these misleading results impact the selection process regarding the suitability of repair mortars, and the design of electrochemical cathodic protection systems.

This thesis presents a simple methodology, utilising established Wenner probe equipment to measure resistivity in atmospheric conditions. The method presented in this paper identifies a relationship with the current AASHTO T358-19 [1] Standard. Further research and testing of this method may lead to the creation of a new concrete resistivity Standard, or the adoption of this methodology into the AASHTO T358-19 [1] Standard for the testing of concrete resistivity in atmospheric conditions. This would mean reduced errors caused by water saturation/surface wetting, and hence provide more representative results both in laboratory conditions and in the field.

3.7.3 Conclusion

The following observations and conclusions can be drawn from this experimental research:

- This experiment establishes the need for a reliable method of achieving sufficient electrolytic contact without the alteration of the concrete surface's moisture content.

- This research identifies that water immersion of dry concrete greatly alters the resistivity measurements significantly, with concrete samples displaying a resistivity measurement decrease of over 80% between dry conditions and after 72-hours of water immersion. Testing concrete resistivity for atmospheric concrete based on AASHTO T358-19 [1] standard by extracting cores and testing the resistivity of these cores under saturated conditions will result in highly inaccurate and non-representative resistivity data for concrete in atmospheric conditions.

- This experiment identifies that by using temporary embedded steel probes, it is possible to eliminate the need for any surface moisture alteration or concrete sample immersion, which would otherwise introduce additional variations. In addition, the method

proposed in this experiment has shown to provide quick accurate and repeatable resistivity data, a method which can be carried out in not only laboratories but also on-site and using the widely adopted and available concrete Wenner probe equipment, without the need for any additional specialised equipment.

- Based on the results from this experiment, a 15mm probe depth was identified to provide the most consistent resistivity measurements of concrete in varied exposure conditions and compositions, with a resistivity measurement decrease of up to 8%, between surface and probe measurements.

- The output from this research work can contribute to the development of guidelines for the measurement of concrete resistivity via the Wenner probe in atmospheric conditions.

3.8 Experiment 4 - Effect of Long-Term Exposure Conditions on Concrete Repair Polymer Modified Repair Grouts.

In the rectification process of reinforced concrete structures, one of the primary considerations made is in the selection of concrete repair methodology and repair products [5]. The suitability of concrete repair products is determined by the structure's function, and some of the main technical aspects which are considered include, compressive strength, bond strength, shrinkage and expansion, tensile strength, chemical resistance, and flow characteristics [5]. In addition, in the case of an electrochemical protection treatment being specified, mortar resistivity becomes the primary consideration. The addition of polymers to concrete repair products is used to improve these characteristics but generally at the expense of increased resistivity. While high concrete resistivity mortar could be beneficial for the long-term corrosion protection when used for conventional patch repairs, the use of high resistivity mortars in conjunction with electrochemical protection systems can be problematic, due to ionic current flow required for electrochemical systems to operate.

A new trend is seeing concrete resistivity beginning to be considered as an important aspect in the selection of concrete repair materials [60] primarily in the repair of corrosion effected reinforced concrete structures, and the compatibility of concrete repair materials with electrochemical protection systems, such as impressed current cathodic protection systems and

galvanic anode systems [9] [51]. This is seen in the international standards such as the Australian Standard AS 2832.5 (R2018) [2] which states:

"Electrical resistivity surveys shall be carried out on representative areas of concrete to provide information for the design of the cathodic protection system. Core samples may also be obtained from the structure to evaluate volumetric concrete resistivity".

"Overlay application may be combined with concrete repair. In such cases, the long-term electrical resistivity of concrete repair materials shall be within the range 50% to 150% of the parent concrete electrical resistivity".

Although there are no exact limits in the applicable standards defining high and low resistivity mortars, providing resistivity data is becoming common for concrete repair mortars. Manufacturers are including resistivity data in their product technical data sheets (TDS) and are advising on the suitability of some of these mortars for repair use in conjunction with electrochemical protection systems.

In most cases, manufacturers publish repair mortar resistivity values at 28 days from casting, in saturated conditions mostly without reference to any standard. Although product resistivity values are commonly being noted in product technical data sheets, there are two areas which require further investigation and research. The first is the study of resistivity change beyond the initial 28-day period. Generally, there is no available data beyond this short-term period and the resistivity performance of the repair mortars after the 28 days is unknown. It has been assumed that the presented data is the maximum resistivity of the mortar under service conditions.

The second aspect which requires research is the environmental condition in which the testing is being carried out in. The current standards AASHTO designation: T358-19 [1] and ASTM C1826-19 [49] require the saturation of samples prior to testing. The actual use of such repair mortars is not in saturated conditions. The repair mortars are designed for use in atmospheric conditions only and the saturated condition data may not be relevant in these circumstances. It is likely that manufacturers assume that the resistivity of mortar is the same under saturated and atmospheric conditions, and the resistivity stops to increase at 28 days.

This thesis presents resistivity data of four commercially available polymer modified concrete repair mortar products. Cylindrical samples of each product were cast and tested in saturated and outdoor conditions. The samples were cast using four commercially available mortars marketed as low resistivity mortars and then tested periodically at the different exposure conditions for a duration of 564 days.

The primary aim of this research is to assess whether the repair mortar resistivity increases over time and whether the manufacturers reported short term resistivity data for repair mortar under saturated condition can be correlated to the actual long-term resistivity of the mortar at saturated and atmospheric conditions.

3.8.1 Materials and Method

Four products were tested in this experiment. For the purpose of confidentiality, the products were labelled L, S, M and H. All products are commercially available concrete repair mortars marketed and extensively used as low resistivity repair mortars in conjunction with electrochemical repair systems. A total of fifteen cylindrical samples were cast. The samples were cast into ø100 x 250mm cylinders and cured for 24-hours in their PVC casts. After 24 hours, the samples were relocated to saturated and outdoor exposure conditions. The sample labelling and exposure conditions are shown in Table 3.11.

Table 3.11 - Experiment 4 sample labelling and exposure condition

Product	Saturated Condition	Outdoor Conditions
L	L1, L2	L5
S	S1, S2	S5, S6
M	M1, M2	M5, M6
H	H1, H2	H5, H6

The testing was performed over a period of 564 days from the date of casting. Twenty sets of readings were carried out during this period. The resistivity testing was performed using a Proceq 50mm four-point Wenner probe, with a testing procedure in accordance to AASHTO designation: T358-19 [1] for the samples in saturated conditions. For samples in outdoor conditions, testing was performed with a four-point Wenner probe with the use of 15mm embedded stainless-steel screws. A total of sixteen 316 stainless steel screws were drilled into each outdoor sample. Four SS screws were drilled at 50mm spacing at 0, 90, 180, and 270 degrees as displayed in Figure 3.19. Embedded SS screws were used to carry out the outdoor measurements in order to attain measurements without the addition of surface saturation

(which can cause variations in measurement accuracy). The outdoor testing was performed during periods of dry conditions and after heavy rain to obtain representative results simulating existing structures located in atmospheric conditions.

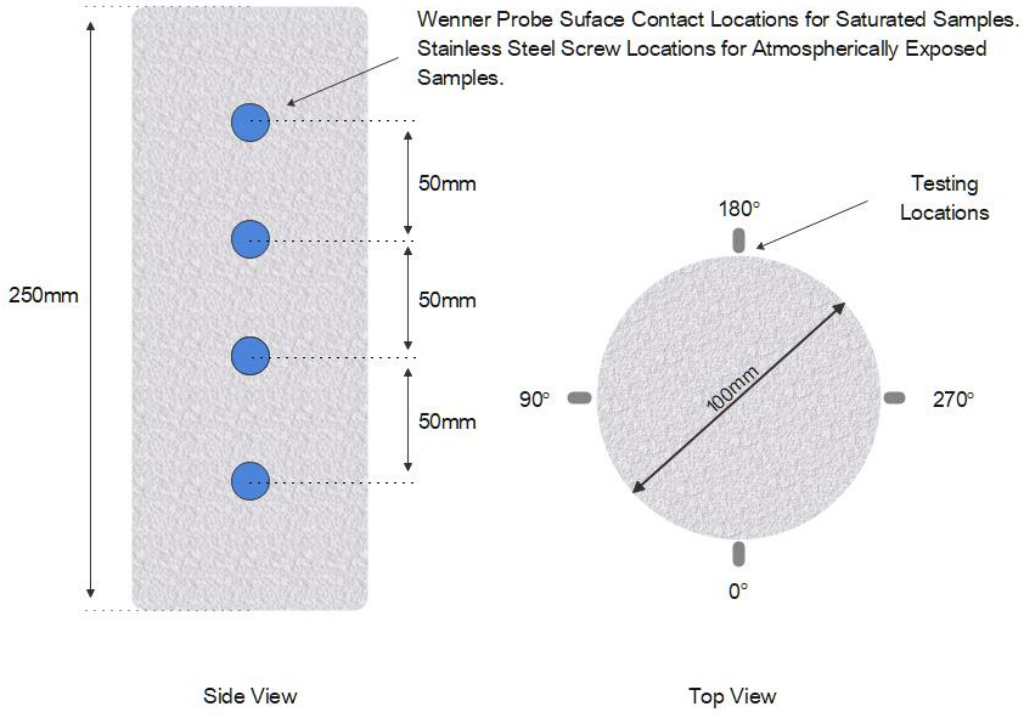

Figure 3.19 - Concrete resistivity testing sample

3.8.2 Results and Discussion

3.8.2.1 Manufacturer TDS vs Laboratory Resistivity Testing

Figure 3.20 displays the resistivity measurement data comparison between the resistivity data presented in each product technical data sheets (TDS) at 28 days and the data obtained from the laboratory conducted saturated condition experimental samples. The reported resistivity data at 28 days saturated conditions for product M and H are equivalent to the data for both products obtained in this experiment. For products L and S, the resistivity data obtained in the experiment at 28 days saturated conditions is substantially greater than the reported resistivity

data by the manufacturers TDS. A possible contributing factor for the inconsistency between the resistivity recorded in the TDS of Samples L and H is that the manufacturer testing is not reported to be performed to any recognised standard. The primary aim of this experiment is not to verify the commercial product resistivity data at 28 days but to assess the changes of the data over time.

The testing in this experiment was performed in accordance with AASHTO designation: T358-19 [1].

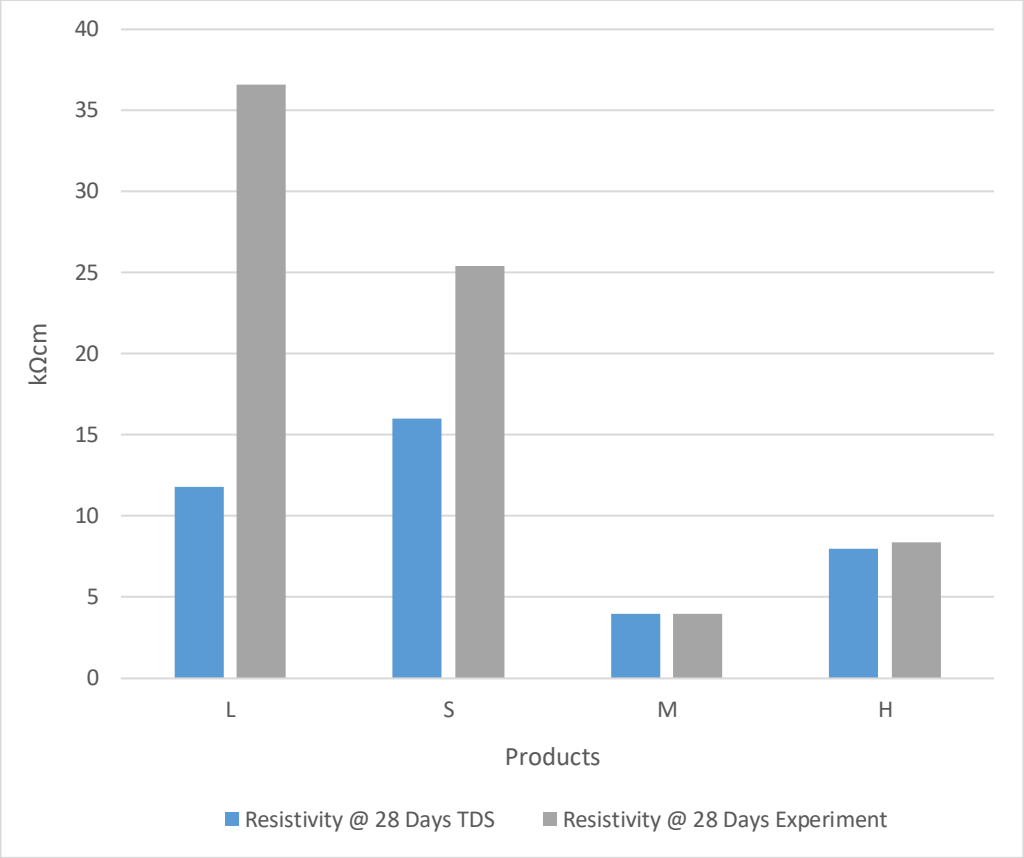

Figure 3.20 - Comparison between resistivity based on manufacturers (TDS) and resistivity based on experiment at 28 Days in saturated conditions

3.8.2.2 Long Term Resistivity Trends

Figure 3.21 and Figure 3.22 display the resistivity trends of saturated and outdoor samples between days 7 and 554 from casting. Figure 3.21 shows a trend of increasing resistivity over time for all products under saturated conditions. There is sharp increase of resistivity for products L, S and M while for product H, the resistivity increase is relatively gradual over time.

Although product M had the initial lowest resistivity value of 3 kΩcm at 7 days, long term resistivity measurements showed a sharper increase in resistivity than product H. The level of resistivity increase over time is related to the type of admixtures/polymers used in each products composition and this is outside the scope of this research. As different mixtures result in different resistivity trends, the long-term testing is necessary to provides an indication of the long-term resistivity performance of the specific product.

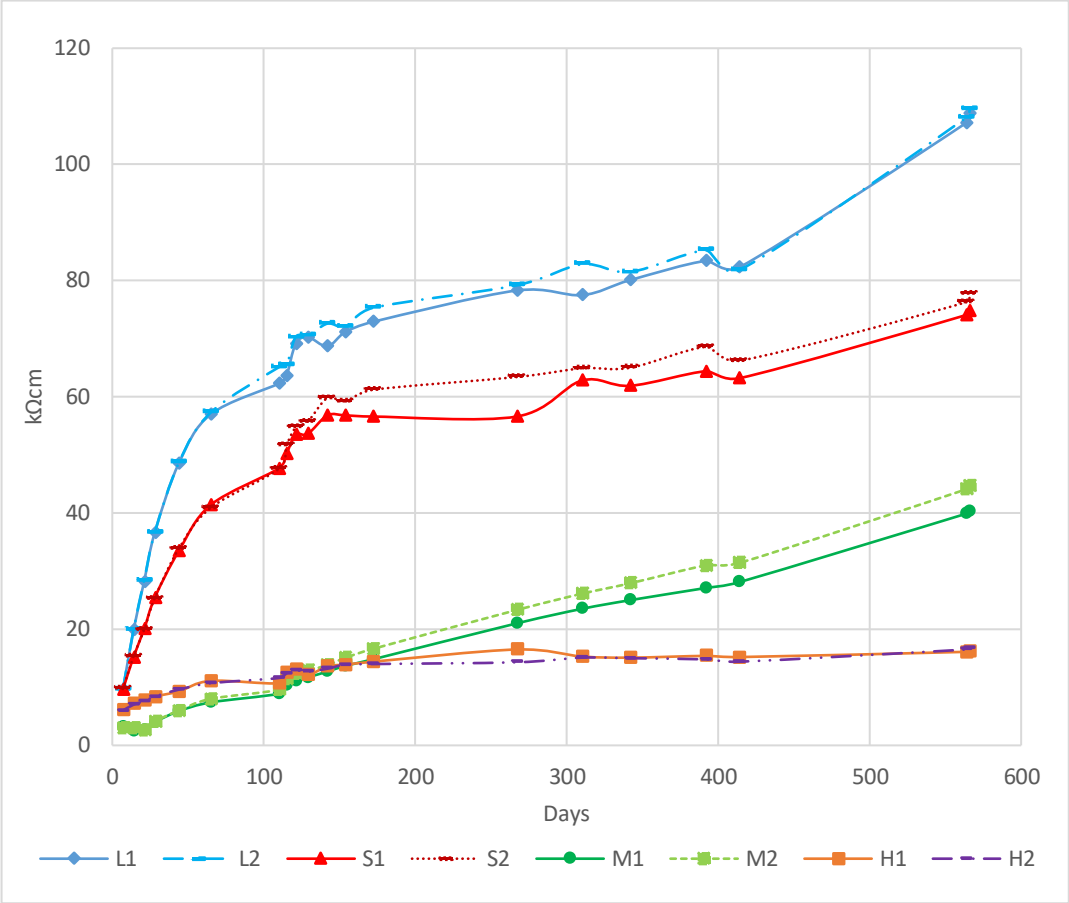

Figure 3.21 - Resistivity trend of saturated samples over 554 days

For the saturated samples between day 7 and day 28 samples L1 and L2 displayed a resistivity increase of 281%. Between day 28 and day 564, L1 resistivity increased by 197% and L2 by 199%.

Between day 7 and day 28 samples S1 and S2 displayed a resistivity increase of 164% and 160%. Between day 28 and day 564, S1 resistivity increased by 194% and S2 by 207%.

Samples L1, L2 and S1, S2 displayed the highest resistivities measured after 28 days in both saturated conditions and based on the TDS data. These samples also have the sharpest overall increase in resistivities in the first 120 days, followed by a period of increasing resistivity, but at a decreasing rate.

Between day 7 and day 28 samples M1 and M2 displayed a resistivity increase of 29% and 36%. Between day 28 and day 564, M1 resistivity increased by 905% and M2 by 987%. Samples M1 and M2 displayed an initially small increase in resistivity in the first 28 days but showed a significant linear increase following the 28-day period, for the entire duration of the testing up to day 564.

Between day 7 and day 28 samples H1 and H2 displayed a resistivity increase of 37% and 40%. Between day 28 and day 564, H1 resistivity increased by 92% and H2 by 98%.

The trends from Figure 3.21 confirm that resistivity continues to increase well after the commonly quoted 28-days.

The results indicate that the polymers used for product M and H are more effective in maintaining lower resistivity beyond the test period than products L and S. While the resistivity of product M was recorded as the lowest resistivity of the four tested products up to approximately 150 days, there was a sharp increase of resistivity for product M beyond this period while product H maintained the lowest resistivity value under saturated conditions of all four products.

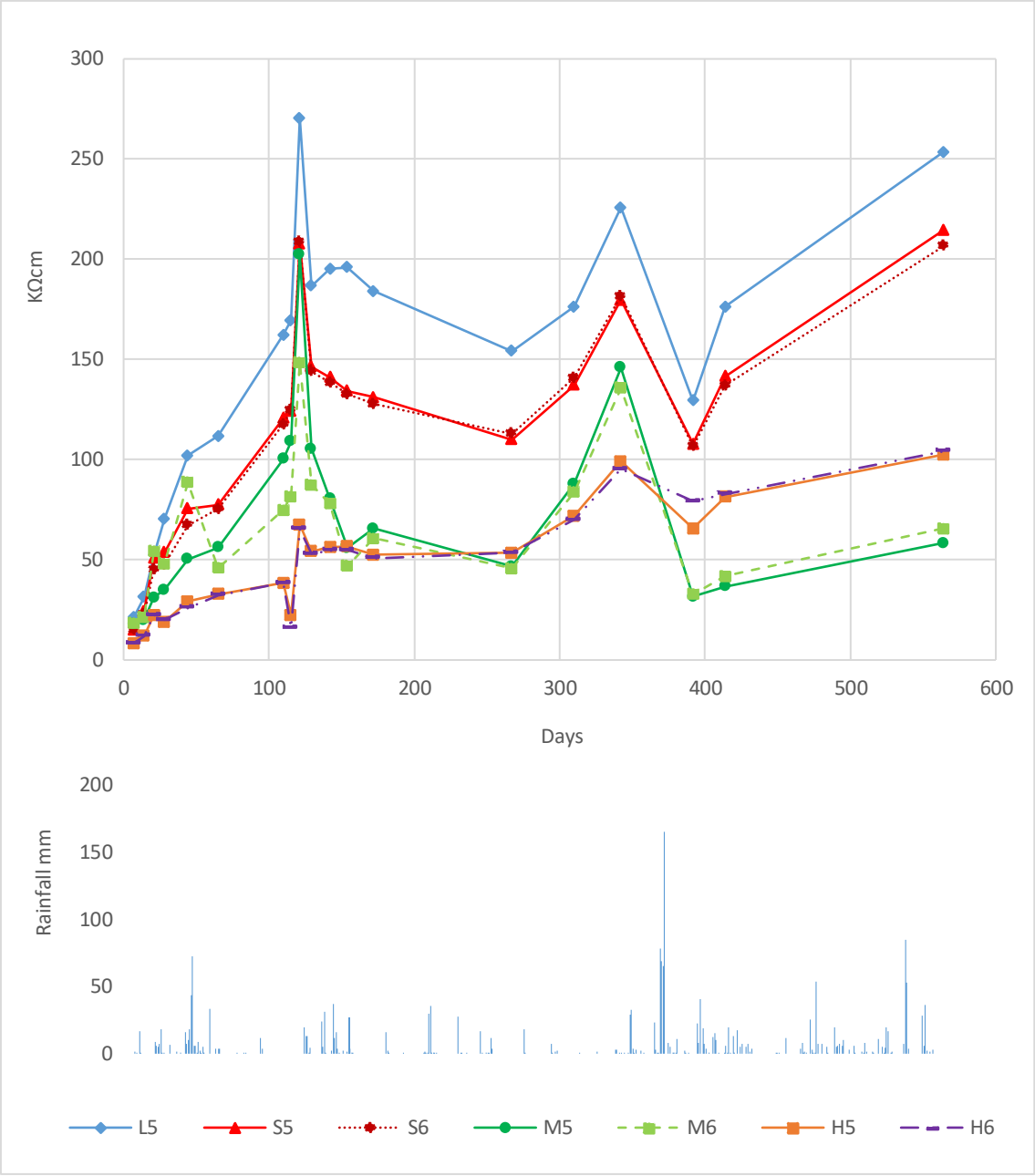

Figure 3.22 - Resistivity trend of outdoor samples over 554 days with rainfall data

Figure 3.22 displays the resistivity trend of the outdoor exposed samples over the 564-day testing period. The figure shows an overall increase in resistivity values with time with a sample range of between 16 kΩcm and 270 kΩcm after 28 days from casting. All four products followed the same trends, with fluctuations in resistivity values influenced by outdoor environmental conditions. The samples were exposed to outdoor temperature fluctuations and precipitation in Sydney, Australia. A spike in resistivity measurement is visible at day 121 and day 129. The spike

at day 121 was caused by 23 days of no rainfall at a monthly mean temperature of 22.7°C. The following testing date at day 129 was carried out after 3 consecutive days of rainfall totalling 36mm at a monthly mean of 18.6°C.

The impact of exposure conditions on the resistivity data is well documented and the fluctuation of resistivity due to rain or dry conditions is well evident in Figure 3.22. The impact of moisture content as identified in the literature review is observed when a comparison between the resistivity magnitude of all saturated samples after 554 days as displayed in Figure 3.21 and the resistivity magnitude of all outdoor samples after 554 days as displayed in Figure 3.22 is undertaken. The presented data in Figure 3.21 and Figure 3.22 confirms the substantial impact of moisture content on electrical resistivity. The electrical conductivity of the saturated samples increases with the increase of moisture content due to the level of direct liquid pore saturation of the saturated samples. Further to this, the correlation between rainfall and dry conditions in Figure 3.22 is very well illustrated in the variation of concrete resistivity in relation to rainfall and dry conditions.

The test data indicates that overall, there is correlation between the resistivity value in saturated and atmospheric conditions. The two products H and M which showed relatively lower long-term resistivity under saturated conditions showed relatively low resistivity under atmospheric conditions although not in the same order. The same applied for products L and S which showed relatively higher resistivity at saturated condition and under atmospheric conditions.

The data in Figure 3.22 shows that product H, although not having the lowest long-term resistivity, is least prone to environmental fluctuations. Product H displayed the most consistent trends during the 564-day experimental period. Sample L exhibited the highest resistivity values.

Two samples of each composition were tested in each exposure condition (only one L sample in outdoor conditions). Regardless of the exposure conditions (fully saturated or in outdoor exposure conditions) all samples in the same exposure conditions displayed consistent resistivity measurements. This indicates that the resistivity data for the samples in these experiments were consistent, accurate, and reproducible.

3.8.2.3 28-Day and 564-Day Resistivity Comparison

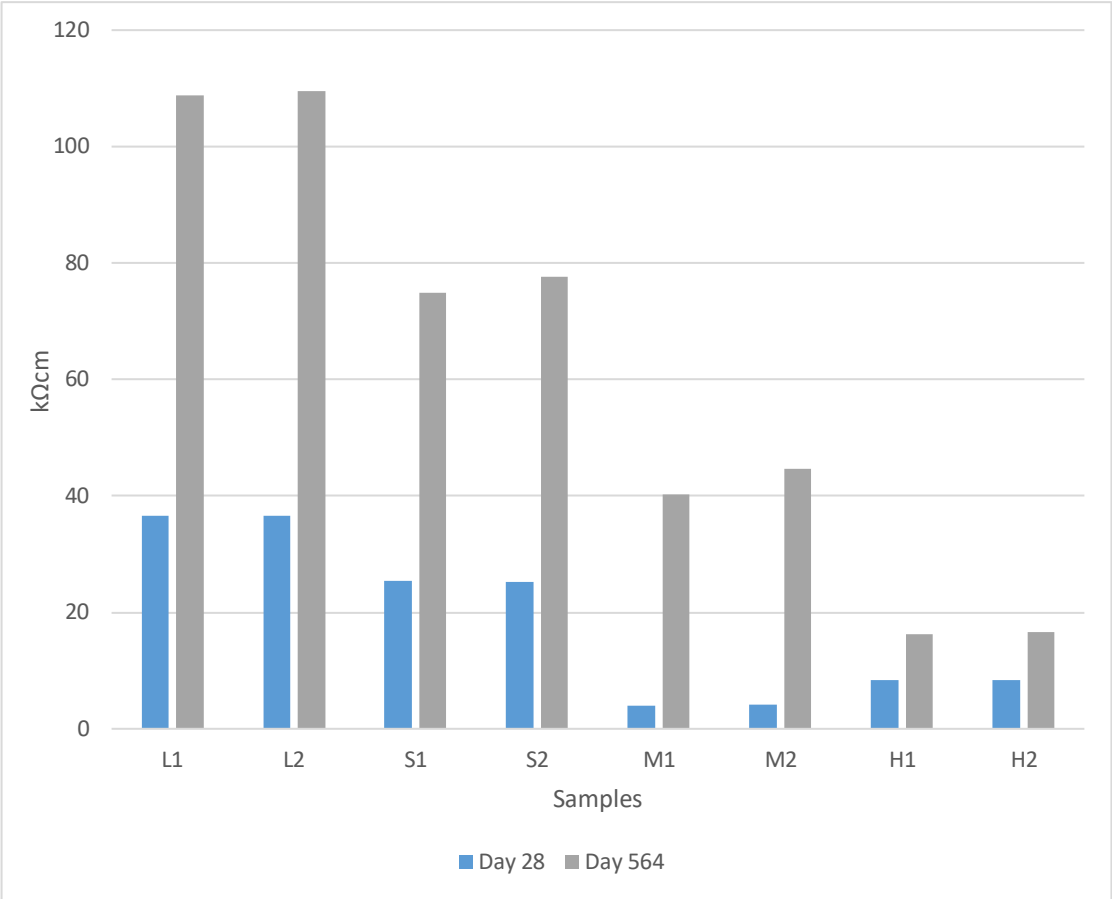

Figure 3.23 - Comparison between resistivity at 28 Days and resistivity at 564 days in saturated conditions

Figure 3.23 displays the resistivity values measured at days 28 and 564 for the water saturated samples. The graph shows a major disparity in resistivity values between the two measurement dates. The graph shows that 28-day data can be unrepresentative of the long-term resistivity values. In the case of these four products, at 28 days, product M displayed the lowest resistivity value, but when conducting long term resistivity monitoring, product H displayed the lowest long-term resistivity values.

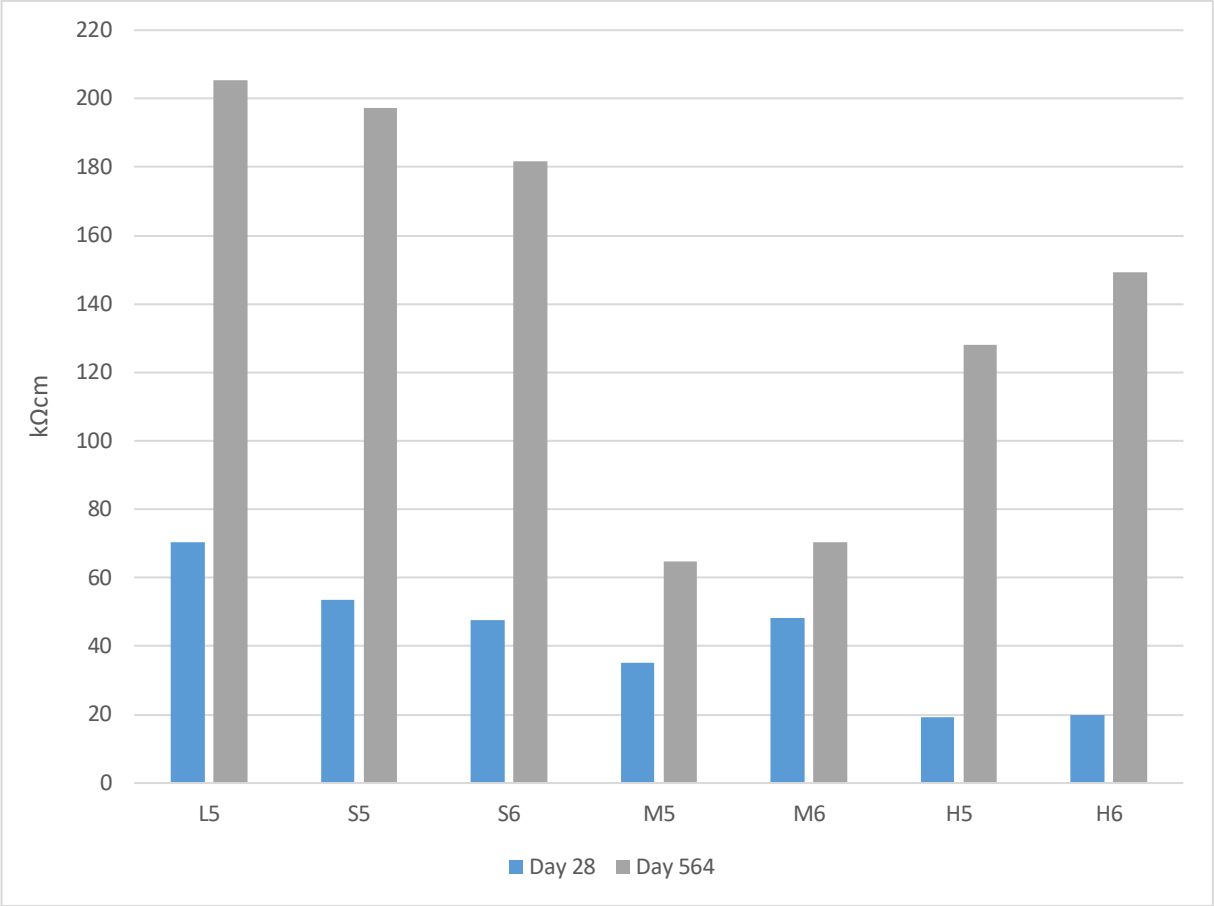

Figure 3.24 - Resistivity comparison of outdoor samples at 28 days and 564 days

Figure 3.24 displays the resistivity values measured at days 28 and 564 for the outdoor samples. Samples L and S displayed the highest overall resistivity values at 28 and 564 days. Resistivity results of products M and H in outdoor conditions were not consistent with the saturated condition data. As shown in Figure 3.24, resistivity in saturated conditions, sample H displayed the lowest resistivity out of the four products. In outdoor conditions, the resistivity measurements of sample H were significantly higher than that of product M. Consistent trends between day 28 and day 564 (Figure 3.23 and Figure 3.24) cannot be identified for products M and H. The data suggest resistivity testing in saturated conditions as per the current standards will in some cases not resemble resistivity behaviour of samples in non-saturated, outdoor conditions.

3.8.2.4 Resistivity Comparison of Saturated and Outdoor Exposed Samples

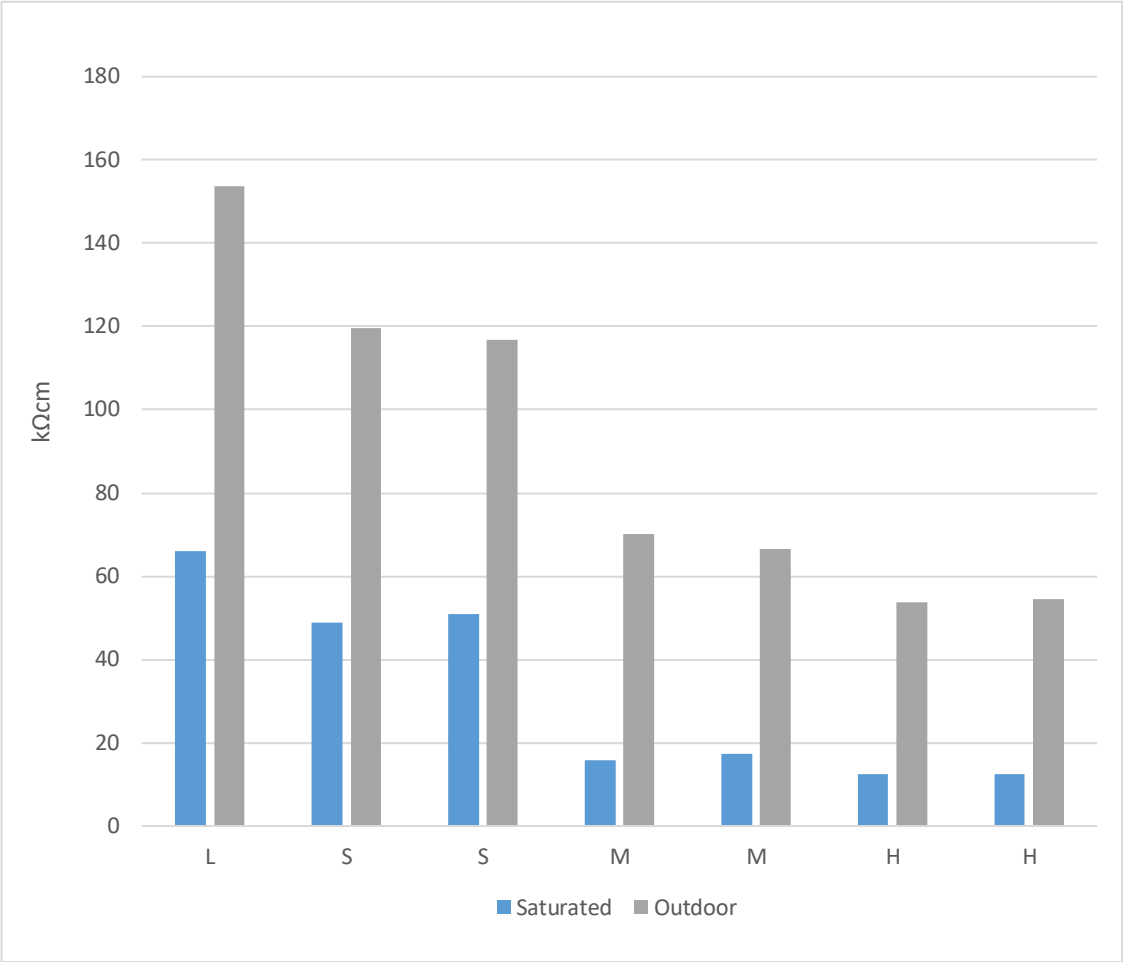

Figure 3.25 - Averaged resistivity of outdoor and saturated samples

Figure 3.25 shows the resistivity values between days 7 and 564 averaged and divided by the number of measurement periods. Product L displayed a 138% resistivity increase, product S, a 137% resistivity increase, product M a 312% resistivity increase and product H, a 335% resistivity increase between saturated and outdoor conditions. When averaging out the total resistivity value of each product, a consistent trend can be observed. Products which displayed the highest resistivity values continued to exhibit the highest outdoor condition values with all products resistivities performing in the same high to low positions. Figure 3.25 highlights a large discrepancy between resistivity measurements conducted using the current standards with samples measured in saturated conditions compared to samples measured in outdoor conditions which is the actual environment exposure conditions.

3.8.2.5 Discussion

Resistivity trends were found to substantially vary with time and between products. The resistivity of the four tested repair mortars increased over time under both saturated and outdoor conditions. Data showed a major difference between resistivity values at 28 days and at 564 days for all products in saturated and outdoor exposure conditions. Based on this experiment, the 28-day resistivity data typically reported in manufacturer technical data sheets is not indicative of the true resistivity of the material under the same conditions over the longer test period of 564 days.

The experiment in outdoor condition reflects the influence of weather condition (temperature, humidity, and direct rain exposure) on concrete resistivity, however, it also confirmed that the overall resistivity trend is toward resistivity increase over time. For outdoor condition, and as expected, the resistivity increase is higher in comparison to saturated conditions.

The average resistivity of the four tested products in saturated conditions was 18.6 kΩcm at 28 days and 61 kΩcm at 564 days. The average resistivity increase in saturated conditions between 28 days and 564 days is 227.9%.

The average resistivity of the four tested products in outdoor conditions was 41.9 kΩcm at 28 days and 142.4 kΩcm at 564 days. The average resistivity increase in saturated conditions between 28 days and 564 days is 239.8%.

The average resistivity of the four tested products in outdoor conditions at 28 days indicates a resistivity increase of 125% in comparison to saturated conditions.

The average resistivity of the four tested products in outdoor conditions at 564 days indicates a resistivity increase of 142.4% in comparison to saturated conditions.

3.8.3 Conclusion

The following observations and conclusions can be drawn from this experimental research:

- Manufacturers in most cases are not noting the methodology for resistivity testing. Inconsistencies with two of the four products were identified during a comparison between the resistivity data presented in each product technical data sheet (TDS) at 28 days and the data obtained from the laboratory conducted saturated condition

experimental samples. Products L and S displayed substantially greater than reported resistivity data than the manufacturers TDS. Manufacturers need to specify the method of resistivity testing utilised.

- Based on the resistivity trend increase of all four products, it is likely that the resistivity will continue to increase beyond the 564 days period. The resistivity mortar data should be tested and reported over an extended period of time up until there is no further increase of resistivity under saturated and outdoor conditions.

- The experiment confirms that the 28-resistivity data of polymer modified repair mortar in saturated conditions is substantially lower than the long-term mortar resistivity under both saturated and atmospheric conditions. 28-day resistivity measurements in saturated conditions cannot be considered as the actual long-term resistivity of the mortar under outdoor conditions.

- Resistivity measurements in outdoor exposure conditions were consistently higher than those in saturated condition. The resistivity measurement under saturated conditions based on the current resistivity standards [1] [49] which measure samples in saturated conditions will not be representative of real exposure condition and would not be applicable for structures located in atmospheric outdoor conditions.

- The test results indicate that the type of admixtures and polymers added to the mortar influences the magnitude of resistivity increase. The increase of concrete resistivity for products M and H was substantially lower than for products S and L.

- The experiment results indicate that the suitability of the use of polymer modified repair mortars in conjunction with electrochemical protection systems must be further investigated. The use of low resistivity mortars in conjunction with galvanic anode systems is essential for system functionality and corrosion protection current delivery. In the absence of any polymer modified mortar with reliable long term low resistivity, the use of cementitious material with no added polymers should be considered to

encapsulate the galvanic anodes within the patch repair areas up until a low resistivity mortar is developed and can be used for the repair work including anode encapsulation.

3.9 Conclusion

Chapter 3 comprised of 4 experiments, all of which provided the necessary foundation required for the following chapters.

Experiment 1 tested samples with different admixture variations to achieve different levels of resistivity. The data gathered in this experiment provided a mixture composition guide to design concrete mixtures for use in laboratory resistivity experiments. Experiment 1 also identified two areas requiring further research.

The first being that a consistent sample specification regarding dimension size and shape is required to provide a consistent and replicable method of concrete resistivity measurements and uniformity between experiments.

The second involved the method of resistivity measurement. In Experiment 1, variations in concrete resistivity readings were found to increase with increasing resistivity. Based on observations, four-point resistivity measurement variations increased over time and with increasing sample resistivity. At higher resistivities, the application of water on the surface was essential to measuring resistivity, and the amount of water and time after surface wetting was found to greatly affect resistivity values.

Building upon the findings in Experiment 1, Experiment 2 involved the adoption of a new concrete test sample design in accordance with AASHTO T358-19 [1] (in order to standardise the following experiments) and also confirmed that surface wetting/temporary water saturation had a substantial impact on resistivity values. Experiment 2 identified that the current Wenner Probe testing Standard AASHTO T358-19 [1] which is based on testing under saturated conditions was found to greatly alter resistivity values. Experiment 2 concluded that in order to test samples located in dry atmospheric conditions, an alternative method of testing must be developed in order to obtain accurate resistivity readings and eliminate the effect of water saturation on the resistivity measurements.

Based on the findings in Experiment 2, Experiment 3 trialled a new method of measuring concrete resistivity in atmospheric conditions, without the need for surface wetting or water

saturation. Experiment 3 identified that water immersion of dry concrete greatly altered resistivity measurements, with concrete samples displaying a resistivity measurement decrease of over 80% between dry conditions and after 72-hours of water immersion. By using temporary embedded steel probes, it was possible to eliminate the need for any surface moisture alteration or concrete sample immersion, which would otherwise introduce additional variations. In addition, the method proposed in Experiment 3 was shown to provide quick, accurate and repeatable resistivity data, a method which can be carried out not only in laboratories, but also on-site and using the widely adopted and available concrete Wenner probe equipment without the need for any additional specialised equipment.

Experiment 4 utilised the laboratory findings in Experiments 2 and 3 to test concrete repair mortars used in the field for commercial applications. Experiment 4 identified that in practice manufacturers of concrete repair mortars are not specifying the methodology of resistivity testing, resulting in inconsistencies between stated product resistivities and the measurements carried out in the laboratory. In addition, a comparison between the impact of exposure conditions between laboratory and atmospheric outdoor environments was carried out. Resistivity measurements in outdoor exposure conditions were found to be consistently higher than those in saturated conditions. The resistivity measurement under saturated conditions based on the current resistivity Standard [1] (which measures samples in saturated conditions) was found not to be representative of real exposure conditions and would not be applicable for structures located in atmospheric outdoor conditions.

In summary, the experiments in Chapter 3 resulted in the identification of major deficiencies with the current methods of concrete resistivity testings (experiment 1 and 2), developed and trialled a new method of concrete resistivity testing utilizing stainless steel probes (Experiment 3) and confirmed the results with data utilizing real commercial concrete repair products. This Chapter provides the foundation to achieve accurate and representative resistivity measurements in the following chapters.

4 Effect of Concrete Resistivity and Anode to Cathode Spacing on the Current Output of Impressed Current Cathodic Protection Systems

The aim of this chapter is to assess the impact of concrete resistivity and spacing between the anode and the embedded rebar on the circuit voltage of impressed current cathodic protection systems. For cathodic protection in reinforced concrete structures in accordance with AS2832.5 – 2008 (R2018) [2], voltage levels applied to bare titanium conductors should be limited to 9V DC in chloride-contaminated concrete. The European Standard [3] ISO 12696 – 2016 further decreases this limit stating:

"Uncoated titanium conductor strips used to connect activated titanium anodes and also various discrete anodes may be at risk of corroding by pitting in chloride environments if operated at in excess of approximately 8V metal/electrolyte potential".

Circuit voltage impacts on the ability of a cathodic protection system to deliver sufficient current to achieve corrosion protection in accordance with the applicable standards. Due to the voltage limitation, high circuit voltage impacts on the amount of current that can be delivered for corrosion protection. No concrete resistivity data is available in the current applicable standards [2] [3] [4], data which is critical for the design and operation of corrosion protection systems. In addition, the current standards do not provide any information related to the impact of spacing between the anode and rebar in a structure where high concrete resistivity could affect the CP system performance.

4.1 Research Background

Chloride-induced corrosion of embedded reinforcement in concrete structures is the major cause of concrete spalling and deterioration for structures in the marine environment. The ingress of chloride to the level of reinforcement through diffusion or through concrete cracking may result in corrosion initiation of the embedded rebar and concrete spalling. In most cases, the corrosion of reinforcement may impact on the structural integrity and the serviceability of

the structure. The rehabilitation process for chloride-induced corrosion affected structures generally includes concrete repair in conjunction with cathodic protection systems such as galvanic anode or impressed current cathodic protection. Both galvanic and impressed current cathodic protection applications require the ability of the anode to impress sufficient cathodic protection current through the concrete to the embedded rebar. The purpose of which is to stop the corrosion process and/or to improve the corrosion resistance of reinforcement based on the applicable standards. This is one of the key considerations in the system selection process.

The design, installation and monitoring of corrosion protection systems for reinforced concrete structures is covered by various local and international standards such as Australian Standard AS2832.5 – 2008 (R2018) [2], European International Standard ISO 12696 – 2016 [3] or NACE (US) Standard SP0290 – 2007 [4].

In AS2832.5 – 2008 (R2018) [2], concrete resistivity testing is required as part of the cathodic protection system design and/or during the selection of the concrete repair materials. However, there is no information related to the input of concrete resistivity values in the design of impressed current cathodic protection or galvanic anode systems. The standard outlines an acceptable resistivity value of the repair mortar in comparison to the resistivity of the original concrete:

"Overlay application may be combined with concrete repair. In such cases, the long-term electrical resistivity of concrete repair materials shall be within the range 50% to 150% of the parent concrete electrical resistivity. The resistivity of anode overlays may exceed 200% of parent concrete electrical resistivity subject to it being a maximum of 1000 Ω.m at ambient conditions and subject to the anode within the overlay being able to pass its design current at the design voltage". [2]

The experiments in this chapter aim to assess three main aspects: to assess the impact of concrete resistivity on the operation of cathodic protection systems; to study the impact of spacing between the anode and embedded reinforcement on the operation of cathodic protection systems; and to assess whether closer spacing of the anode to the reinforcement may allow corrosion protection systems to operate at a higher resistivity.

Two experiments were carried out as part of this chapter:

1. The impact of concrete resistivity and spacing between anode and rebar on the cathodic protection current delivery for ICCP applications.

2. The effect of concrete resistivity on the ongoing application of ICCP and the effect of anode placement

4.2 Experiment 5 – The Impact of Concrete Resistivity and Spacing Between Anode and Rebar on the Cathodic Protection Current Delivery for ICCP Applications.

The objective of experiment 5 was to assess the impact of current output on reinforced concrete samples with various resistivities and at different anode-to-rebar spacing.

Four concrete samples with identical dimensions (90mm (H) x 180mm (W) x 340mm (L)) steel layout, anode layout and operating cathodic protection current density were used in this experiment. The only variable for all samples was the concrete resistivity. The samples were designed based on achieving a progressive level of resistivity increases from low to high between the three selected testing sessions.

For each of the samples, the cathodic protection current was calculated based on the steel surface area. A current of 2mA for each sample circuit (two circuits per samples – 30mm and 60mm circuits) was used. The current was calculated based on current density of 20mA/m² of steel surface area for each sample.

The duration of each testing session was 60 minutes to allow for the voltage to stabilise. The testing sessions were carried out at 8-day intervals to allow for an increase of concrete resistivity during the experiment. The circuit voltage was monitored at 5-second intervals during the 60-minute test period.

In order to determine accurate concrete resistivity for each of the four samples, cylindrical samples (100mm diameter and 200mm height) using the same concrete mix of each of the four samples were cast and the resistivity was measured in accordance to AASHTO Designation: T358-19 [1]. The primary reason for using the cylinder for resistivity testing of the concrete instead of using the concrete block was to eliminate the influence of embedded rebar on the concrete resistivity value.

4.2.1 Materials and Method

Four test sample composition mixtures were created: A, D1, G1 and H1, labelled 1-4. Table 3.2 and

Table 4.1 display the materials and mixture compositions of the samples.

Table 4.1 - Experiment 5 sample mixture by weight %

Mixture Composite		Material Composition by weight %					
		GP Cement	Fly Ash	Silica Sand	Silica Fume	Denka Sigma	Water
Mixture	A	41%	-	41%	-	-	18%
	D1	25%	16%	41%	-	-	18%
	G1	14%	32%	31%	5%	-	18%
	H1	14%	37%	26%	-	5%	18%

Sample compositions were determined based on the experiment data in Chapter 3. For each sample, a forced action mixer was used to mix the material composites at a slow speed. With the mixer in operation, the material composites and water were progressively added. Mixing was carried out for 5 minutes for each sample until a fully homogeneous mortar was obtained. The mixed mortar was cast into a concrete block with pre-installed rebar and ribbon anodes and into a cylinder for the purpose of performing concrete resistivity testing.

The dimensions of the concrete block for each sample were 90mm (H) x 180mm (W) x 340mm (L). The anode used for the experiment was activated titanium expanded mesh ribbon anode for cathodic protection in concrete. The current rating for the mesh ribbon is 5.3mA/m. The width of the ribbon anode was 20mm and the thickness was 0.9mm. The anode substrate was titanium grade 1 and the catalyst was noble Mixed Metal Oxide (MMO). Four equal lengths of 180mm of ribbon anode were installed in each concrete block sample. The total length of ribbon anode in each concrete block sample was 720mm. The cathode for each concrete block consists of eight 12mm mild steel rebar. The total length of each rebar was 450mm. The effective cathode within the concrete block under the influence of the ICCP system was 2720mm.

Eight mild steel rebar were placed at equal spacing of 20mm distance from the base of the concrete block. Two ribbon anodes were placed at 30mm spacing from the rebar and two ribbon anodes were placed at 60mm spacing from the rebar. The anodes and the rebars were held in

place using penetrations in the container formwork, and these penetrations were blocked with sealant during the mortar casting. The eight rebar were made continuous outside the concrete block. The continuity of all embedded rebar was verified by resistance measurements between all embedded rebar. The measured resistance between the rebar was less than 0.2 Ω. For each concrete sample, the first circuit was comprised of the two anodes at 30mm spacing from the rebar and the second circuit comprised of the two anodes at 60mm spacing from the rebar. 30 and 60mm anode-to-rebar spacing was selected to provide sufficient variation in spacing while minimising the concrete samples' size and weight. Diagrams of the samples are displayed in Figure 4.1. Figure 4.2 displays a photo of the samples used in Experiment 5.

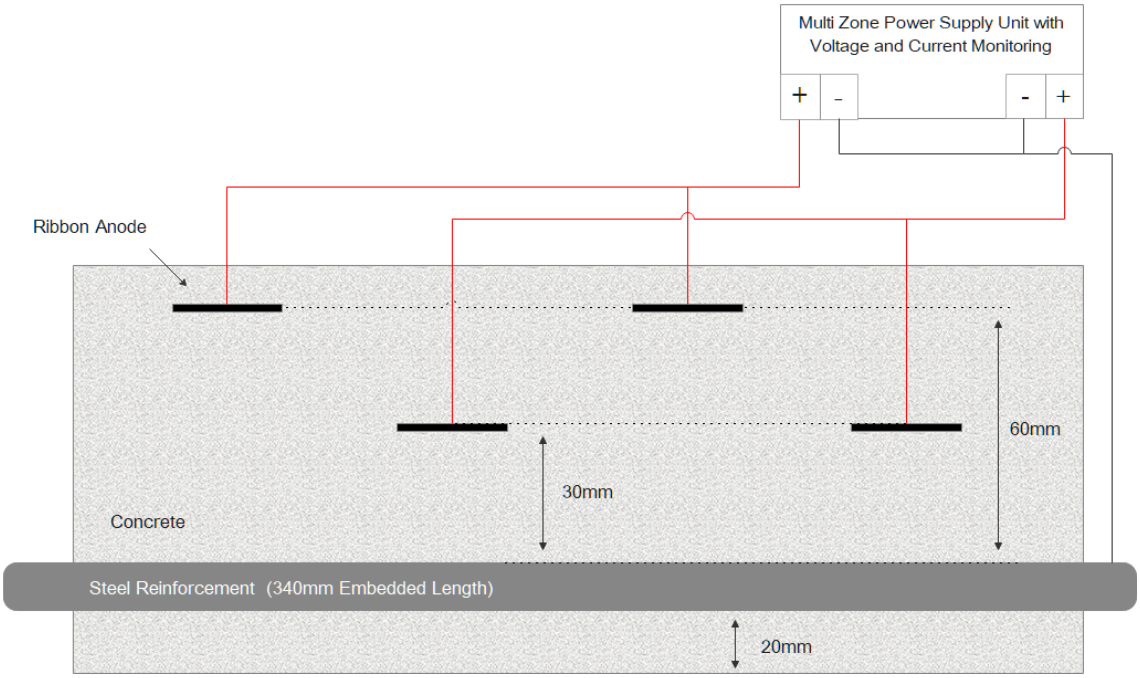

(A)

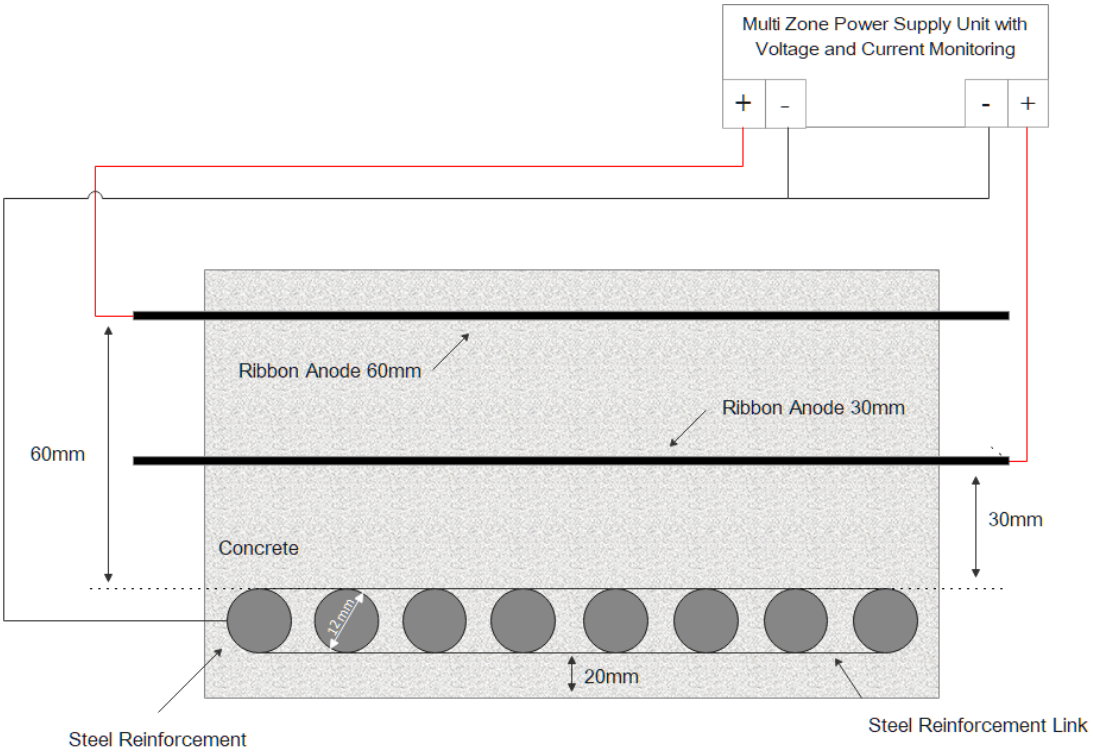

(B)

Figure 4.1 - Experiment 5 - (A) Sample design side view, (B) Sample design front view

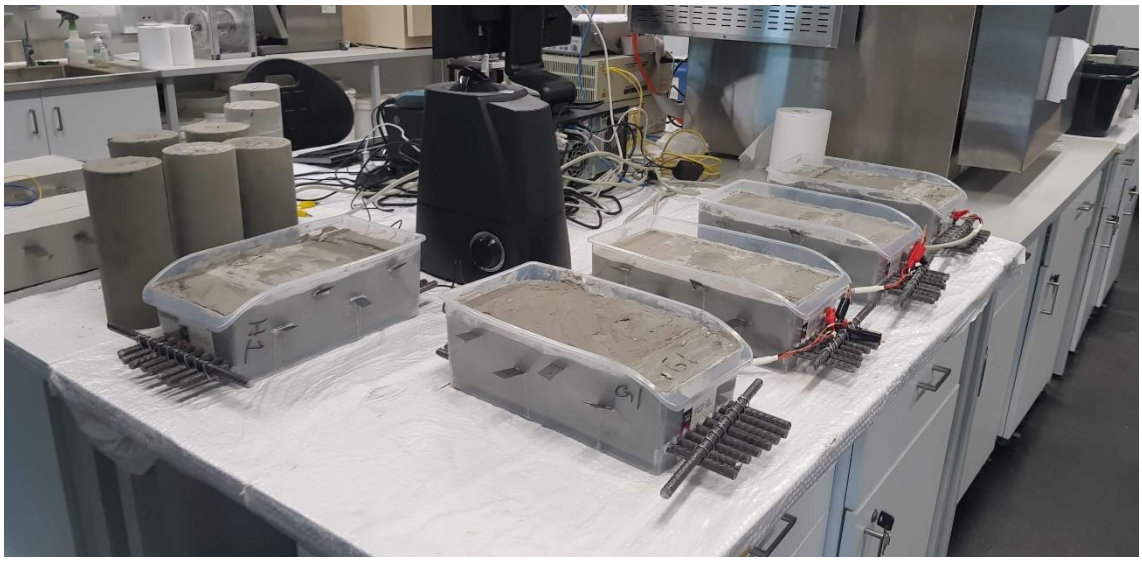

Figure 4.2 - Photo of Experiment 5 Samples

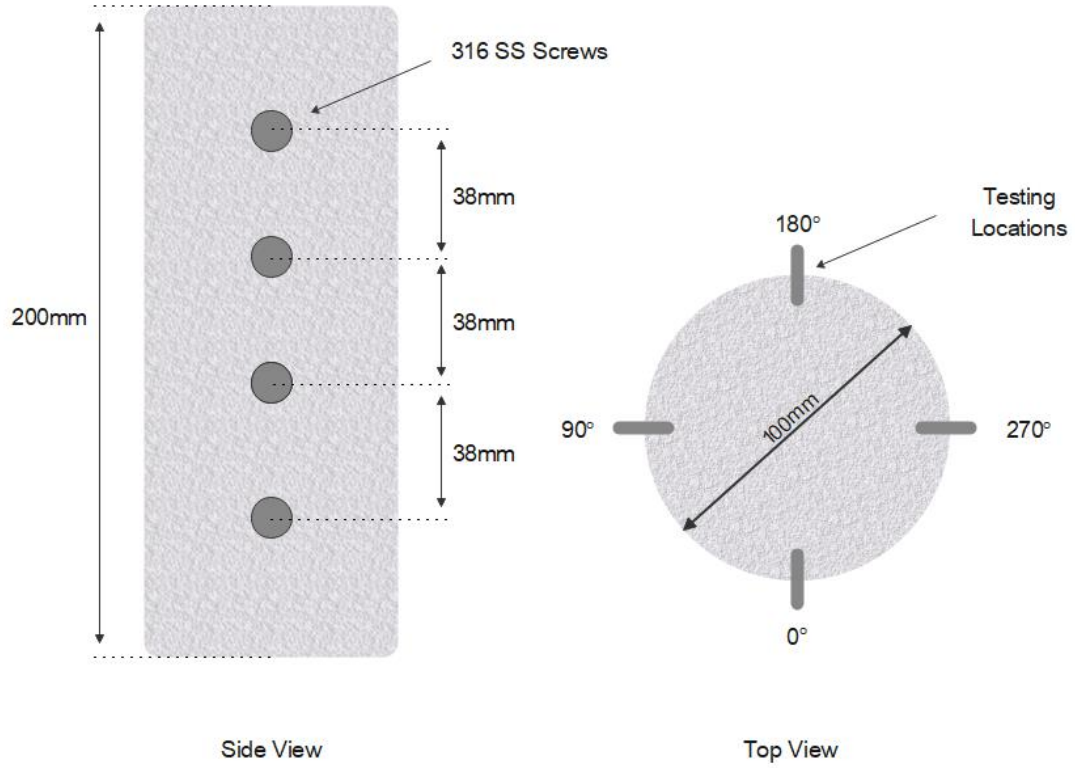

Figure 4.3 - Experiment 5 - Resistivity measurement cylinder

In conjunction with the four concrete test samples, four cylinders with 100mm diameter and 200mm height were cast for resistivity testing. The cylinders were formed in polyvinyl chloride (PVC) piping and the base of each cylinder was sealed using 100mm cap. A diagram of the cylinder is displayed in Figure 4.3.

All concrete samples were cast at the same time. All samples were left to cure in their PVC casts for 24 hours at room temperature (23 ± 1°C and a humidity of 55 ± 10%). The samples were then removed from their PVC cast and stored in the laboratory. The samples were kept at a room temperature of 23 ± 1°C and a humidity of 55 ± 10%. As 3 testing sessions (60 minutes each) were carried out in this experiment, samples were stored for 20 days prior to the testing to allow for the resistivity of the concrete to increase to a level where the different samples had sufficiently varied resistivities. The same curing and exposure conditions applied for all samples used in this experiment. Resistivity measurements were carried out in accordance with the methodology in Experiment 3 using 38mm stainless steel probe spacing in a 4-pin Wenner probe array. The measurement process included taking eight readings from four locations around the samples at 0°, 90 ° ,180 ° and 270 ° and calculating the average resistivity. Resipod (Wenner Probe) set to measurement mode: surface measurement; contact spacing: default; geometric

correction factor: Flat. Resistivity measurements were carried out using no correction (K) value as per Section 4.4 of AASHTO Designation: T358-19 [1].

Table 4.2 displays the current density calculation used in this experiment.

Table 4.2 - ICCP design current calculation

Steel Bars	Bar Length (m)	Bar Radius (m)
8	0.340	0.006
$A = 2\pi * 0.006 * 0.340 * 8$ = 0.1025m^2 0.1025 m^2 steel surface area Design current for ICCP 20mA/m^2 $20\text{mA}/m^2 \ * \ 0.1025m^2 \ = \ 2.05\text{mA}$		

A total of 8 power supply units were used for cathodic protection current delivery in this experiment. For each concrete block, two separate power supply units were used to provide CP current for each of the two circuits. All power supply units were operated in constant current mode, delivering 2mA to each circuit for the 60 minutes test duration. Following impressing the cathodic protection current for each sample for 60 minutes, the system was switched off until the next test date to allow depolarisation of the embedded rebar and an increase of the concrete sample resistivities. Testing of the samples was carried out during three testing sessions. The testing sessions were at eight-day intervals; at 28 days, 36 days and at 44 days after the casting of the samples.

4.2.2 Results and Discussion

Figure 4.4, Figure 4.5, Figure 4.6 and Figure 4.7 display the voltage data of each sample after switching on the ICCP current for each circuit and the data plotted over the 60-minute testing period.

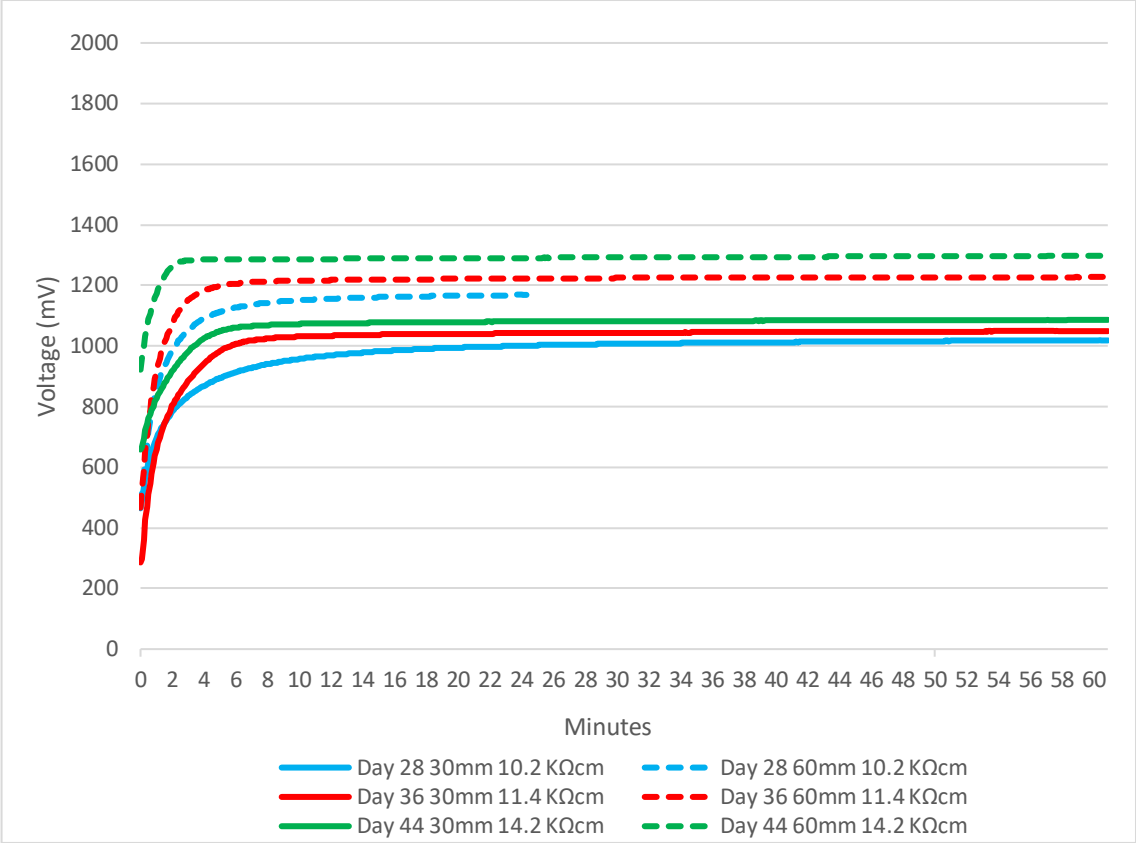

Figure 4.4 - Sample A start up ICCP voltage

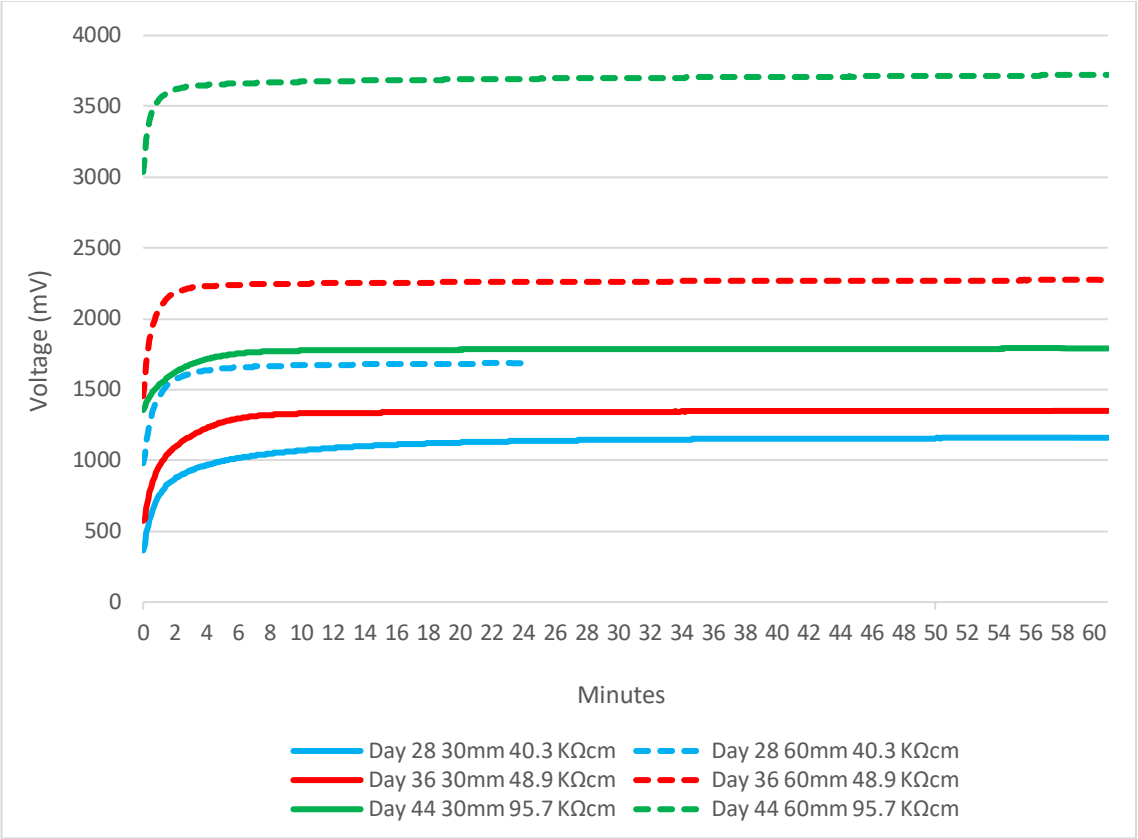

Figure 4.5 - Sample D1 start up ICCP voltage

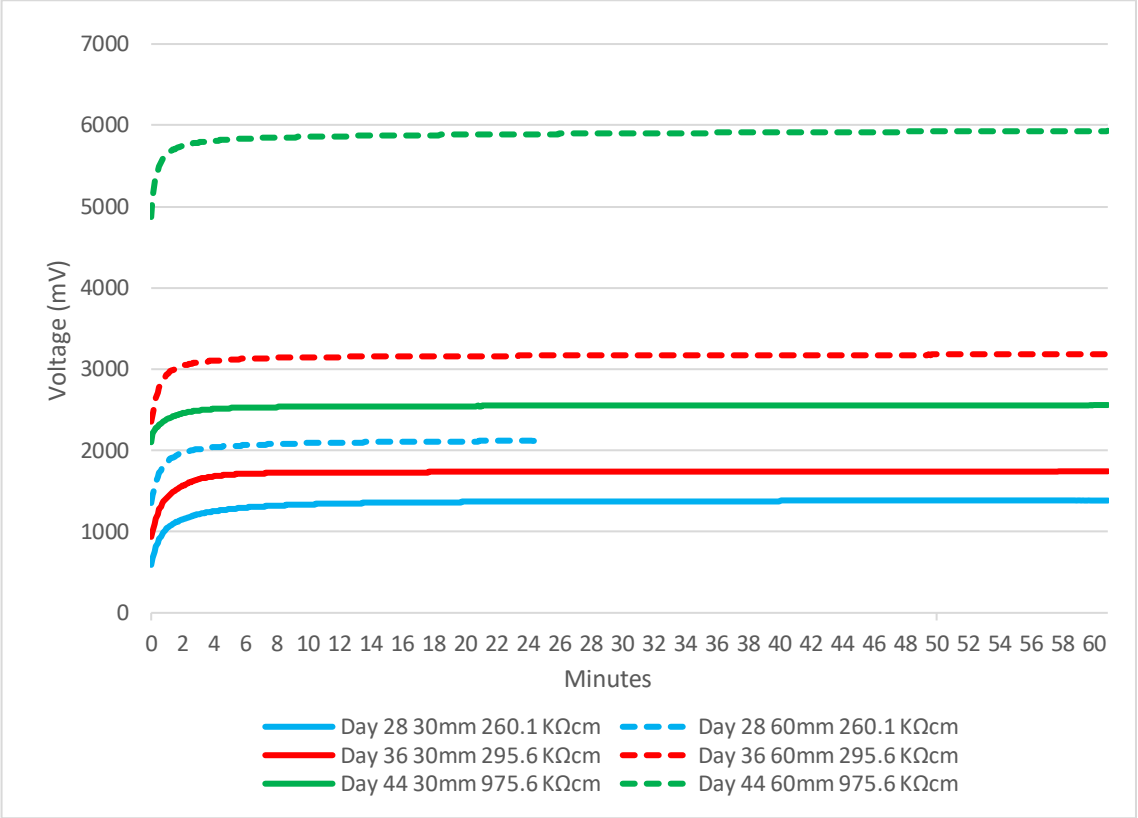

Figure 4.6 - Sample G1 start up ICCP voltage

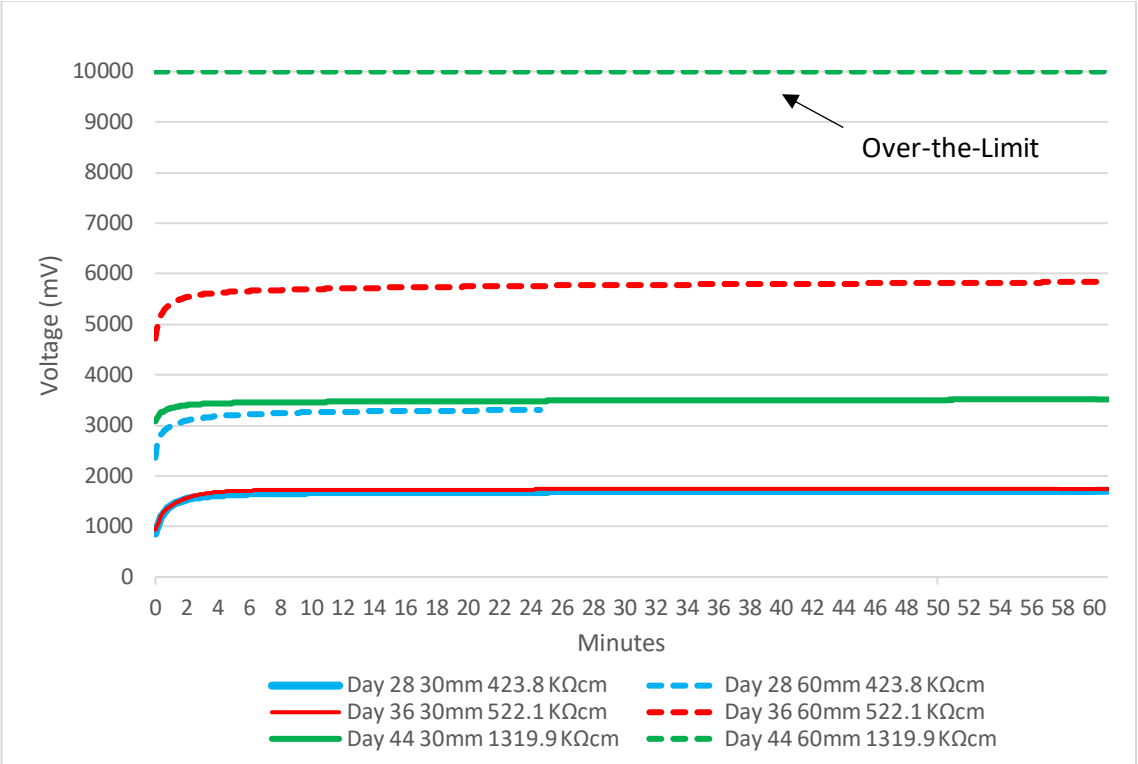

Figure 4.7 - Sample H1 start up ICCP voltage

The data from Figure 4.4, Figure 4.5, Figure 4.6, and Figure 4.7 identifies an initial voltage increase which is visible for all samples tested at both 30mm and 60mm spacing, regardless of mixture compositions and resistivity values. This was not recorded for Sample H1 Day 44 at 60 mm due to the circuit reaching the maximum voltage set limit of the power supply unit. Polarisation of the circuits ranged between 0.38 and 0.97 volts with an average value of 0.68 volts calculated among all samples between the time of system start-up and 10-minute voltage readings.

The graphical data displays the voltage spike in the initial two minutes from the ICCP system being switched ON. Following this initial spike in voltage, all circuit voltages continued to increase up to the recorded 60-minutes experiments during the three testing sessions. An average increase of 0.037 volts was identified between the 10-minute and 60-minute testing period. There was no clear relationship between the initial voltage spike and concrete resistivity.

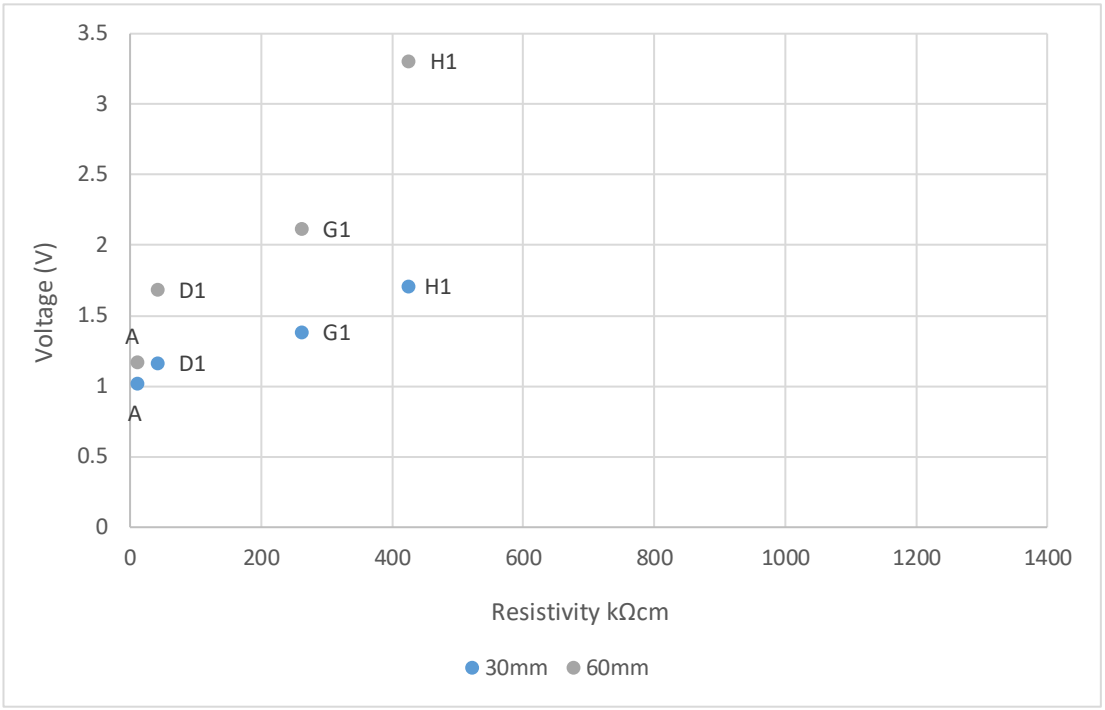

Figure 4.8 - Test 1 Day 28, ICCP voltage at different concrete resistivity values at 60 minutes from start up

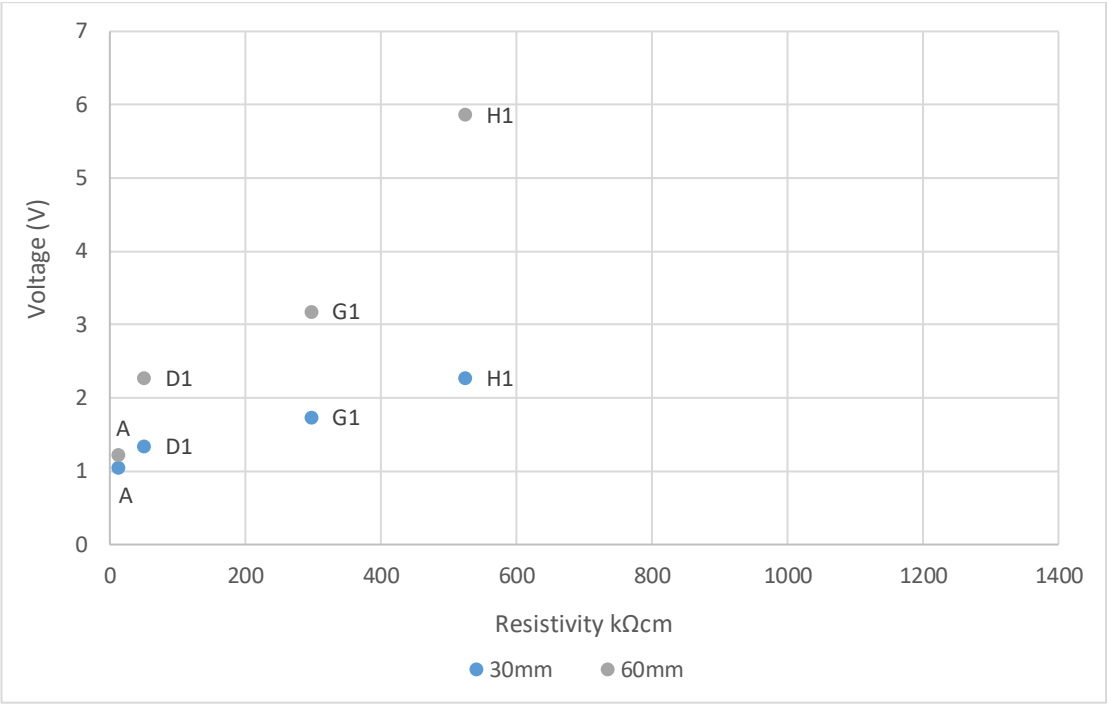

Figure 4.9 - Test 2 Day 36, ICCP voltage at different concrete resistivity values at 60 minutes from start up

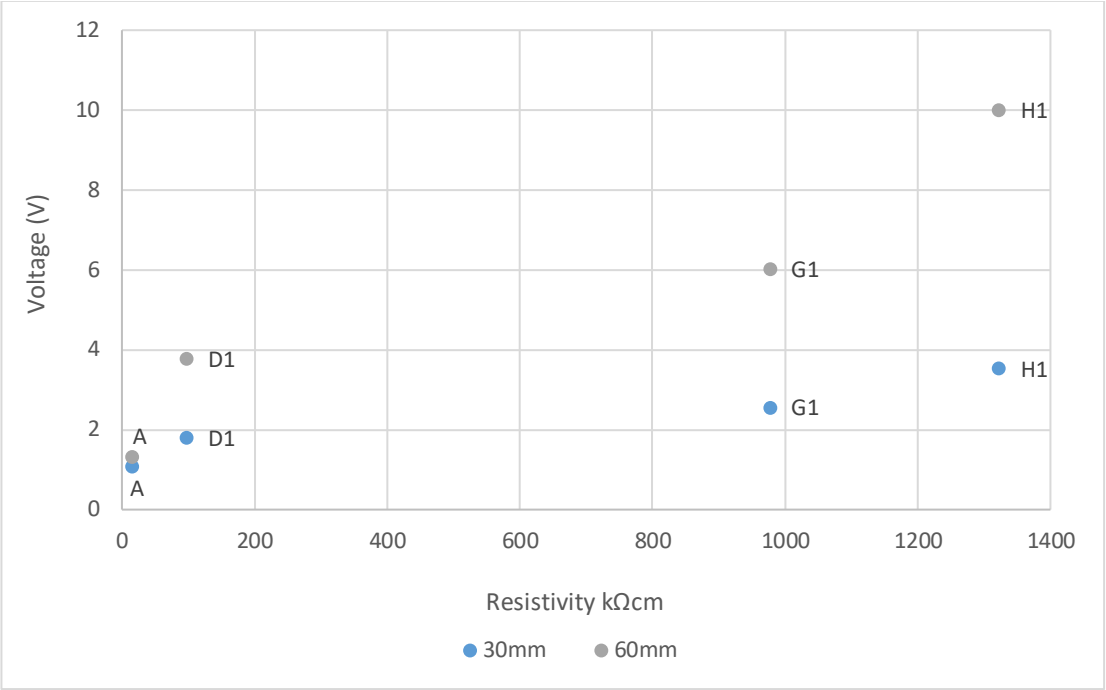

Figure 4.10 - Test 3 Day 44, ICCP voltage at different concrete resistivity values at 60 minutes from start up

Figure 4.8, Figure 4.9, Figure 4.10 display the ICCP voltage at different concrete resistivity values after 60 minutes of current.

For test 1 (at day 28), the resistivity values of the four samples were recorded at 10.2 kΩcm 40.4 kΩcm, 260.1 kΩcm and 423.8 kΩcm.

For test 2 (at day 36), the resistivity values of the four samples were recorded at 11.4 kΩcm 48.9 kΩcm, 295.6 kΩcm and 522.1 kΩcm.

For test 3 (at day 44), the resistivity values of the four samples were recorded at 14.2 kΩcm 95.7 kΩcm, 975.6 kΩcm and 1319.9 kΩcm.

Based on the above data, it can be concluded that regardless of the anode-to-rebar spacing, the circuit voltage increased progressively with the increase of resistivity value for each test. This confirms the correlation between the mortar resistivity value and circuit voltage. The higher the resistivity of the mortar (smaller capillary pore size), the higher the circuit voltage required is to impress the same amount of current.

The circuit voltage at each resistivity value was measured at 30mm and 60mm anode-to-rebar spacing. The data from the experiment indicates that for all measurements at day 26, day 36

and day 44 at 60mm anode-to-rebar spacing, the circuit voltage is greater than the circuit voltage at 30mm anode-to-rebar spacing. This confirms the effect of anode-to-rebar spacing on the circuit voltage for mortar at various resistivities.

This experiment indicates that for the same concrete resistivity value, the circuit voltage is lower (current output is higher) when the anode is located closer to the rebar. While the impact of anode spacing is relatively negligible for low concrete resistivity, this impact is considerable at high concrete resistivity values.

The resistivity and voltage data from the samples is presented in Table 4.3. Voltage measurements displayed in Table 4.3 were taken at the 60-minute mark of each test.

Table 4.3 - Experiment 5 resistivity, voltage, and percentage change data

Day	Sample	Resistivity	30mm anode-to-steel spacing	60mm anode-to-steel spacing	Change	
		kΩcm	Volts	Volts	Volts	%
Test 1 (Day 28)	A	10.2	1.0212	1.1687	0.1475	14.44
	D1	40.3	1.1625	1.6858	0.5233	45.01
	G1	260.1	1.3839	2.1161	0.7322	52.90
	H1	423.8	1.7100	3.3029	1.5929	93.15
Test 2 (Day 36)	A	11.4	1.0509	1.2301	0.1792	17.05
	D1	48.9	1.3516	2.2780	0.9264	68.54
	G1	295.6	1.7441	3.1876	1.4435	82.76
	H1	522.1	2.2805	5.8692	3.5887	157.36
Test 3 (Day 44)	A	14.2	1.0856	1.3113	0.2257	20.79
	D1	95.7	1.7912	3.7760	1.9848	110.80
	G1	975.6	2.5607	6.0119	3.4512	134.77
	H1	1319.9	3.5249	10.0012	6.4763	183.73

Based on the data presented in Table 4.3; At a concrete resistivity value of 10.2 kΩcm, the increase of the circuit voltage limit at 60mm anode-to-rebar spacing is 14.44% greater than at 30mm anode-to-rebar spacing. At a concrete resistivity value of 1319.9 kΩcm, the increase of the circuit voltage limit at 60mm anode-to-rebar spacing is 183.73% greater than at 30mm anode-to-rebar spacing.

Based on the test data in the case of high resistivity concrete, an increase in current output can be obtained by decreasing the anode-to-rebar spacing. Placing the anodes closer to the rebar

may impact on the current distribution of the impressed current cathodic protection system and may necessitate system designs based on greater anode current density to achieve corrosion protection. This effect on current distribution is outside the scope of this research.

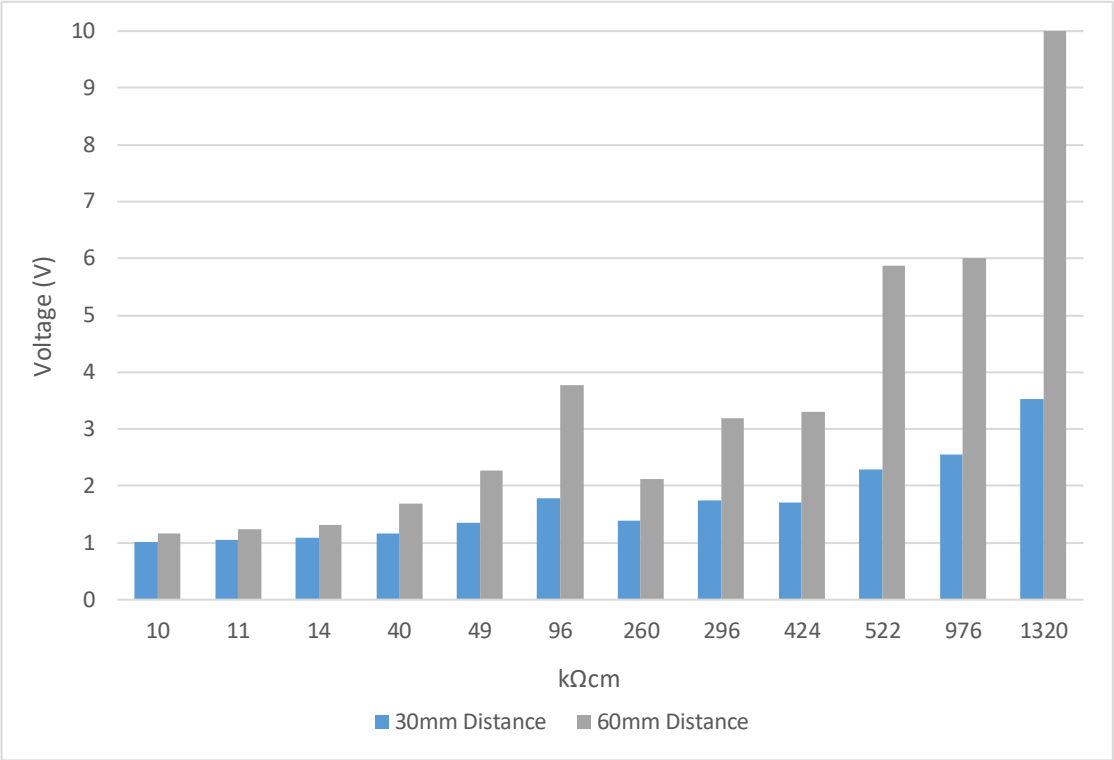

Figure 4.11 - ICCP energisation voltage vs resistivity results

Figure 4.11 displays the correlation between circuit voltage, resistivity and anode-to-rebar spacing. The impact of spacing increases with the increase of concrete resistivity.

The data indicates that in high resistivity concrete, the location of the anode can be adjusted to achieve a lower output voltage and consequently higher cathodic protection current. This is due to the decrease in resistance brought upon a shorter path of ionic flow between the anode and rebar. Ohm's law states that the current flowing through a conductor is directly proportional to the circuit resistance. For impressed current cathodic protection in concrete, the current flowing from the anode to the rebar through the electrolyte (concrete) is proportional to the concrete resistivity. By placing the anode closer to the rebar there is a shorter current path between the anode and the rebar lowering the circuit resistance. Based on ohms law, by lowering the circuit resistance (R) and applying the same current (I), the circuit voltage (V) is lower. In practice, anode to steel spacing is determined by the structure in which the CP is being installed. For concrete

structures, anode installation can be grouped into two categories. The first is for cathodic prevention, where anodes are installed during construction of new structures. The second is for cathodic protection, where anodes are installed in existing structures.

Cathodic prevention is a system commonly installed on structures which require extended design service life. During construction, anodes are installed as close to the reinforcement as possible, in most cases tied to the reinforcement (spacing of only 10mm) with a plastic spacer. The spacer is used to isolate the anode from the steel in order to stop short circuits. As the anode installation is carried out to exposed reinforcement prior to any concrete, additional anodes can be easily installed to increase current distribution.

In new structures and particularly in structures where extended design service life is required (where cathodic prevention systems are commonly installed), high performance concrete is used due to its advantages in durability, strength, and workability. High performance concrete includes admixtures such as fly ash, silica fume, slag and other chemical admixtures resulting in high concrete resistivity. Fortunately, as the anode is installed very close to the steel in cathodic prevention systems, no notable issues regarding voltage limits have been identified in the literature. The data in this experiment supports the concept that anodes can operate in high resistivity concrete when anode to steel spacing is decreased. For the highest resistivity measurement in this experiment (1320 kΩcm), the installation of the anode at 30mm instead of 60mm, would result in the reduction of operating circuit voltage by 183.73% from 10 volts to 3.5 volts, well below the maximum voltage limit for CP systems operation. Based on this finding, it can be assumed that further decreases in anode spacing, such as those used in cathodic prevention (10mm) will allow for systems to perform at low voltages in high resistivity concrete.

Cathodic protection involves the installation of anodes to existing concrete structures, commonly decades after the structure's construction. Unlike cathodic prevention system installations, constructability of a CP system is constrained to the existing structure's design and characteristics. Some notable design considerations include the concrete cover to reinforcement, design of reinforcement and the concrete resistivity. Installation is significantly more complex than that of a cathodic prevention system, as the installation of anodes for existing concrete structures requires labour intensive destructive cut slots (for ribbon anodes) or cores (for discrete-cylindrical) anodes to be carried out. The labour-intensive nature of

retrofitting CP may impact the cost to benefit ratio in cases where concrete resistivity is high and sufficient current flow would require close anode to steel spacing.

Currently a lack of data regarding the impact of concrete resistivity and the performance of CP has resulted in structures being installed with CP which operate at a maximum 8 volts with insufficient current outputs. The data presented in Figure 4.11 can be utilised to identify a suitable anode to steel spacing at different concrete resistivities and further assess the cost to benefit ratio of installing CP.

It is important to note that the recorded circuit voltage at the measured concrete resistivity was only performed after 60 minutes of ICCP system operation. It is expected that circuit voltage increases over time, albeit at a smaller rate. The actual circuit voltage data reported for this short-term test are indicative only and presented for the purpose of establishing a correlation between resistivity values, circuit voltage and anode-to-rebar spacing and not long-term performance.

4.3 Experiment 6 - Effect of Concrete Resistivity on the Ongoing Application of Impressed Current Cathodic Protection and the Effect of Anode Placement

Experiment 5 provided initial short-term testing data related to concrete resistivity, circuit voltage and anode-to-rebar spacing. The data was obtained for a relatively short period of time (44 days). The data from experiment 5 was assessed and used for the preparation of a more detailed assessment of the correlation between concrete resistivity, circuit output and anode-to-rebar spacing over a longer period of time. Experiment 6 was performed over a 13-month duration and the anode-to-rebar spacing of 30mm and 60mm was performed in separate concrete test blocks.

The aim of this experiment is to provide correlation between concrete resistivity and system current output at 30mm and 60mm anode-to-rebar spacing over 13 months. Such correlation between anode resistivity, system current output and anode-to-rebar spacing can be an effective design tool for the design of impressed current cathodic protection systems, especially when these systems are installed in high resistivity concrete or in conjunction with polymer modified resistivity mortar where resistivity may increase over time.

4.3.1 Materials and Method

Eight reinforced concrete test samples and four concrete cylinders were used for this experiment. Concrete cylinders as per experiment 5, were used in order to obtain accurate resistivity measurements based on AASHTO Designation: T358-19 [1].

Four composition mixtures were used in this experiment: G, H, D1 and F1. Table 3.2 and Table 4.4 display the materials and mixture compositions of the samples.

Table 4.4 - Experiment 6 sample mixture by weight %

Mixture Composite		Material Composition by weight %						
		GP Cement	Ground Slag	Fly Ash	Silica Sand	Silica Fume	Denka Sigma	Water
Mixture	G	14%	32%	-	31%	5%	-	18%
	H	14%	37%	-	26%	-	5%	18%
	D1	25%	-	16%	41%	-	-	18%
	F1	14%	-	27%	41%	-	-	18%

For each sample mixture (G, H, D1 and F1), a forced action mixer was used to mix the mixture components and the water. Water was placed into the container and with the mixer in operation the material was added, and mixing was carried out for 5 minutes for each sample until a fully homogeneous mortar was obtained. For each sample mixture, the mixed mortar was cast into two concrete test blocks with pre-installed rebar and ribbon anodes, and into one cylinder for the purpose of performing resistivity testing of concrete based on the requirements of AASHTO Designation: T358-19 [1].

The dimensions of the concrete block for each sample were 90mm (H) x 110mm (W) x 170mm (L). The anode used for the experiment was activated titanium expanded mesh ribbon anode for cathodic protection in concrete. The current rating for the mesh ribbon is 5.3 mA/m. The width of the ribbon anode was 20mm and the thickness was 0.9mm. The anode substrate was titanium grade 1 and the catalyst was noble Mixed Metal Oxide (MMO). 100mm of ribbon anode were installed in each concrete block sample. Table 4.5 displays the current density calculation used in this experiment.

Table 4.5 - ICCP Design Current Calculation

Steel Bars	Bar Length (m)	Bar Radius (m)
4	0.17	0.006
$A = 2\pi * 0.006 * 0.17 * 4$ = 0.0256m^2 0.0256 m^2 steel surface area Design current for ICCP 20mA/m^2 $20\text{mA}/m^2 \ * \ 0.0256m^2 \ = \ 0.51\text{mA}$		

The cathode for each concrete block consists of four 12mm mild steel rebar. The total length of each rebar was 450mm. The effective length of the cathode within the concrete block under the influence of the ICCP system was 680mm. The four mild steel rebar were placed at equal spacing at 20mm distance from the base of the concrete block. For each sample mixture, the first block included one ribbon anode placed at 30mm spacing from the rebar and the second block included one ribbon anode placed at 60mm spacing from the rebar. The anodes and the rebars were held in place using penetration in the container formwork and these penetrations were blocked with sealant during the mortar casting. The four rebar in each block extended outside the concrete block and made continuous. The continuity of all embedded rebar was verified by resistance measurement between all embedded rebar post establishing continuity. The measured resistance between the rebar was less than 0.2Ω. Diagrams of the samples are displayed in Figure 4.12 and Figure 4.13. Figure 4.14 displays a photo of the samples used in Experiment 5.

In conjunction with the eight concrete test samples, four cylinders with 100mm diameter and 200mm height were cast for resistivity testing. The cylinders were formed in polyvinyl chloride (PVC) piping and the base of each cylinder was sealed using 100mm PVC cap. A diagram of the cylinder is displayed in Figure 4.13.

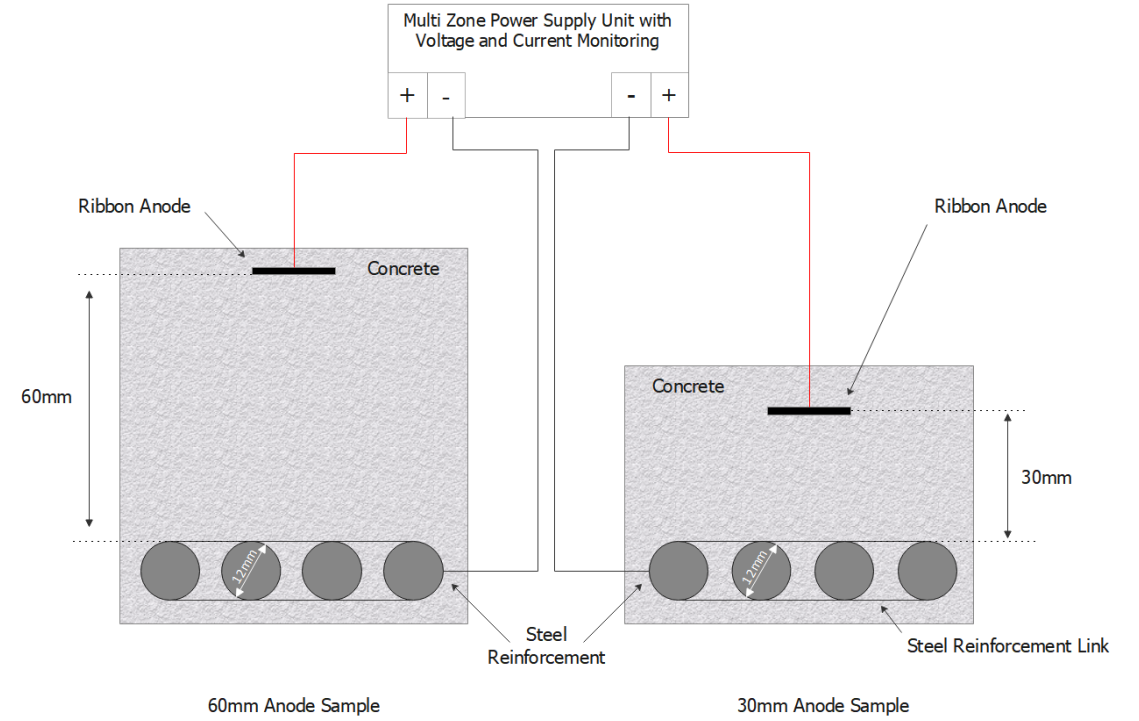
Multi Zone Power Supply Unit with Voltage and Current Monitoring
+
-
-
+
Ribbon Anode
Concrete
60mm
12mm
Steel Reinforcement
Ribbon Anode
Concrete
30mm
12mm
Steel Reinforcement Link
60mm Anode Sample
30mm Anode Sample

(A)

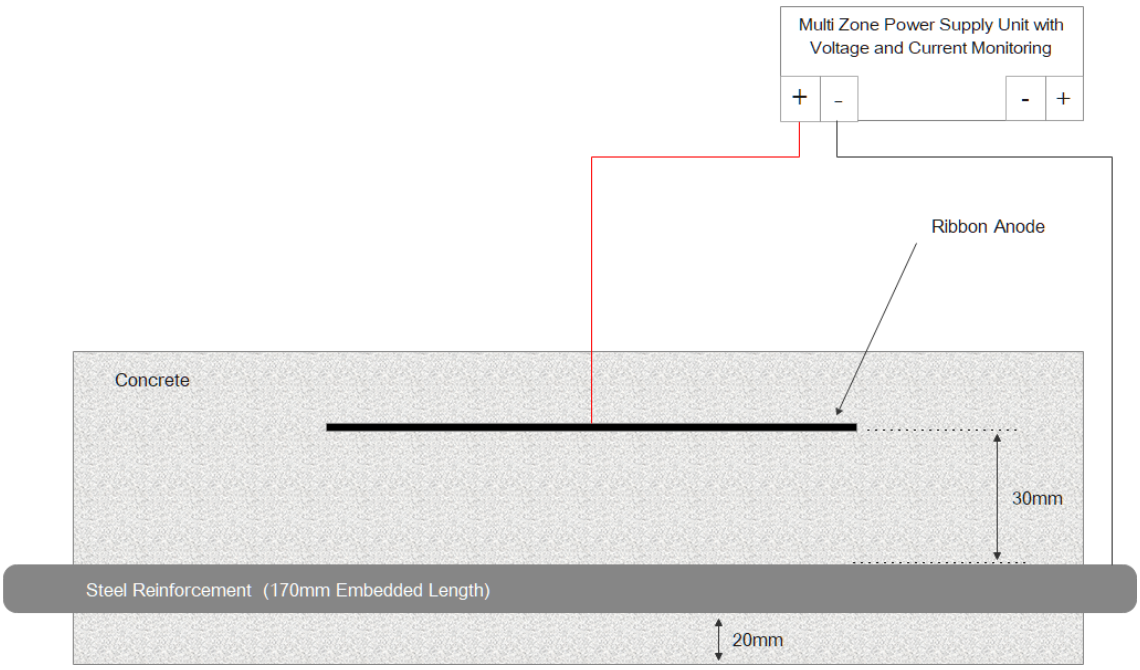
Multi Zone Power Supply Unit with Voltage and Current Monitoring
+
-
-
+
Ribbon Anode
Concrete
30mm
Steel Reinforcement (170mm Embedded Length)
20mm

(B)

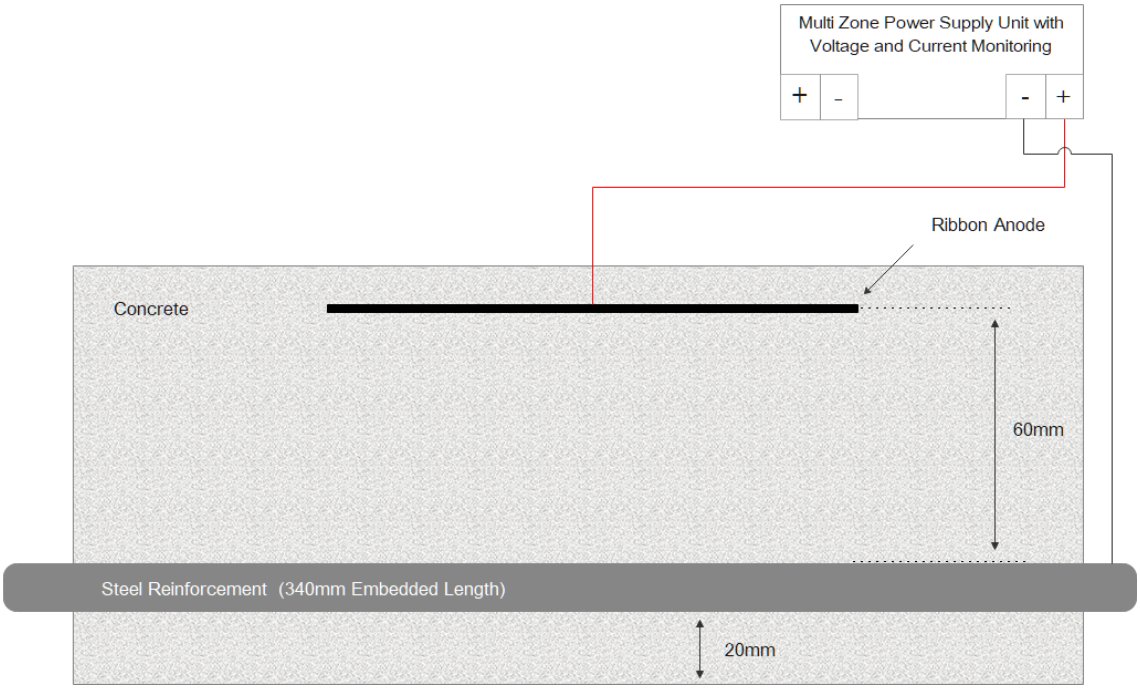

(C)

Figure 4.12 - Experiment 6 – (A) Sample design front view, (B) 30mm anode spacing side view, (C) 60mm anode spacing side view

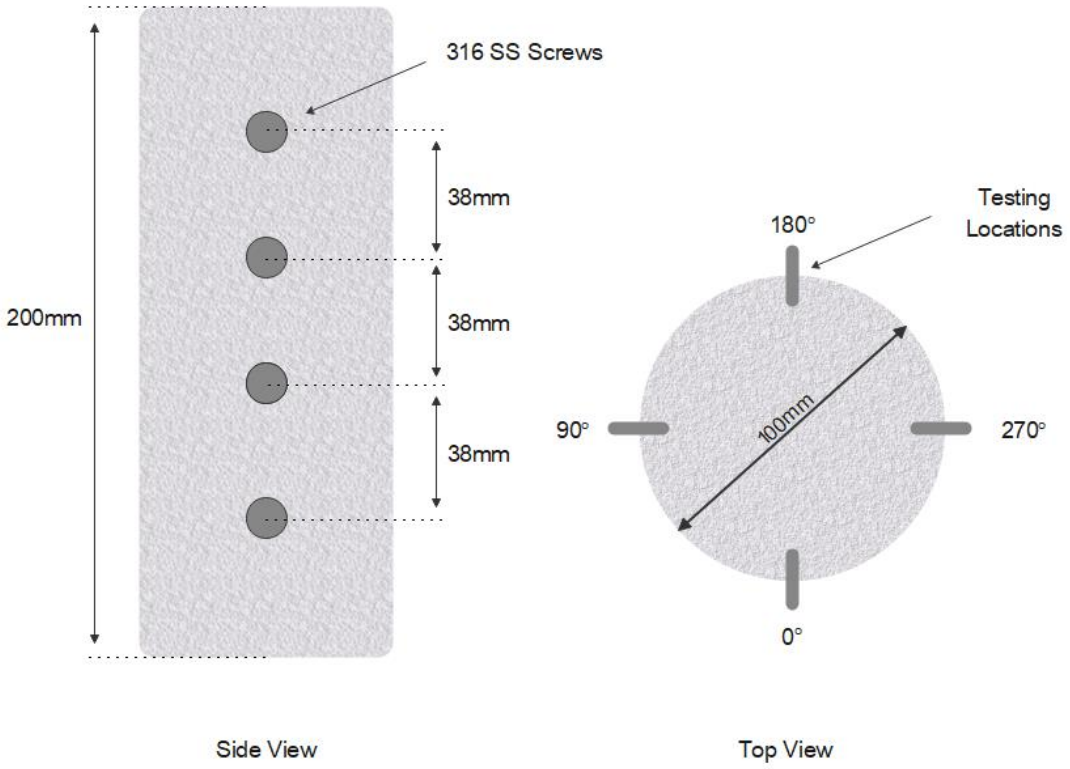

Figure 4.13 - Experiment 6 - resistivity measurement concrete sample

(A)

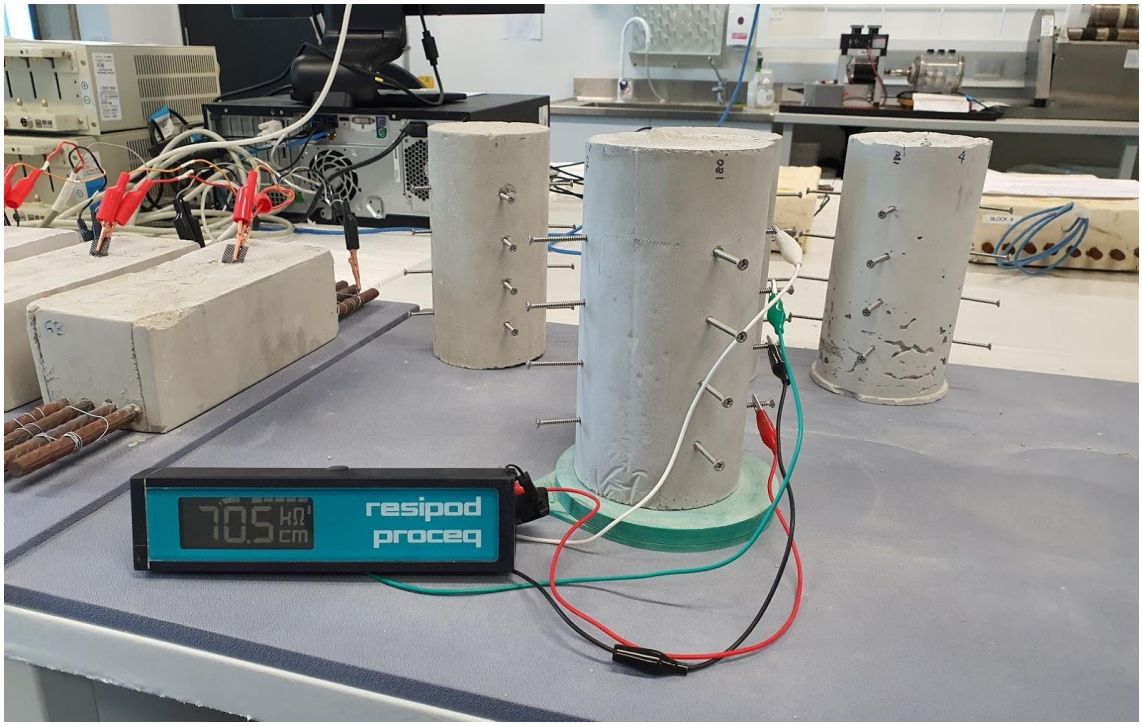

(B)

Figure 4.14 - Photo of Experiment 6 samples - (A) samples with ICCP, (B) samples for resistivity testing with resistivity meter

The same curing and exposure condition applied for all samples used in this experiment. All concrete samples were cast at the same time. All samples were left to cure for 24 hours, removed from their formwork, and stored in a laboratory at room temperature. From the date of casting, the samples were kept at a temperature of 23 ± 1^{o}C and a humidity of 55 ± 10% for 96 hours before testing commenced. Unlike Experiment 5 which consisted of 3 isolated test sessions, Experiment 6 was conducted continuously for the duration of the 384-day experiment, allowing for the experiment to commence within a shorter 96-hour timeframe once the samples were sufficiently set and the experiment setup completed.

A total of 8 power supply units were used for the cathodic protection current delivery. Cathodic protection current was ON for the full 384-day experimental duration. A total of 50 testing sessions were carried out in this experiment. For each session, the resistivity of the four sample compositions (G, H, D1 and F1) were measured and the circuit voltage/current for each of the eight circuits was recorded.

The testing was conducted in two stages. In stage 1 all power supply units were set to operate at constant current mode delivering 0.5mA for each circuit. The procedure for this test was based on changing the operating mode of each power supply unit from constant current to constant voltage once the circuit reaches the maximum set voltage limit for ICCP systems of 8 volts. While the power supplies operated in constant current mode the circuit voltage was recorded. Once the 8-volt limit was reached, stage 2 involved switching each circuits' power supply output to operate in constant voltage mode (at 8 volts), where the current output was recorded (highlighted in blue in Table 4.6). The current output measurements highlighted in blue were used to calculate the current density output. A current output of 0.5mA equates to a current density of 20mA/m^2.

4.3.2 Results and Discussion

Table 4.6 - Experiment 6 data

	G			H			D1			F1		
Day	Resistivity kΩcm	30mm Voltage (V)	60mm Voltage (V)	Resistivity kΩcm	30mm Voltage (V)	60mm Voltage (V)	Resistivity kΩcm	30mm Voltage (V)	60mm Voltage (V)	Resistivity kΩcm	30mm Voltage (V)	60mm Voltage (V)
1	15.3	1.145	1.188	15.4	1.141	1.183	6.2	0.949	1.064	12.7	1.093	1.102
5	23.0	1.332	1.454	21.1	1.349	1.468	12.1	1.088	1.302	35.4	1.645	2.652
8	29.4	1.465	1.608	24.9	1.489	1.623	17.2	1.199	1.511	56.4	2.198	4.754
13	37.9	1.651	1.849	37.3	1.682	1.882	26.2	1.402	1.894	102.7	3.467	10.000
16	42.2	1.766	2.011	36.6	1.804	2.062	33.0	1.562	2.238	142.5	4.674	0.037
20	50.1	1.906	2.202	42.1	1.956	2.285	42.2	1.762	2.693	205.3	6.499	0.018
22	54.2	1.998	2.342	45.3	2.052	2.465	48.5	1.939	3.222	245.9	0.499	0.012
26	61.2	2.152	2.560	50.2	2.219	2.746	58.4	2.219	4.252	307.5	0.329	0.013
28	64.6	2.213	2.652	53.8	2.294	2.850	63.6	2.313	4.725	345.3	0.296	0.014
33	77.7	2.413	2.922	61.5	2.496	3.172	81.6	2.684	6.457	473.0	0.211	0.012
35	78.2	2.483	3.104	61.2	2.607	3.462	84.4	2.997	9.528	513.3	0.171	0.011
37	80.8	2.569	3.202	64.3	2.698	3.566	90.0	3.090	0.347	553.0	0.164	0.012
40	87.1	2.688	3.385	68.5	2.834	3.819	98.6	3.336	0.244	630.4	0.143	0.012
42	90.7	2.811	3.604	70.4	2.971	4.201	106.5	3.764	0.135	716.4	0.115	0.011
44	94.8	2.905	3.785	72.1	3.082	4.478	113.5	4.172	0.067	794.9	0.095	0.011
47	98.7	3.083	4.092	75.9	3.271	5.071	127.5	5.068	0.024	951.9	0.068	0.011
50	99.2	3.341	4.497	77.8	3.563	5.566	134.7	5.869	0.017	1016.5	0.045	0.011
54	105.2	3.452	4.759	83.2	3.701	6.285	153.1	6.866	0.013	1304.4	0.022	0.011
56	110.2	3.537	4.945	87.7	3.827	6.641	164.0	7.429	0.012	1411.6	0.013	0.011
57	105.6	3.616	5.071	95.3	3.910	6.954	166.0	7.903	0.012	1480.6	0.011	0.011
61	119.0	3.829	5.439	95.0	4.183	7.656	186.6	0.449	0.011	1530.0	0.009	0.010
63	144.5	3.951	5.602	99.1	4.317	7.889	196.3	0.436	0.012	2000	0.009	0.011
64	141.9	3.981	5.668	104.3	4.367	7.995	199.5	0.429	0.012	2000	0.009	0.010
68	134.4	4.220	6.070	108.3	4.664	8.872	224.3	0.382	0.011	2000	0.009	0.010
70	148.5	4.442	6.429	114.2	4.927	0.401	238.9	0.347	0.010	2000	0.008	0.010
72	149.0	4.485	6.657	114.7	5.037	0.376	284.4	0.313	0.009	2000	0.008	0.011
75	155.6	4.726	7.122	119.1	5.348	0.327	273.6	0.258	0.009	2000	0.008	0.011
77	161.0	4.827	7.328	124.2	5.507	0.323	282.3	0.252	0.009	2000	0.008	0.011
79	169.2	5.082	7.757	129.4	5.823	0.294	305.1	0.227	0.009	2000	0.008	0.010
83	175.8	5.252	0.487	135.5	6.053	0.267	316.8	0.197	0.009	2000	0.008	0.011
89	187.6	5.711	0.441	143.8	6.613	0.242	366.8	0.164	0.010	2000	0.008	0.010
92	202.8	5.791	0.432	150.9	6.762	0.237	370.6	0.162	0.010	2000	0.008	0.011
99	208.2	6.177	0.401	164.9	7.269	0.223	404.4	0.153	0.011	2000	0.007	0.011
111	233.2	7.205	0.329	187.9	0.454	0.170	497.4	0.108	0.009	2000	0.008	0.010
124	283.8	7.627	0.305	216.1	0.427	0.170	544.9	0.103	0.011	2000	0.008	0.011
127	287.0	0.503	0.291	218.9	0.397	0.156	547.6	0.098	0.010	2000	0.008	0.010
135	289.9	0.476	0.275	233.8	0.372	0.143	548.4	0.098	0.010	2000	0.008	0.010
139	310.9	0.455	0.262	239.8	0.352	0.136	574.4	0.094	0.010	2000	0.008	0.011
146	326.4	0.408	0.234	254.9	0.314	0.112	647.9	0.069	0.009	2000	0.008	0.010
148	321.5	0.417	0.237	259.0	0.320	0.120	628.4	0.074	0.009	2000	0.008	0.010
153	345.9	0.388	0.221	268.4	0.296	0.104	674.1	0.058	0.009	2000	0.008	0.011
155	334.9	0.394	0.224	270.5	0.300	0.109	657.3	0.060	0.010	2000	0.009	0.011
160	364.6	0.385	0.219	283.6	0.293	0.106	651.9	0.058	0.010	2000	0.008	0.010
170	409.3	0.322	0.182	300.3	0.239	0.072	795.9	0.020	0.009	2000	0.008	0.011
176	428.5	0.330	0.186	316.3	0.245	0.080	774.0	0.021	0.009	2000	0.008	0.011
183	434.2	0.308	0.174	330.4	0.226	0.069	809.4	0.017	0.009	2000	0.007	0.011
189	486.4	0.293	0.163	339.4	0.217	0.061	844.1	0.014	0.009	2000	0.007	0.011
272	660.0	0.218	0.125	472.5	0.159	0.040	940.1	0.019	0.009	2000	0.008	0.011
294	706.6	0.201	0.116	504.6	0.144	0.035	1003.5	0.016	0.011	2000	0.009	0.011
384	1022.5	0.088	0.064	727.0	0.070	0.012	1255.9	0.010	0.009	2000	0.008	0.011

The data from this experiment is presented in Table 4.6. The resistivity for sample G ranges from 15.3 kΩcm at day 1 testing to 1022.5 kΩcm at test day 384. The resistivity for sample H ranges from 15.4 kΩcm at day 1 testing to 727 kΩcm at test day 384. The resistivity for sample D1 ranges from 6.2 kΩcm at day 1 testing to 1255.9 kΩcm at test day 384. The resistivity for sample F1 ranges from 12.7 kΩcm at day 1 testing to 2000 kΩcm at test day 63.

Figure 4.15 displays the resistivity increase of each of the four samples over time. While similar increasing trends were observed for all four samples, for sample F1 the maximum resistivity of 2000 kΩcm (limit of resistivity measurement equipment) was reached at day 63. Although outside the scope of this research, based on the composition of the samples, fly ash had a significant impact on concrete resistivity. Higher levels of fly ash in samples F1 (28%) when compared to sample D1 (16%) significantly increased the speed of the resistivity increase. This observation suggests that in cases where new grouts are being developed for CP, the use of fly ash significantly increases resistivity.

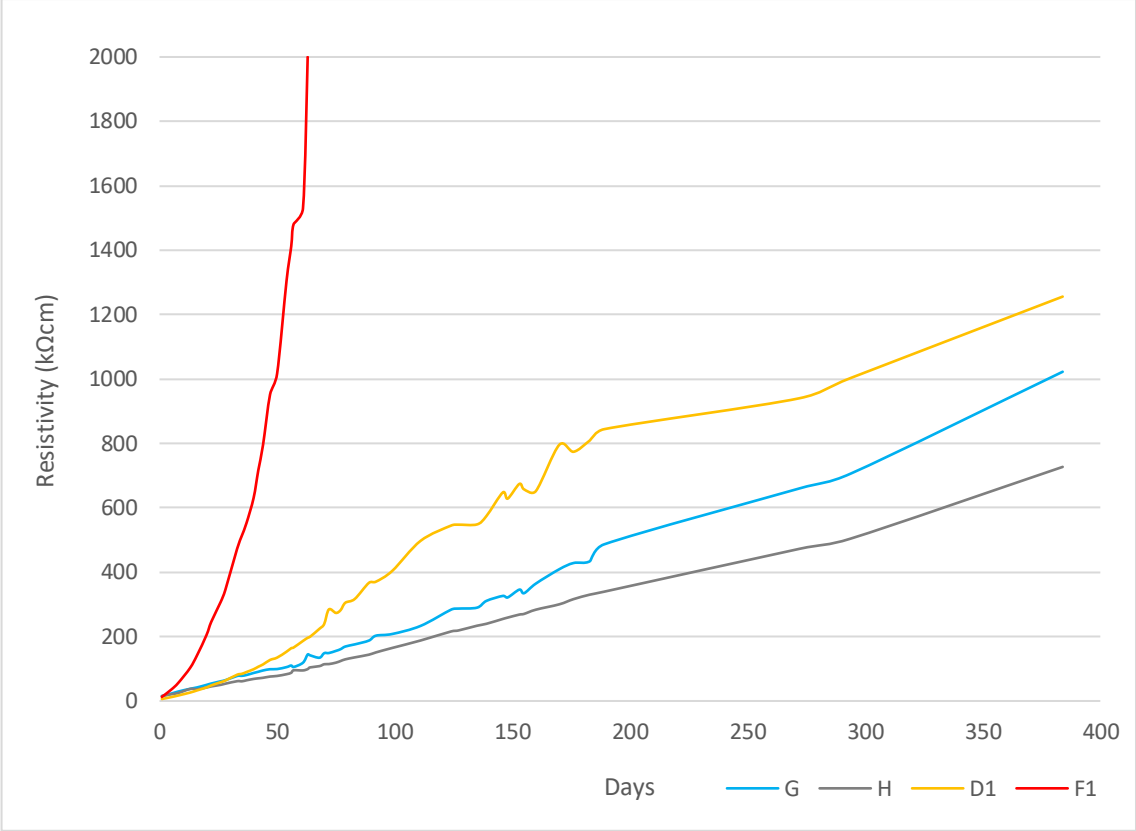

Figure 4.15 - Resistivity over time

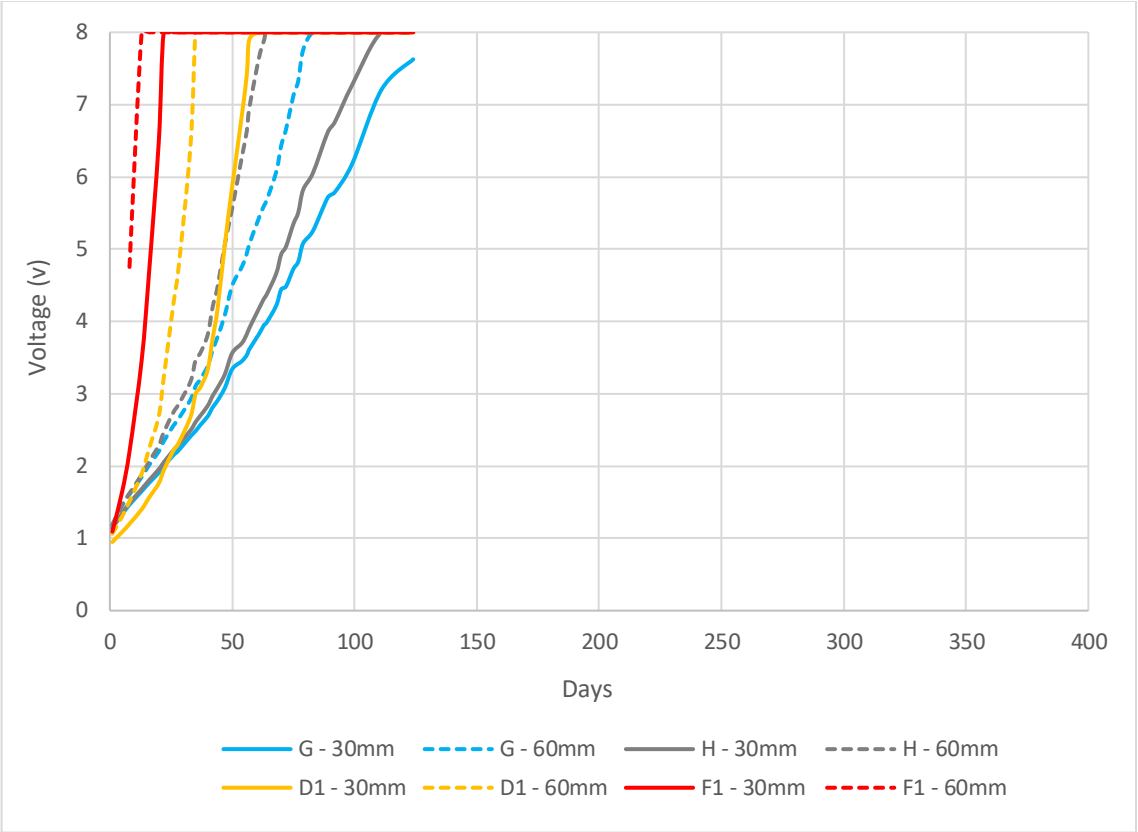

Figure 4.16 - Voltage over time

Figure 4.16 displays the circuit voltage increase of each of the eight samples over 124 days. The data in Figure 4.16 identifies that for all samples/compositions, the 60mm anode to reinforcement spacing will reach maximum voltage before the corresponding 30mm anode sample.

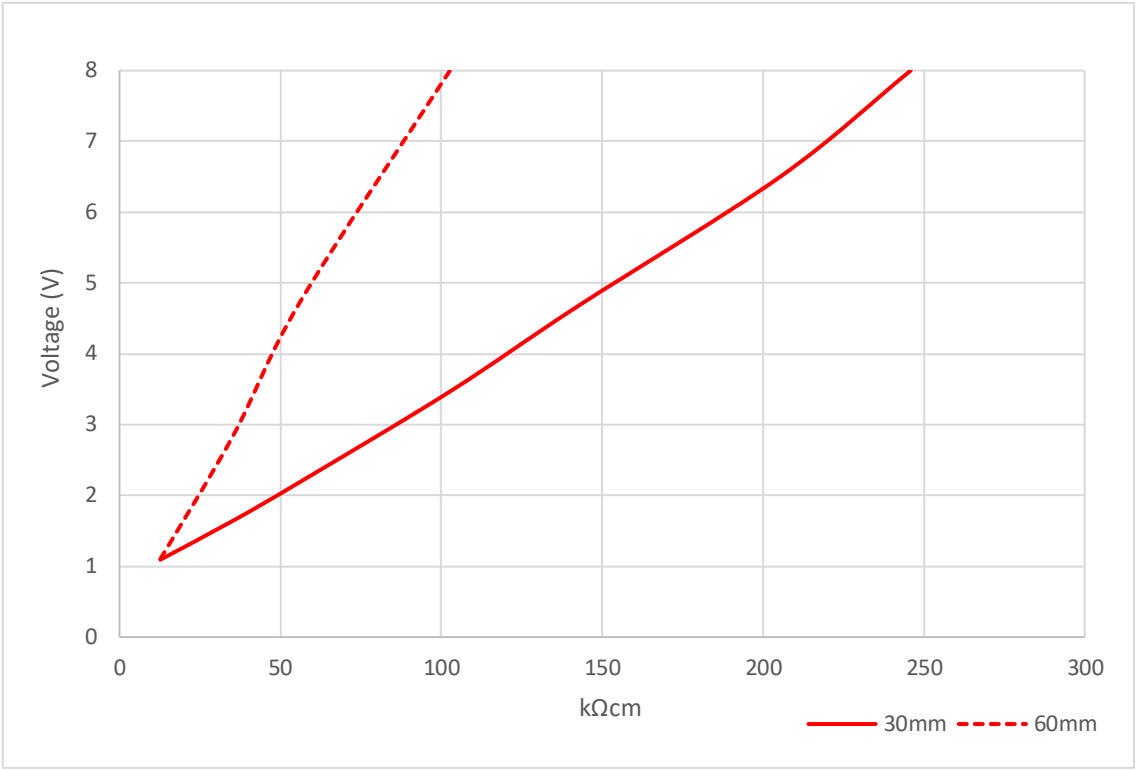

Figure 4.17 - Sample F1 voltage vs resistivity at 30mm and 60mm anode-to-rebar spacing

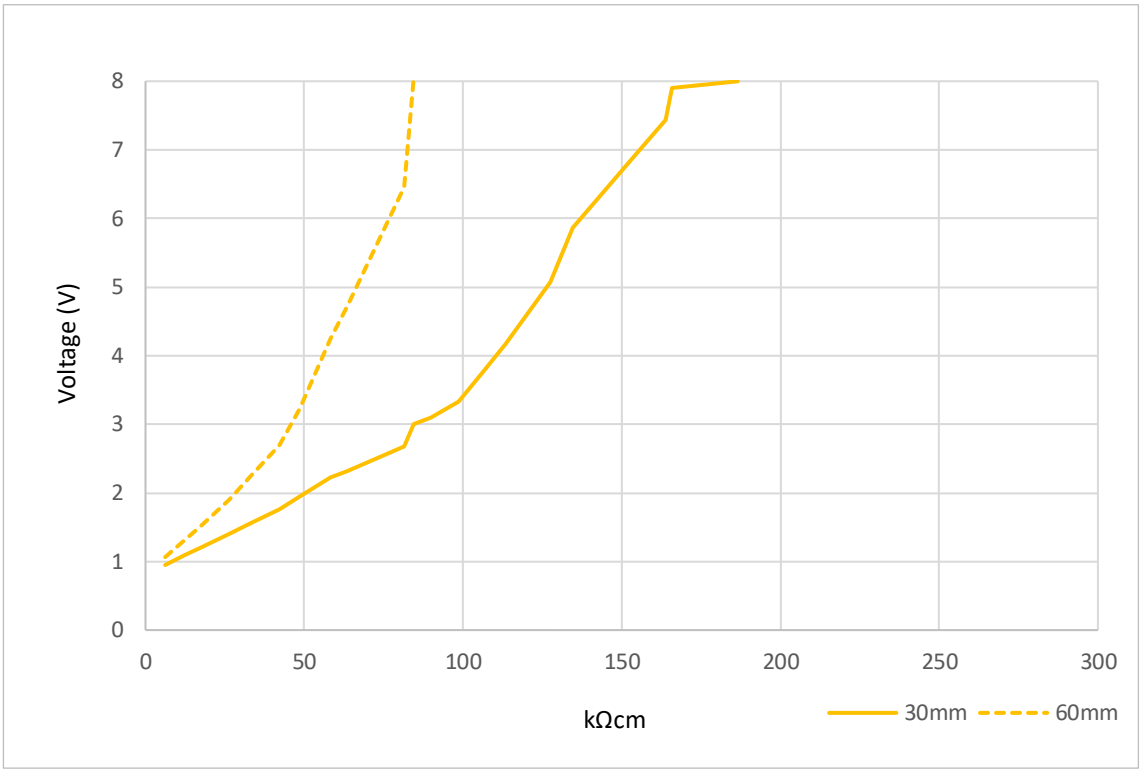

Figure 4.18 - Sample D1 voltage vs resistivity at 30mm and 60mm anode-to-rebar spacing

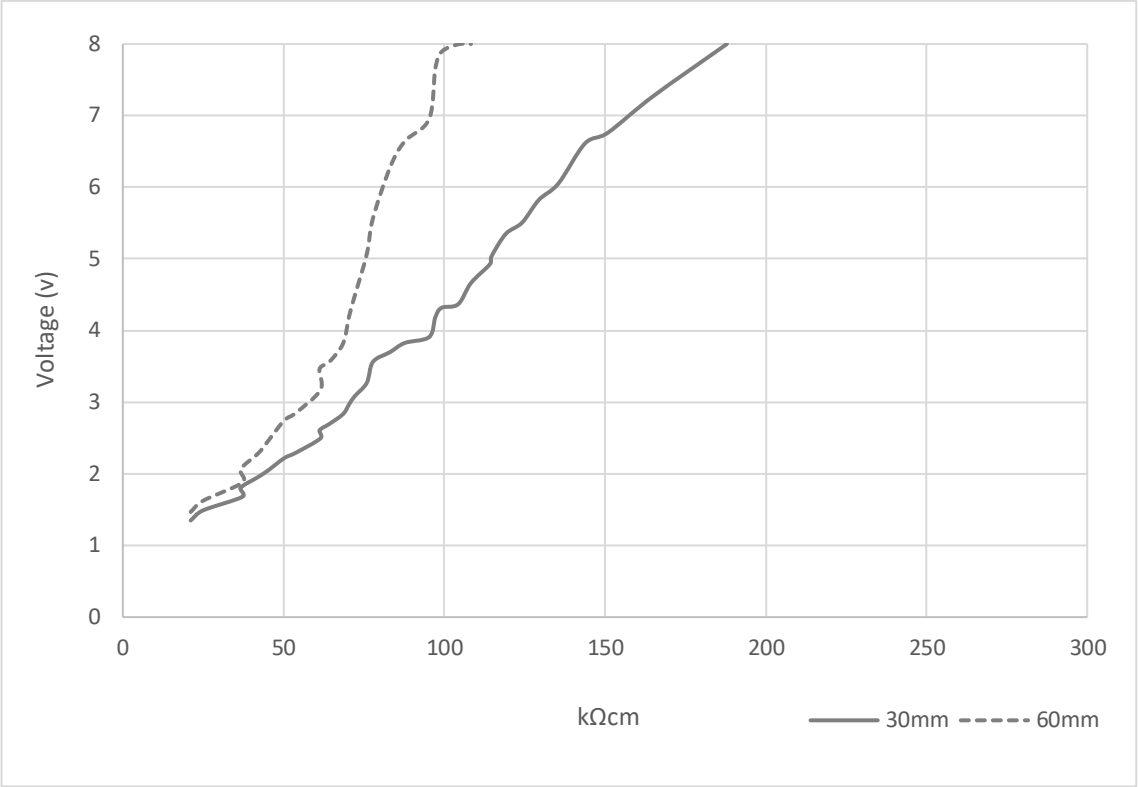

Figure 4.19 - Sample H voltage vs resistivity at 30mm and 60mm anode-to-rebar spacing

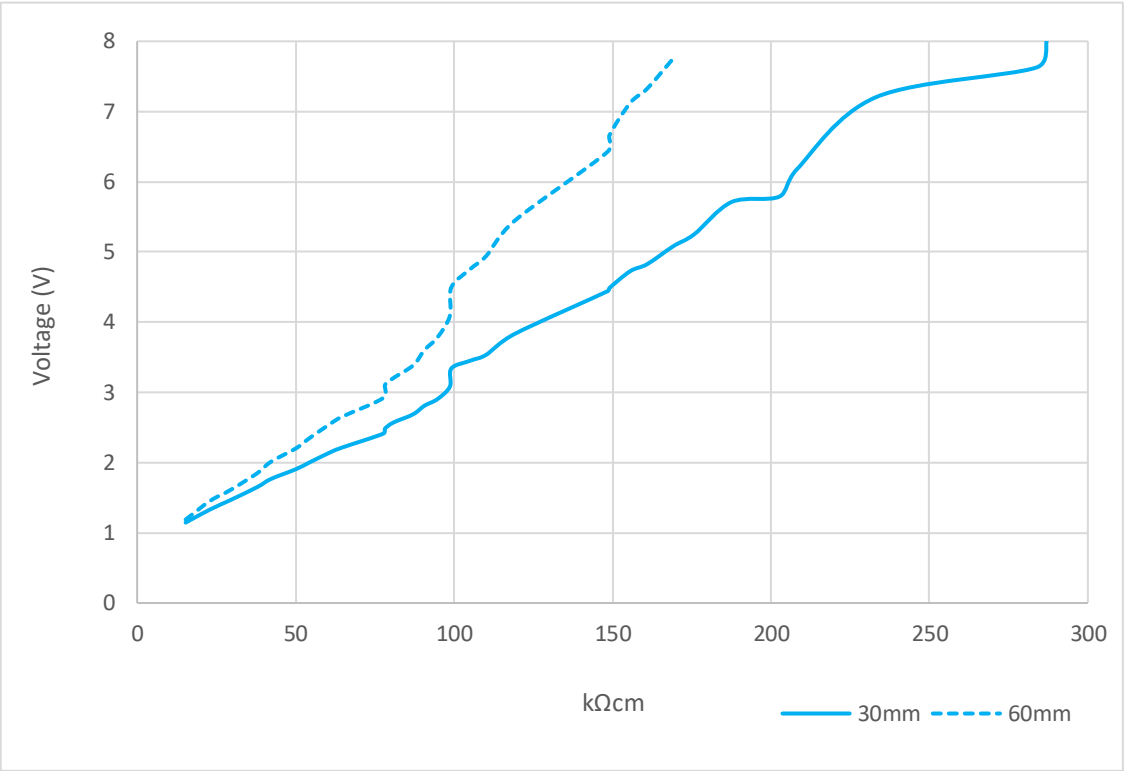

Figure 4.20 - Sample G voltage vs resistivity at 30mm and 60mm anode-to-rebar spacing

Figure 4.17, Figure 4.18, Figure 4.19 and Figure 4.20 display voltage vs resistivity for each of the samples at 30mm and 60mm anode-to-rebar spacing.

For sample F1, the maximum circuit voltage limit was reached at 102.7 kΩcm at 60mm anode-to-rebar spacing and at 245.9 kΩcm at 30mm anode-to-rebar spacing.

For sample D1, the maximum circuit voltage limit was reached at 84.4 kΩcm at 60mm anode-to-rebar spacing and at 186.6 kΩcm at 30mm anode-to-rebar spacing.

For sample H, the maximum circuit voltage limit was reached at 108.3 kΩcm at 60mm anode-to-rebar spacing and at 187.9 kΩcm at 30mm anode-to-rebar spacing.

For sample G, the maximum circuit voltage limit was reached at 175.8 kΩcm at 60mm anode-to-rebar spacing and at 287.0 kΩcm at 30mm anode-to-rebar spacing.

Samples F1, D1, H and G displayed similar trends where 60mm anode-rebar spaced samples reached the limiting 8 volts prior to the corresponding 30mm samples. It is evident from Figure 4.17, Figure 4.18, Figure 4.19 and Figure 4.20, that resistivity and voltage increase in a linear trend. It is also identified that although all samples followed similar voltage to resistivity trends, variations in the final resistivity value where the 8-volt limit is reached were found. The data shows that the concrete with different variations in admixtures will result in varying ICCP voltage limits. Due to the limited comparable research that has been carried out on the topic of ICCP voltage and resistivity, limited conclusions on how admixtures affect the voltage variations can be made. As the impact of admixtures is not the focus of this research, further in-depth research into the effect of admixtures can be undertaken in the future.

Table 4.7 - Concrete resistivity measurement for each of the eight samples at maximum circuit voltage of 8-volt limit

Resistivity of Samples at 8-Volt Limit			
Sample	60mm	30mm	% Variation
	kΩcm	kΩcm	
F1	102.7	245.9	139%
D1	84.4	186.6	121%
H	108.3	187.9	73%
G	175.8	287.0	63%
Average	117.8	226.8	91%
Standard Deviation	34.6	42.1	

The voltage limit data from this experiment presented in Table 4.7, confirms the impact of anode-to-rebar spacing on the ability of the ICCP system to operate at a higher resistivity value. The circuit voltage reaches the maximum limit of 8 volts at an average resistivity of 117.8 kΩcm for the 60mm anode-to-rebar spacing while for the closer anode-to-rebar spacing of 30 mm, the maximum circuit voltage was reached at an average resistivity of 226.8 kΩcm. The percentage variation between 60mm and 30mm anode spacing was calculated for each sample to display the variation between anode spacing for each composition. In addition, the total average and standard deviation of all 60mm and 30mm anodes was calculated. The purpose of averaging the data is to identify a universal trend which may be relevant to all concrete structures.

For the eight operated circuits, once the maximum voltage limit was reached for each circuit, the operational mode was switched from constant current to constant voltage and the operating current of each circuit versus resistivity was recorded and plotted as shown in Figure 4.21, Figure 4.22,

Figure 4.23 and Figure 4.24. The current output for each circuit was based on 20 mA/m² of steel surface area. The change from constant current to constant voltage was carried out to continue to monitor the power output and obtain further data relating to the decrease in anode current output capacity after the 8-volt limiting voltage.

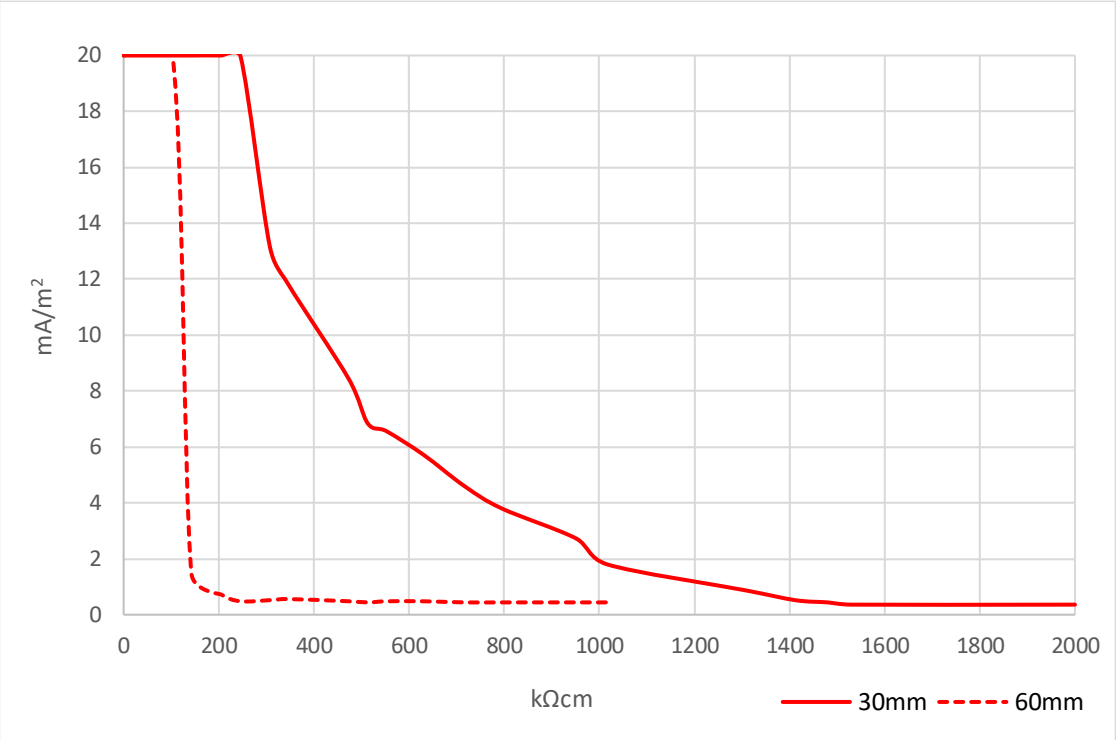

Figure 4.21 - Sample F1 current density vs resistivity at 30mm and 60mm anode-to-rebar spacing

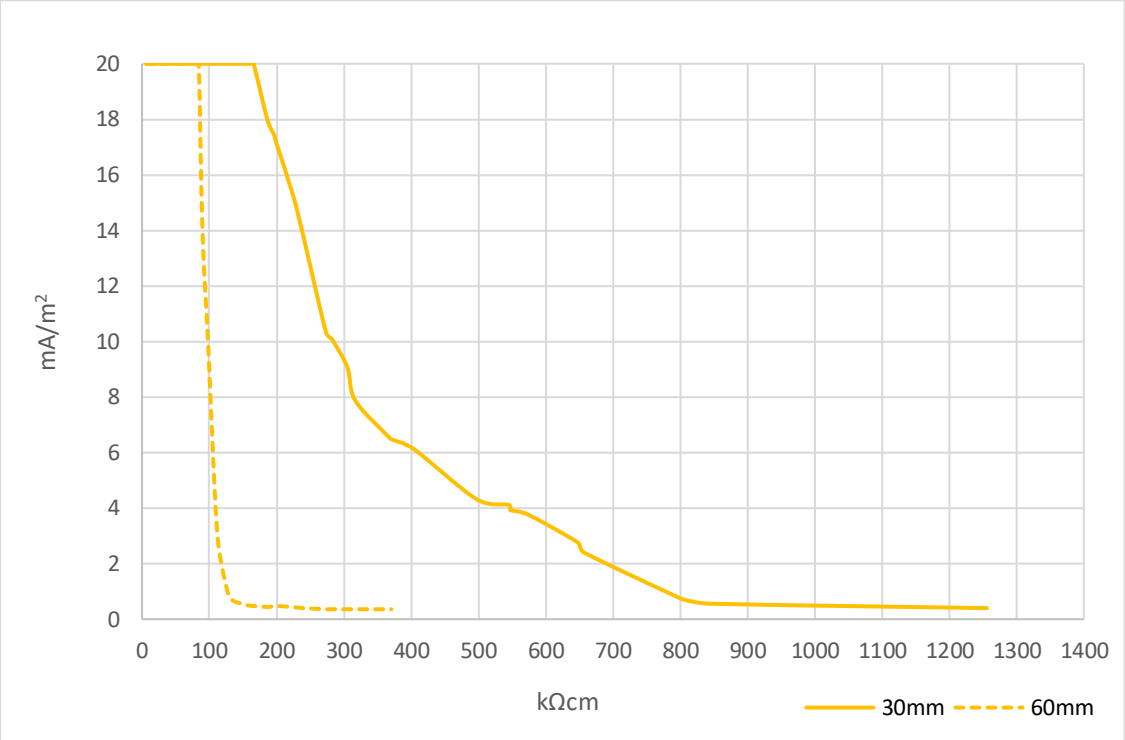

Figure 4.22 - Sample D1 current density vs resistivity at 30mm and 60mm anode-to-rebar spacing

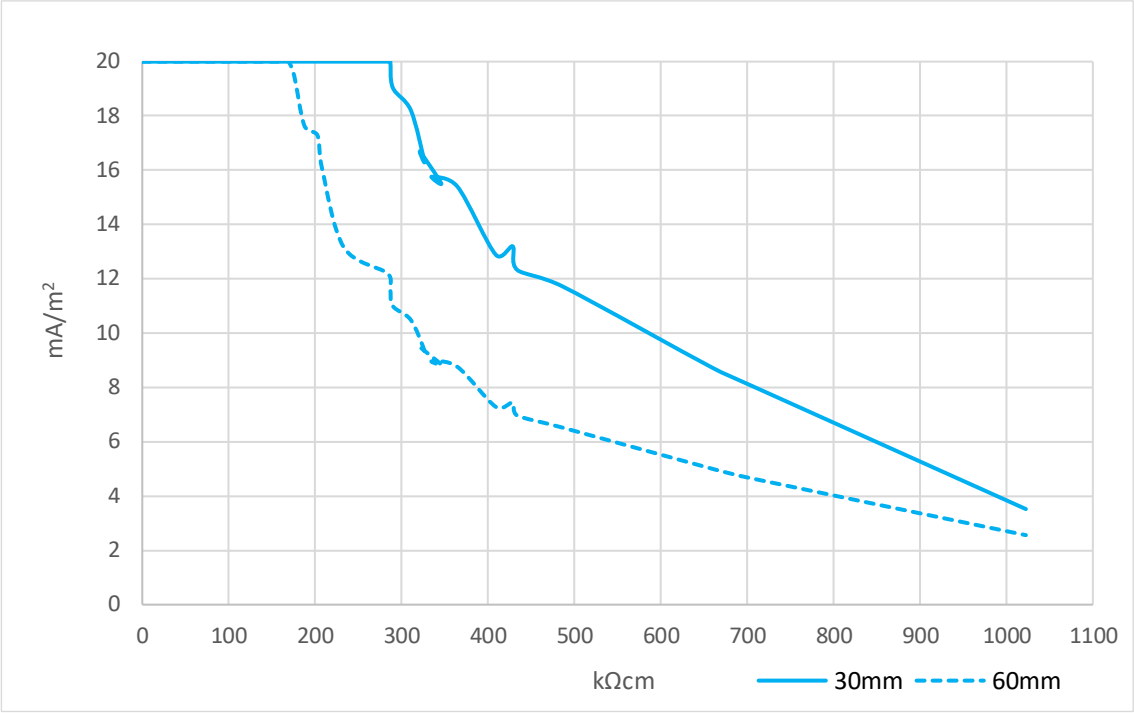

Figure 4.23 - Sample G current density vs resistivity at 30mm and 60mm anode-to-rebar spacing

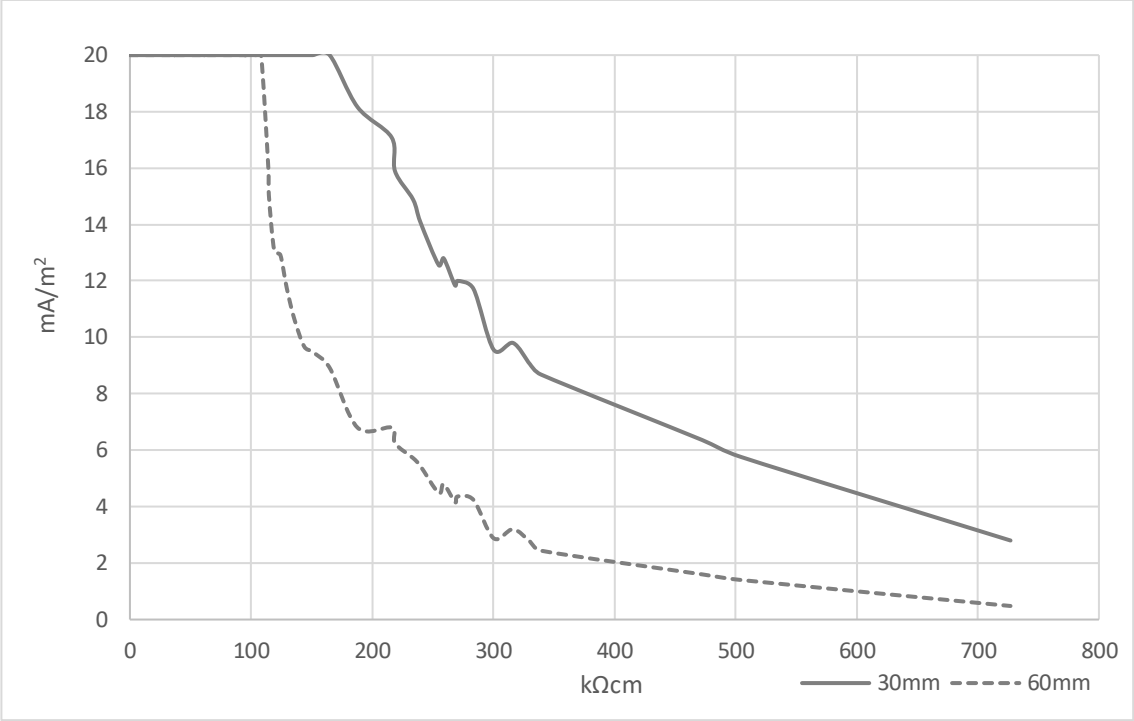

Figure 4.24 - Sample H current density vs resistivity at 30mm and 60mm anode-to-rebar spacing

Figure 4.21 and Figure 4.22 display a steep decline of the circuit current output for samples F1 and D1 at 60mm spacing in comparison to the gradual decline of current output for samples G and H at 60mm spacing. This variation of current decline could be related to the admixture used for these samples – fly ash was used for samples F1 and D1, while ground slag was used for samples D and H. Although the effect of admixtures is outside the scope of this experiment, the observation of fly ash greatly increasing resistivity suggest that fly ash will severely impact on the performance of ICCP, particularly regarding the voltage limit.

The voltage limit at 8 volts was reached at lower concrete resistivities for sample H than for sample G for both the 30mm and 60mm anode-to-rebar spacing samples. For samples F1 and D1, there is considerable impact of the anode-to-rebar spacing on the current output. At an anode-to-rebar spacing of 30mm, the current output for both circuits is much higher than for the samples at 60mm anode-to-rebar spacing. Future research can be carried out to further understand the relationship between admixtures and resistivity.

For samples G and H as displayed in Figure 4.23 and Figure 4.24, there is a similar trend of decline for current output for the 30mm and 60mm anode-to-rebar spacing.

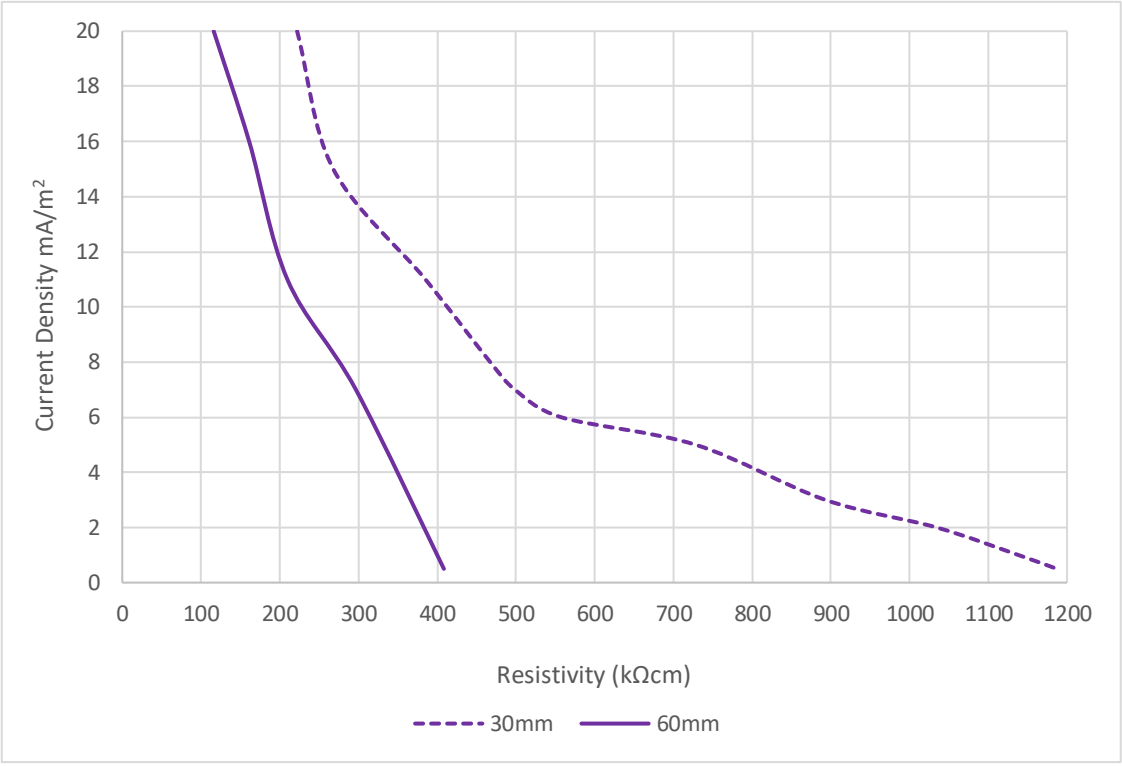

Figure 4.25 - Averaged trend of current density vs resistivity

The graph presented in Figure 4.25 provides a correlation between current density and concrete resistivity at the 30mm and 60mm anode-to-rebar spacing by averaging the data from Samples F1, D1, G and H.

Based on the average trend in Figure 4.25, at 60mm anode-to-rebar spacing the current output decreased to less than 1mA/m² at a resistivity of 408 kΩcm. At 30mm anode-to-rebar spacing, the current output decreased to less than 1mA/m² at a significantly higher resistivity of 1187 kΩcm.

It is important to note that while the 20mA/m² of steel surface is an estimated current density used normally for design purposes, normally ICCP systems operate at current density between 5mA/m² and 15mA/m² subject to corrosion activity and exposure conditions. Based on data extracted from operating impressed current cathodic protection systems [61], the average current densities of multiple operating impressed current cathodic protection systems ranged from 4.4mA/m² to 17.2mA/m².

Based on the average trend of current density versus resistivity (Figure 4.25), concrete resistivity of 296 kΩcm for anode-to-rebar spacing of 60mm and concrete resistivity of 467 kΩcm for anode-to-rebar spacing of 30mm, the ICCP system can deliver current output equivalent to 10mA/m² of steel surface area.

The graph in Figure 4.25 could be incorporated in the design of impressed current cathodic protection systems. The graph provides an indication of current output at different levels of concrete resistivity. Based on the input of current density required for the design of a cathodic protection system and the measured concrete resistivity of the subject structure, the anode-to--rebar spacing can be modified to achieve the desired current output for the system operation.

AS2832.5 – 2008 (R2018) does not specify minimum spacing between the anode and the rebar. The requirement is to avoid a short circuit during installation:

"In the case of impressed current systems particular attention shall be paid to avoid short circuits occurring between the anode system and any reinforcement steel, ancillary metallic components, reinforcement tie wire or debris steel in the surface of the concrete".

On this basis and based on the average trend for current density versus resistivity (Figure 4.25), impressed current cathodic protection systems can operate at relatively high concrete resistivities by modifying the spacing between the anode and rebar.

In practice, achieving closer spacing between the anode and rebar may not be possible in different structures. Considerations related to the existing concrete cover to embedded rebar and the required grout cover to the anode to achieve proper encapsulation within the concrete cover may limit anode positioning. It is likely that placing the anode at closer spacing to the rebar may result in greater current output in high resistivity concrete, however it is likely that this may impact on the current distribution offered by the anodes to the embedded rebar. The CP system in this case could be designed at a higher current density with more anodes at a closer anode spacing.

4.4 Conclusion

The average trend for current density versus resistivity indicates that an impressed current cathodic protection system can operate at 20 mA/m² at a concrete resistivity up to 116 kΩcm for an anode-to-rebar spacing of 60mm. Impressed current cathodic protection systems can operate at 20 mA/m² at a concrete resistivity up to 221 kΩcm at an anode-to-rebar spacing of 30mm. The level of current output decreases with the increase of concrete resistivity for anode-to-rebar spacing at both 30mm and 60mm anode-to-rebar spacing.

Overall, the data from this research suggests that for high resistivity concrete, the desired current output can be achieved by reducing the spacing between the anode and the rebar.

The data presented in Figure 4.25 could be incorporated in the design of impressed current cathodic protection systems Standards. The data identified in this experiment provides an indication of current output at different levels of concrete resistivity. Based on the input of current density required for the design of a cathodic protection system and the measured concrete resistivity of the subject structure, the anode-to-rebar spacing can be modified to achieve the desired current output for the system operation.

5 Performance of Impressed Current Cathodic Protection in an Operational Reinforced Concrete Structure

The purpose of this chapter is to verify the concrete resistivity, anode-to-rebar spacing, and system current output data presented in Chapter 4. Data obtained from an impressed current cathodic protection system operating on a wharf structure in NSW has been analysed and assessed against the average trend of current density versus resistivity graph (Figure 4.25) presented in Chapter 4.

5.1 The Structure

The structure is a reinforced concrete wharf, approximately 37m x 9m comprising of piles, concrete headstocks and a composite pre-cast/cast in-situ concrete deck.

Figure 5.1 - Structure photo taken from under wharf structure

The primary cause of concrete spalling and deterioration of the structure was chloride contamination of the concrete. The repair of the structure was carried out using “low resistivity” polymer modified repair mortar. The same concrete repair material (Material H) from Experiment 4 was used during installation of the ICCP system in 1999. Material H was used for patch repair areas as well as for the installation of the ICCP system as the anode encapsulating grout.

5.2 Cathodic Protection System Description

The impressed current cathodic protection system was installed to the headstocks and selected sections of the deck soffit. The system was commissioned in 1999.

The anode used for this ICCP system was activated titanium expanded mesh ribbon anode for cathodic protection in concrete (the same anode used in Chapter 4, Experiments 5 and 6). The current rating for the mesh ribbon is 5.3mA per linear metre. The width of the ribbon anode was 20mm and the thickness was 0.9mm. The anode substrate was titanium grade 1 and the catalyst was noble Mixed Metal Oxide (MMO). The anode was installed in concrete slots within the concrete cover.

The cathodic protection system was divided into 6 zones (circuits). Figure 5.2 displays the cathodic protection transformer rectifier unit, which is used to control current output, measure voltage and measure embedded concrete reference electrodes. The anode, rebar, reference electrodes and reference return cables were terminated in junction boxes along the wharf and extended to a transformer rectifier unit. The transformer rectifier unit houses 6 power supply units, each feeding one zone. The power supply units operate in constant current mode.

Figure 5.2 - Photo of cathodic protection transformer rectifier unit

Seventeen silver/silver chloride reference electrodes were installed for the system monitoring.

The system zoning was based on the exposure conditions for the various elements of the wharf and the type of protected element (headstock or deck soffit).

The system zoning and exposure conditions are detailed in Table 5.1.

Table 5.1 - Structure zoning and environmental exposure condition

Zone	Element	Environmental Exposure Condition
3	Rear deck soffit bays 1-4	Splash zone
4	Rear deck soffit bays 5-8	Atmospheric zone
5	Middle & front deck soffit bays 1-3	Splash zone
7	Middle deck soffit bays 6-8	Atmospheric zone
9	Headstock top bays 1-9	Tidal zone
10	Headstock bottom bays 1-9	Tidal zone

Figure 5.3 display the zoning and plan view of the reinforced concrete wharf structure. The structure consists of a reinforced concrete slab and nine headstock beams. Zones 3, 4, 5 and 6 are located in the soffit of the reinforced concrete slab, and zones 9 and 10 located in the headstock beams. Figure 5.4 displays a photograph taken of the headstock.

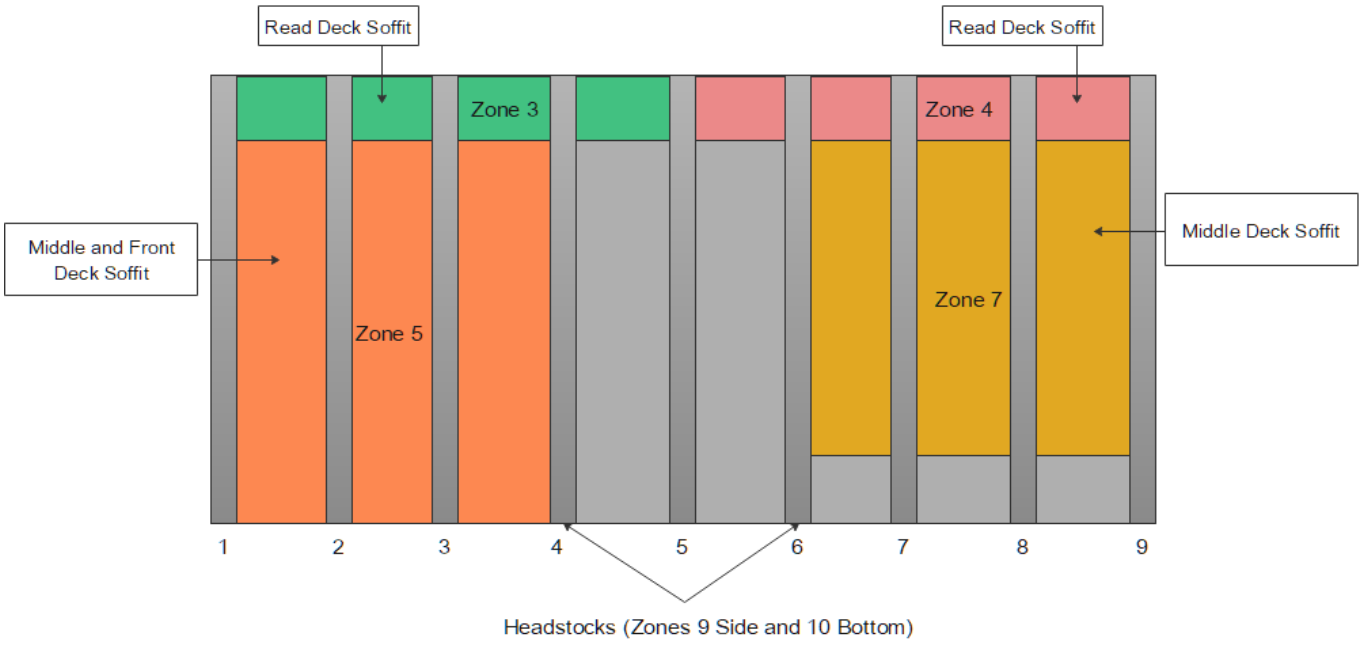

(A)

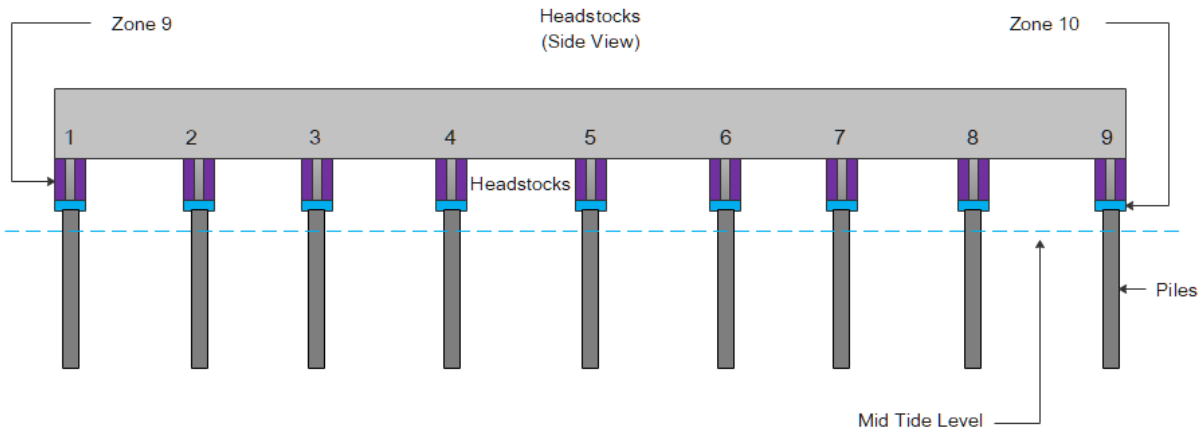

(B)

Figure 5.3 - Structure ICCP system zoning plan – (A) top view of structure main slab soffit, (B) side view of structure

Figure 5.4 - Photo of headstock 8

5.3 Assessment Methodology

Resistivity testing, cover to reinforcement measurements, verification of steel layout within the concrete, and a review of circuit voltage data were performed as a part of the testing. Testing was carried out to the underside of the wharf structure with a boat.

Resistivity testing was performed for the elements of the structure protected by the cathodic protection system. Resistivity data was obtained onsite using a four-point Wenner probe (Proceq 50mm). Testing of this structure was conducted prior to the tested methodology using stainless steel probes for resistivity measurements detailed in Chapter 3 Section 3.7. The commonly used surface resistivity testing method was applied [10]. As shown in Figure 5.5 prior to resistivity testing, scabbling of the concrete surface was carried out in order to remove the external layer of concrete. This was carried out using a handheld portable angle grinder.

Figure 5.5 – Cleaning of surface using angle grinder

Figure 5.6 – Onsite resistivity testing using Proceq Resipod

A system performance report was attained. The report includes circuit zoning, maximum design current and zone output current and voltage data. A summary of the systems data is presented on the following page in Table 5.2.

Cover meter testing was carried out using a Proceq cover meter. The concrete cover to existing rebar was measured and verified at various breakout locations in order to confirm the exact cover to the rebar. The cover to the ribbon anode was measured on-site and anode-to-rebar spacing was calculated.

5.4 Results and Discussion

5.4.1 System Performance Data

Table 5.2 presents data extracted from a system performance report detailing the ICCP systems circuit zoning, location of each zone, the maximum design current based on 20mA/m² of embedded rebar surface area, and the output current and voltage of each circuit.

Table 5.2 - Structures cathodic protection system data

Zone/Circuit	Location	Exposure Conditions	Maximum Design Current	Output Current	Measured Voltage
			(mA)	(mA)	(V)
3	Soffit Rear Bay 1-4	Splash	800	150	2.8
4	Soffit Rear Bay 5-8	Atmospheric	800	10	9.0
5	Soffit Middle and Front Bays 1-2-3	Splash	2190	250	2.5
7	Soffit Middle Bays 6-7-8	Atmospheric	1590	170	8.1
9	Headstock Top	Tidal	1800	1050	2.4
10	Headstick Bottom	Tidal	1750	570	2.2

Zones 4 and 7 highlighted in yellow in Table 5.2 were both located in atmospheric exposure conditions and were found to be operating above the maximum recommended voltage for ICCP systems (8 volts). Voltage will fluctuate due to environmental exposure conditions. The ICCP transformer rectifiers operate in constant current mode. During the last monitoring session (commonly annually), the current output would have been set with a measured voltage under 8 volts. Due to the changing environmental conditions, voltage limits in some cases may be exceeded. In cases where an 8-volt limit is reached, the current output decreases during the next testing and adjustment session.

The design current for zone 4 (atmospheric) was 800mA based on 20mA/m² of steel surface area. Zone 4 operated above the maximum voltage limit of 8 volts. The output current for this circuit was 10mA which is equivalent to 1.25% of the design current.

The design current for zone 7 (atmospheric) was 1590mA based on 20mA/m² of steel surface area. Zone 7 operated above the maximum voltage limit of 8 volts. The output current for this circuit was 170mA which is equivalent to 10.69% of the design current.

Zones 3, 5 (splash zones), 9 and 10 (tidal zones) operated below 40% of the voltage limit of 8 volts.

5.4.2 Resistivity Data

The following data in Figures 5.7 – 5.14 were obtained by onsite four-point Wenner probe resistivity measurement testing. Resistivity measurements were averaged out from 8 to 10 readings at each data point location/zone (Figure 5.6). Measurements were carried out immediately one after the other within a 300x300mm area and within the specific zone. The Proceq Resipod four-point Wenner probe automatically calculates the mean value (f) of the measurements (N) in the test location (displayed in Figures 5.7 – 5.14). A mean value is used for resistivity measurements as measurements do range (as seen in the minimum and maximum measurements) when carrying out onsite measurements. These variations can be caused by the location of rebar, influence of aggregate, temperature, moisture content, carbonation, and concrete-to-probe contact resistance [10]. Concrete-to-probe contact resistance is believed to be the main cause of these variations. A solution to this issue is detailed in Chapter 3 Section 3.7. The site testing was carried out prior to the development of the methodology in Section 3.7. For the Proceq equipment settings, contact spacing is based on the equipment's probe spacing (50mm), and the specimen shape was set to flat–default setting, used for onsite measuring. These setting are in accordance with the Wenner probe operation manual [10].

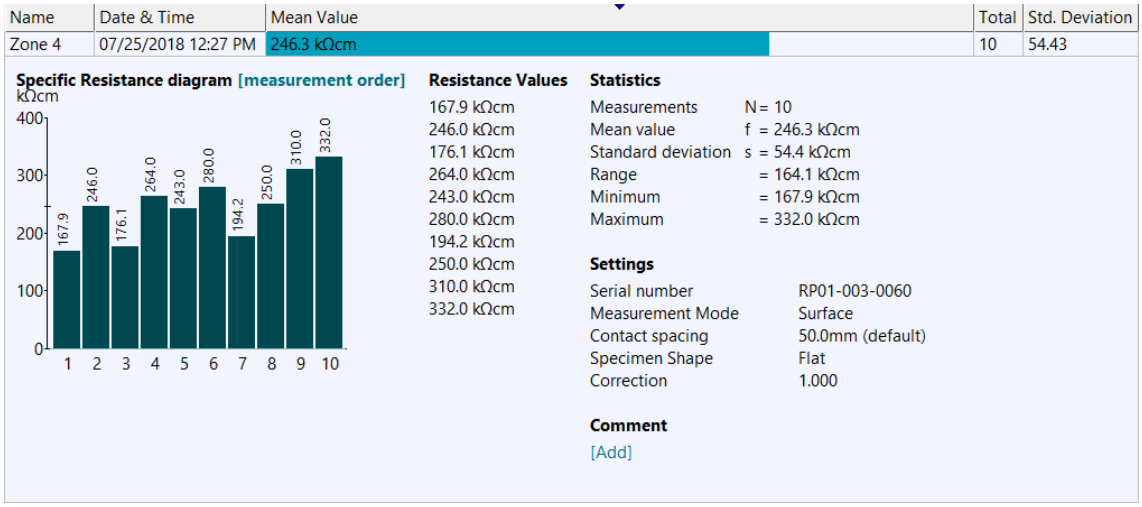

Figure 5.7 - Zone 4 (atmospheric) resistivity measurements

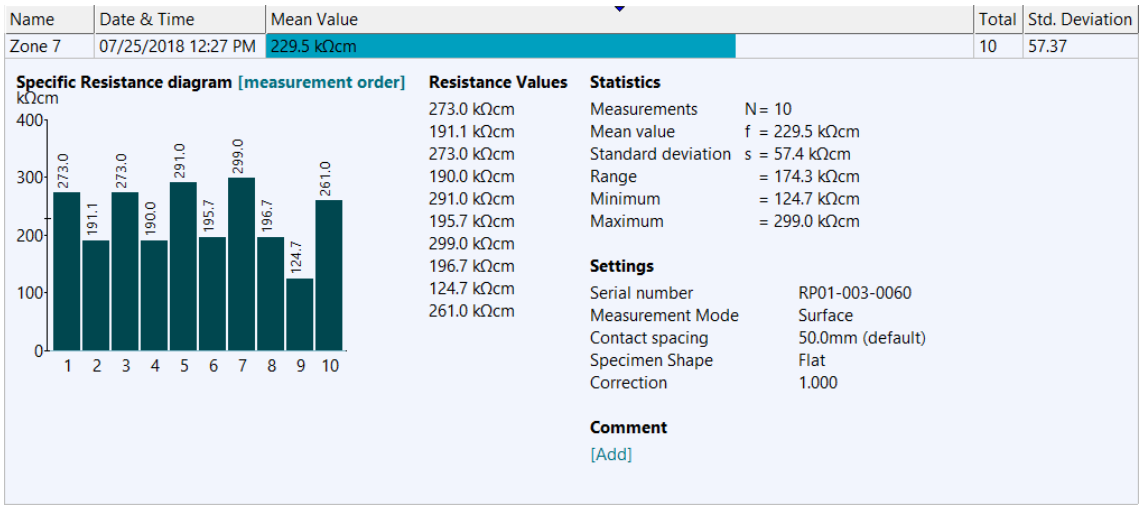

Figure 5.8 - Zone 7 (atmospheric) resistivity measurements

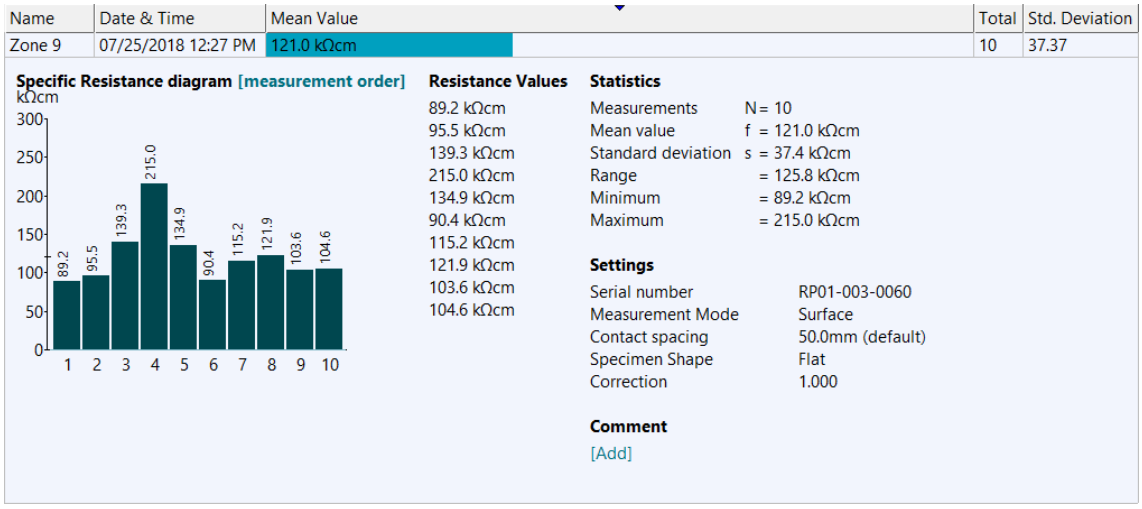

Figure 5.9 - Zone 9 (tidal) resistivity measurements

Name	Date & Time	Mean Value	Total	Std. Deviation
Zone 5	07/25/2018 12:27 PM	117.2 kΩcm	10	13.90

Specific Resistance diagram [measurement order]

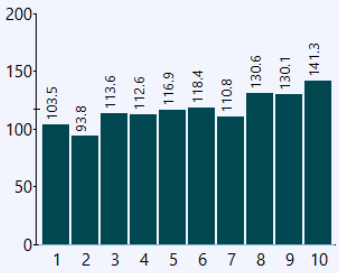

Resistance Values

103.5 kΩcm
93.8 kΩcm
113.6 kΩcm
112.6 kΩcm
116.9 kΩcm
118.4 kΩcm
110.8 kΩcm
130.6 kΩcm
130.1 kΩcm
141.3 kΩcm

Statistics

Measurements	N = 10
Mean value	f = 117.2 kΩcm
Standard deviation	s = 13.9 kΩcm
Range	= 47.5 kΩcm
Minimum	= 93.8 kΩcm
Maximum	= 141.3 kΩcm

Settings

Serial number	RP01-003-0060
Measurement Mode	Surface
Contact spacing	50.0mm (default)
Specimen Shape	Flat
Correction	1.000

Comment

[Add]

Figure 5.10 - Zone 5 (splash) resistivity measurements

Name	Date & Time	Mean Value	Total	Std. Deviation
Zone 3	07/25/2018 12:27 PM	49.2 kΩcm	10	11.47

Specific Resistance diagram [measurement order]

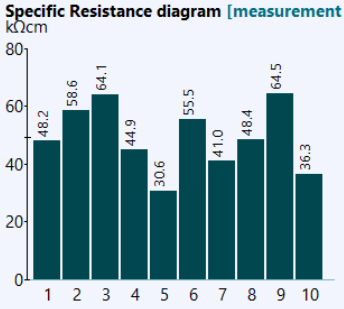

Resistance Values

48.2 kΩcm
58.6 kΩcm
64.1 kΩcm
44.9 kΩcm
30.6 kΩcm
55.5 kΩcm
41.0 kΩcm
48.4 kΩcm
64.5 kΩcm
36.3 kΩcm

Statistics

Measurements	N = 10
Mean value	f = 49.2 kΩcm
Standard deviation	s = 11.5 kΩcm
Range	= 33.9 kΩcm
Minimum	= 30.6 kΩcm
Maximum	= 64.5 kΩcm

Settings

Serial number	RP01-003-0060
Measurement Mode	Surface
Contact spacing	50.0mm (default)
Specimen Shape	Flat
Correction	1.000

Comment

[Add]

Figure 5.11 - Zone 3 (splash) resistivity measurements

Name	Date & Time	Mean Value	Total	Std. Deviation
Zone 10 Top	07/25/2018 12:27 PM	79.1 kΩcm	10	6.48

Specific Resistance diagram [measurement order]

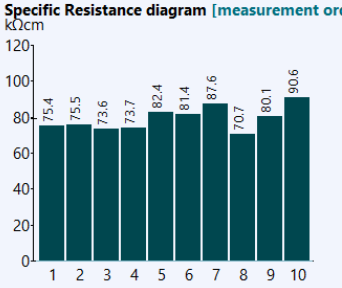

Resistance Values

75.4 kΩcm
75.5 kΩcm
73.6 kΩcm
73.7 kΩcm
82.4 kΩcm
81.4 kΩcm
87.6 kΩcm
70.7 kΩcm
80.1 kΩcm
90.6 kΩcm

Statistics

Measurements	N = 10
Mean value	f = 79.1 kΩcm
Standard deviation	s = 6.5 kΩcm
Range	= 19.9 kΩcm
Minimum	= 70.7 kΩcm
Maximum	= 90.6 kΩcm

Settings

Serial number	RP01-003-0060
Measurement Mode	Surface
Contact spacing	50.0mm (default)
Specimen Shape	Flat
Correction	1.000

Comment

[Add]

Figure 5.12 - Zone 10 headstock (tidal) top resistivity data

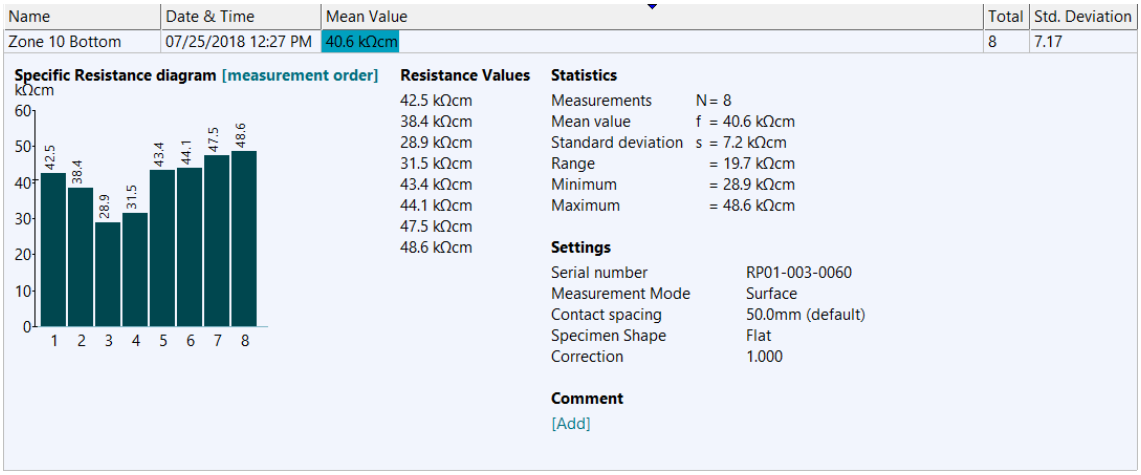

Figure 5.13 - Zone 10 headstock (tidal) bottom resistivity data

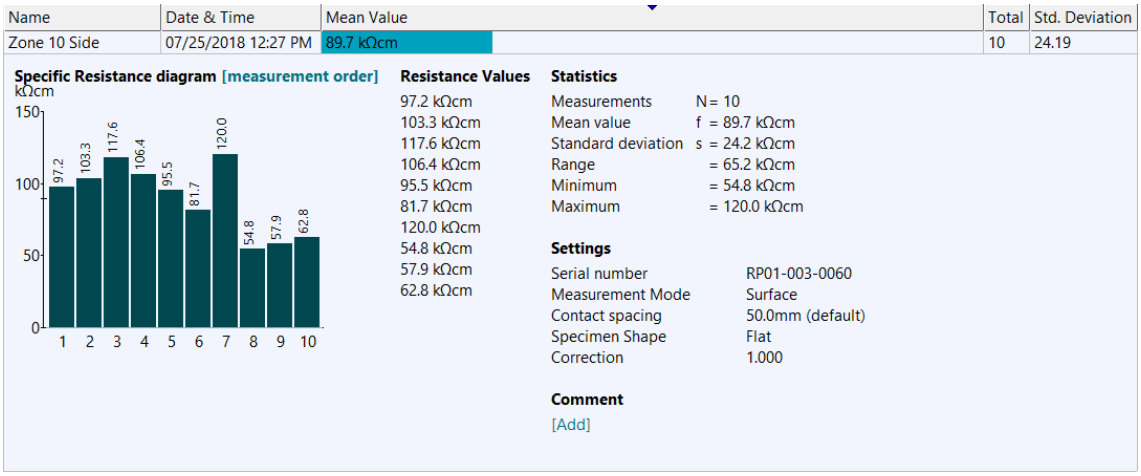

Figure 5.14 - Zone 10 headstock (tidal) side resistivity data

Table 5.3 - Circuit, voltage, resistivity, and exposure condition data

Circuit/Zone	Voltage (V)	Resistivity (kΩcm)	Exposure conditions
3	2.8	49.2	Splash
4	9.0	246.3	Atmospheric
5	2.5	117.2	Splash
7	8.1	229.5	Atmospheric
9	2.4	121	Tidal
10	2.2	69.8	Tidal

Table 5.3 displays the circuit/zone, operating voltage, resistivity, and exposure condition data. The data shows that the highest resistivity measurements of 246.3 kΩcm and 229.5 kΩcm (Zones 4 and 7) were in the atmospheric zones. Zones 4 and 7 also exhibited the highest voltages of 9 volts and 8.1 volts. Averaging the data between the exposure conditions, voltage in the tidal zones (9 and 10) was 2.30 volts, 2.60 volts in the splash zones (3 and 5) and 8.55 volts in the atmospheric zones (4 and 7). This data identifies a correlation between operating circuit voltage and exposure conditions. The impact of circuit voltage limitation is more relevant for atmospheric zones (dry conditions) than for tidal and splash zones.

5.4.3 Current Density Output

Table 5.4 - ICCP design vs operating current density

Zone	Design current density based on 20mA/m^2	Operating current (mA)	Operating current ÷ design density	Output current density (mA/m^2)
3	800	150	0.1875	3.75
4	800	10	0.0125	0.25
5	2190	250	0.1142	2.28
7	1590	170	0.1069	2.14
9	1800	1050	0.5833	11.67
10	1750	570	0.3257	6.51

Table 5.4 displays the output current density calculated by dividing the operating current density by the design current density (based on 20mA/m² of steel surface area).

The exposure condition of the wharf can be divided into three categories. Atmospheric, splash and tidal. For the elements located in the atmospheric zones (zone 4 and zone 7), the concrete resistivity ranged between 229.5 kΩcm and 246.3 kΩcm with an average resistivity of 237.9 kΩcm. The average circuit's operating voltage was 8.55 volts, and the average current density was 1.19mA/m².

For the elements located in the splash zone (zone 3 and zone 5), the concrete resistivity measured was 49.2 kΩcm and 117.2 kΩcm with an average resistivity of 83.2 kΩcm. The average circuit's operating voltage was 2.65 volts, and the average current density was 3.01mA/m².

For the elements located in the tidal zone (zone 9 and zone 10), the concrete resistivity was 95.4 kΩcm. The average circuit's operating voltage was 2.3 volts, and the average current density was 9.09mA/m².

Based on the data presented in Table 5.4, it can be observed that while all zones are designed to a current density of 20mA/m² of steel surface area, the actual operating current density greatly varied between zones. The tidal zones operated at a current density of 9.09mA/m², the splash zones operated at a current density of 3.01mA/m², and the atmospheric zone operated at a current density of 1.19mA/m². This data identifies a correlation between operating current density and exposure conditions of different elements/zones of the structure. This is related to the conductivity in each zone. The atmospheric zones have the lowest water content as they are least exposed to tidal fluctuations and understandably were found to have the highest resistance (resistivity).

5.4.4 Anode-to-Rebar Spacing

Cover-to-reinforcement measurements were performed for the elements of the wharf. The average cover-to-embedded rebar was 60mm and the average spacing between the rebar was 200mm.

Ribbon anodes were installed in slot cuts within the concrete cover. The average depth of ribbon anode cover was 20mm.

Figure 5.15 displays the anode and steel layout and spacing.

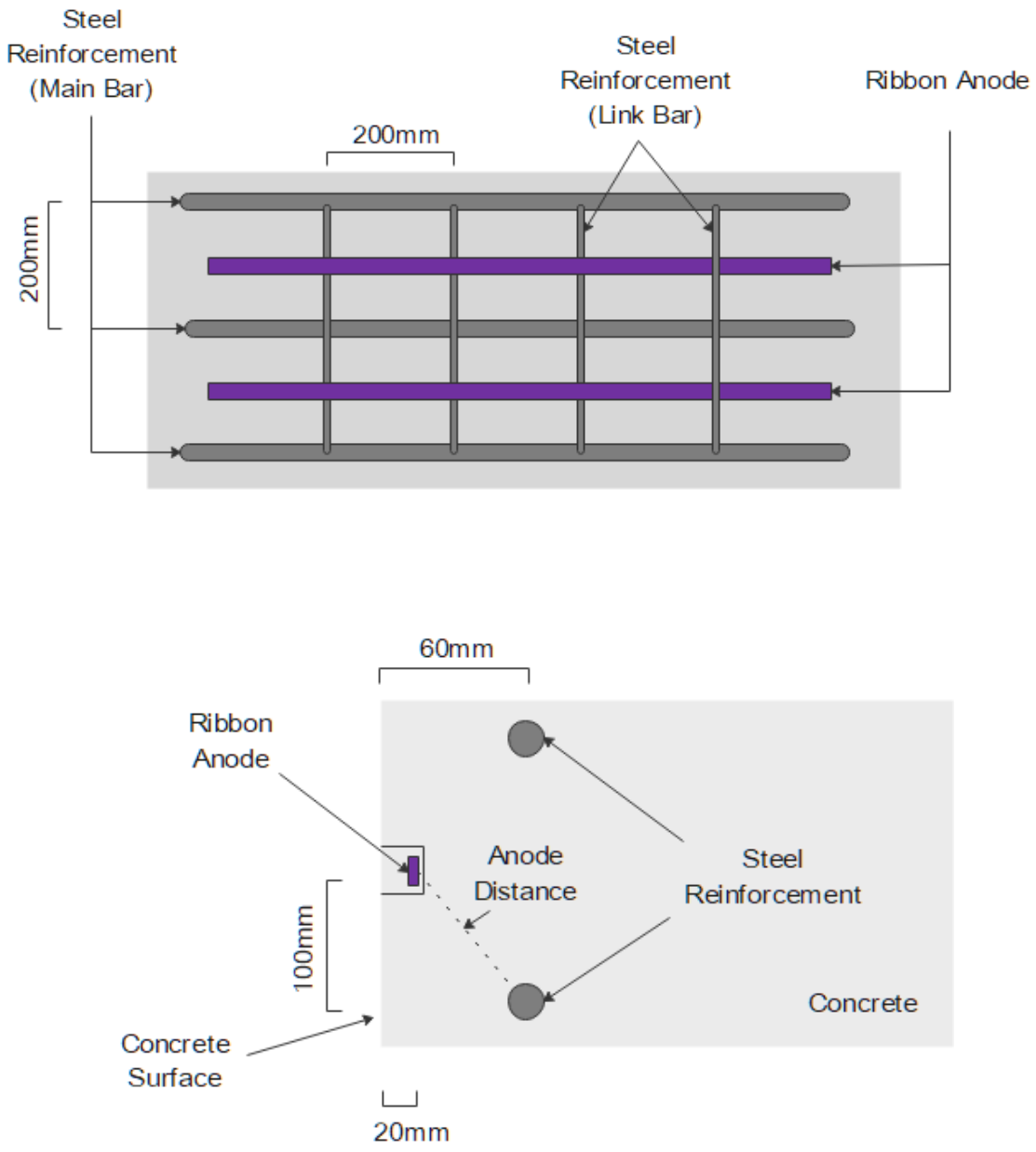

Figure 5.15 - Typical ribbon anode and rebar layout and spacing

Based on the distances between the anode and steel reinforcement as pictured in Figure 5.15, Pythagoras theorem was used to calculate the anode-to-steel distance. A typical anode spacing for all zones/circuits of approximately 107mm between anode and steel was calculated.

5.4.5 Current Density Comparison Between Site and Laboratory Data

The laboratory data gathered in Chapter 4 identified a correlation between operating current density (mA/m²), concrete resistivity and anode-to-rebar spacing. The averaged trend line laboratory data from Chapter 4 (previously presented in Figure 4.25) has been incorporated with the structure data obtained in this Chapter.

Figure 5.16 displays the two data sets. The purple trend lines display the 30mm and 60mm anode-rebar spacing data from Chapter 4. The current density and resistivity data obtained from the ICCP structure in this Chapter is also displayed in Figure 5.16.

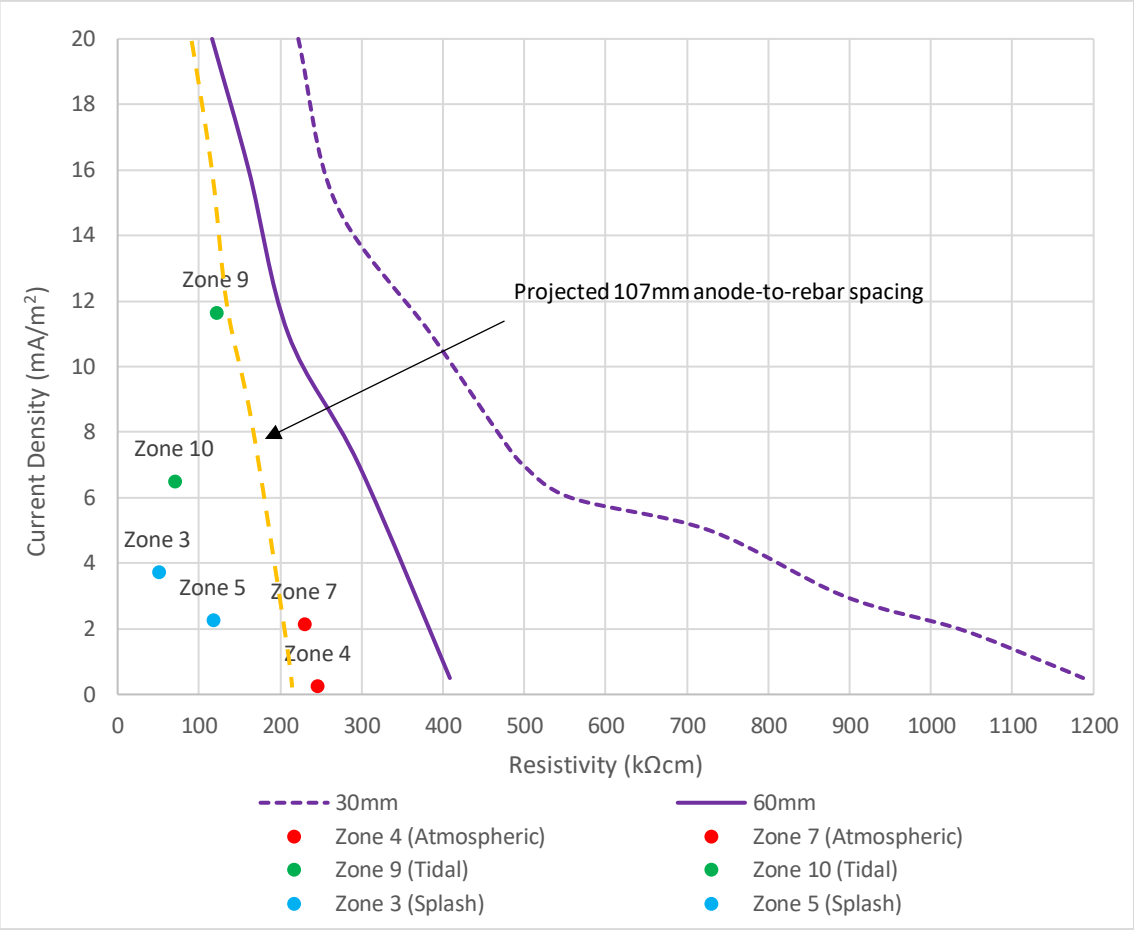

Figure 5.16 - ICCP laboratory and on-site data comparison

From the structures tidal and splash zones 3, 5, 9 and 10 all operated under the 8-volt limit threshold, while atmospheric zones 4 and 7 exceeded the 8-volt limit. Based on this data, a trend line was estimated depicting the current density to resistivity trend line limit for the structure at the measured anode-to-rebar spacing of 107mm. This projected trend line limit is displayed in Figure 5.16 as an orange dash line. The zones which operate under the 8-volt limit (tidal and splash zones 3, 5, 9 and 10) are on the left of the trendline, while the zones (atmospheric zones 4 and 7) exceeding the 8-volt limit are on the right. If the zones are displayed on the right, at the specific anode spacing, they will operate above the 8-volt limit.

Based on the data from Chapter 4 it was evident that as anode-to-rebar spacing increases, current density output decreases (due to the voltage limit). When the anode-to-rebar distance increases, the trend line will move to the left. In the case of the wharf structure, an anode-to-rebar spacing of 107mm is more than that of the tested 30mm and 60mm anode-to-rebar samples tested in Chapter 4. The trends presented in Figure 5.16 are consistent and a correlation between current-output, concrete-resistivity and anode-to-rebar spacing of laboratory data and data from a real operating structure is established.

The consistent trends between the laboratory and site data presented in Figure 5.16 indicate that the anode-to-rebar spacing can be used as a tool to estimate the current output for an impressed current cathodic protection system at different concrete resistivity. Anode-to-rebar spacing can be adjusted to achieve the optimal performance.

For example, the data suggests that if we take a structure with a measured concrete resistivity 200 kΩcm at 30mm anode-to-rebar spacing, the ICCP zone will operate at a full 20 mA/m^2 within the 8 volts limit, but at a 60mm anode-to-rebar spacing, the ICCP zone will exceed the 8-volt limit. It will however at 60mm and 8 volts operate at a limited current density of approximately 11 mA/m^2. Increasing/doubling of the amount of installed anode may be one solution if the minimum anode spacing is limited to 60mm and a full 20 mA/m^2 output is required.

The data presented in Figure 5.16 provides vital design information currently absent in ICCP international design Standards [2] [4] [3]. The data provides information which identifies how the manipulation of anode-to-rebar spacing can be adjusted in order to design efficient and effective ICCP systems.

5.4.6 Long Term Repair Mortar Resistivity Trends

As noted in Section 5.1, the same concrete repair material (Material H) from Experiment 4 (Section 3.8) was used during installation of the ICCP system in 1999. Material H was used for patch repair areas as well as for the installation of the ICCP system for the anode encapsulating grout. Figure 5.17 plots the data of grout Material H from Experiment 4 (564 days of testing) alongside the resistivity data taken from the real structure 22 years after grout repairs and ICCP installation.

As displayed in Figure 5.17, the measurements of laboratory saturated samples (H1 and H2) were significantly lower than all structure resistivity measurements. Supporting the theory in Experiment 4, resistivity measurements carried out in saturated conditions (H1 and H2), (particularly after 28 days) will not yield representative results for concrete located in tidal, splash or atmospheric zones. The site data in the splash and tidal zones was found to be within the range of the outdoor samples (H5 and H6), while the atmospheric zones 4 and 7 were significantly higher than both the saturated and outdoor samples (H1, H2, H6 and H7) from Experiment 4.

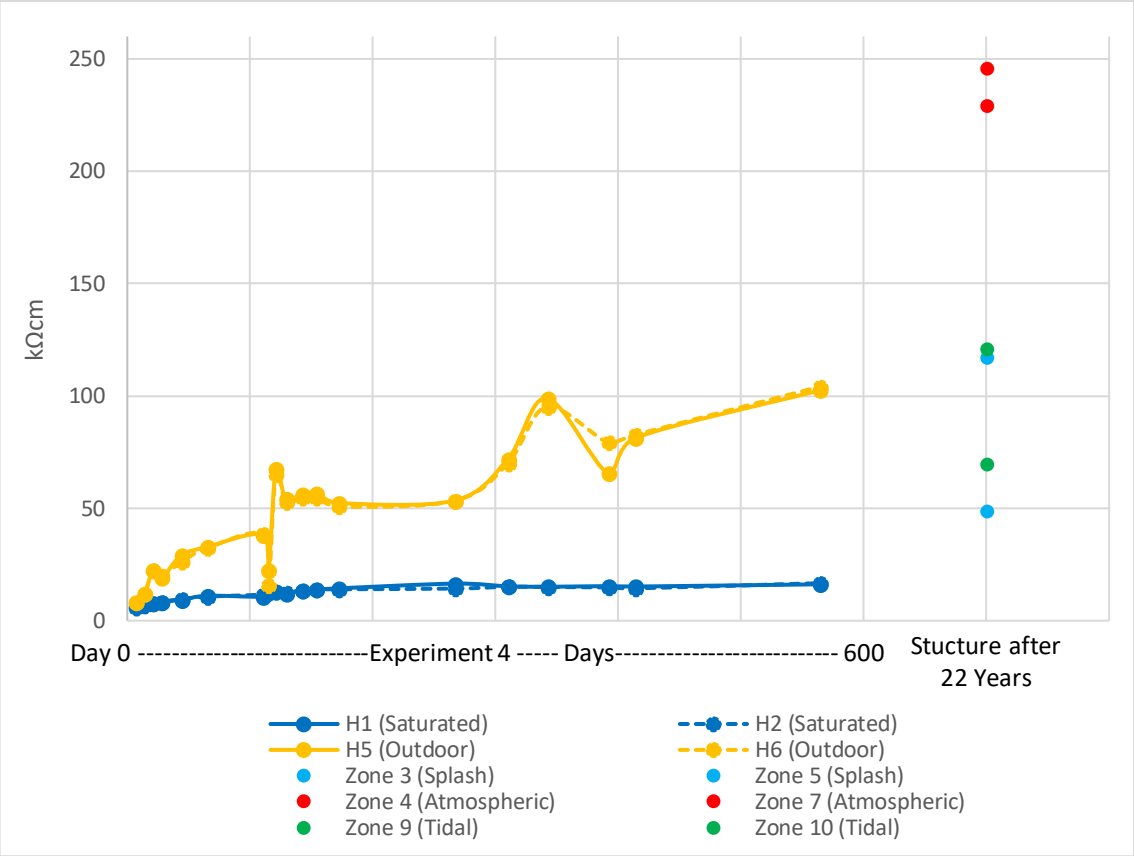

Figure 5.17 - Resistivity data from Experiment 4 vs structure site resistivity after 22 years

The data presented in Figure 5.17 supports the theories in Experiment 4 (Section 3.8). Further research into the resistivity development over long periods of time of polymer modified materials is required.

5.5 Conclusion

This chapter involved the analysis of data from a reinforced concrete structure with an operating impressed current cathodic protection system. Operational data from the structure was obtained and site resistivity and cover-metre testing was undertaken. Based on the site data obtained in this chapter, the average concrete resistivity of 95.4 kΩcm was measured in the tidal zones, 117.2 kΩcm in the splash zones, and 229.5 kΩcm in the atmospheric zones. At a calculated anode-to-steel spacing of 107mm, the ICCP performed under the 8-volt limit in the tidal and splash zones, while in the higher resistivity atmospheric zones the ICCP exceeded the 8-volt limit. In the case of the ICCP system operating on the structure, the maximum operating voltage limit was reached in the atmospheric zones around the vicinity of 229.5 kΩcm.

The data was analysed in conjunction with the laboratory data gathered in Chapter 4. The information gathered was plotted in Figure 5.17, confirming the correlation between resistivity, current output and anode-to-rebar spacing between a real operational ICCP system and the laboratory data gathered in Chapter 4.

This is the first research to identify the relationship between concrete resistivity, current output and anode-to-rebar spacing. The data presented in Figure 5.17 can be incorporated into the International ICCP design Standards as it provides significant data on the impact of resistivity on the current output of ICCP systems.

6 Conclusions & Future Work

The primary aim of this research was to expand the body of knowledge on the impact of concrete resistivity on the performance of impressed current cathodic protection (ICCP) systems used in conjunction with concrete repairs.

To achieve this aim in an under-researched area in the field of concrete repair and corrosion protection, it was necessary to carry out a series of laboratory and field experiments. The key challenges associated with this research work are summarised below:

- The absence of an accurate and practical method for laboratory and field concrete resistivity testing under atmospheric conditions. As a result of this issue, a new method of concrete resistivity testing utilising existing Wenner probe equipment was proposed in Chapter 3 Section 3.7. The innovative method allows for resistivity testing to be carried out in dry atmospheric conditions, without the need for sample water saturation.

- The lack of data related to the resistivity development over time under saturated and atmospheric conditions. This was exhibited by all manufacturers of repair mortars used in conjunction with electrochemical protection systems reporting short term resistivity data under saturated conditions. The common assumption that saturated and short-term data was indicative of the long-term resistivity of the material in atmospheric conditions was identified to be incorrect in Chapter 3, Section 3.8.

- The lack of design guidelines in the applicable Standards for cathodic protection regarding the potential impact of concrete resistivity on the design and performance of cathodic protection systems. Chapter 4 resulted in the development of a trend line graph for current density output at different resistivities and at different anode-rebar spacing. Chapter 5 further confirmed the trendline with data from a real structure with an operating cathodic protection system.

6.1 Development of Concrete Mixtures For Resistivity Testing

In order to perform laboratory research on the topic of concrete resistivity, it was necessary to develop different concrete mixtures in order to test concrete resistivities at different levels. Seven commonly available materials in nine compositions were tested. The following conclusions was identified from this experimental work:

- Where low resistivity concrete is required, a simple composition of sand, cement, and water (sample A) displayed the lowest resistivity values. At 63 days from casting, the resistivity value was measured at 37 kΩcm.

- If medium resistivity values are required within the same period (63 days), the addition of ground slag was found to increase resistivity by 132%. The increase of ground slag from 16% to 27% (gravimetric) increased concrete resistivity by 294% (sample F).

- If medium to high resistivity values are required, the addition of Silica fume increased resistivity by 448% (sample G), and the addition of Denka Sigma increased the resistivity by 602% (sample H).

- To achieve the highest resistivity values, the substitution of fly ash for ground slag would result in a 2600% increase (sample F1), 4021% increase (sample G1) and 5305% increase (sample H1) in concrete resistivity.

Experiment 1 provided the plotted resistivity trends for each of these tested compositions in atmospheric exposure conditions. By varying the materials and compositions, the increase of resistivity can be controlled allowing for the creation of samples with concrete resistivity from 37 kΩcm to 2000 kΩcm at 63 days. The data gathered in this experiment provides a mixture composition guide to design concrete mixtures for use in laboratory resistivity experiments, where varied concrete resistivities are required within a short testing schedule.

6.2 Effect of Water Saturation on Wenner Probe Resistivity Measurements

Section 3.6 involved the resistivity measurement of concrete samples under dry laboratory conditions. A major issue was identified during the resistivity testing process using the four-point Wenner probe resistivity equipment. While stable and accurate resistivity measurements were achieved for the concrete samples in atmospheric conditions up to approximately 10 days from casting, no accurate data could be achieved beyond this point. For concrete resistivity testing the AASHTO T358-19 [1] is commonly adopted, as it is the only current Standard for the measurement of concrete resistivity using the four-point Wenner probe. Unfortunately, this Standard is based on testing under saturated conditions only, requiring concrete samples to be water saturated. It was suspected that water saturation of atmospheric dry concrete will greatly impact resistivity values.

Section 3.6 found a considerable drop in resistivity values after the water saturation of the dry concrete sample. A significant drop (70.1%) for the sample with a high initial resistivity value of 420 kΩcm and a relatively minor drop (2.94%) for the sample with a low initial resistivity value of 10 kΩcm was recorded.

Resistivity measurement standard deviation was smaller for saturated samples, and larger for the dry samples. This indicates that for concrete in atmospheric conditions, there is a large variation of resistivity data, and the stability and replicability of measurements cannot be achieved.

Water saturation was found to decrease standard deviation between measurements. However, the effect of water saturation was found to greatly affect resistivity measurement results. This thesis identified and confirmed a major flaw with the current method of concrete resistivity measurement and identified the need for the development of a reliable and accurate method for the resistivity measurement of concrete in atmospheric conditions. Hence a new concrete resistivity testing method which would allow for concrete resistivity testing of atmospherically exposed concrete without the need for any water is proposed in the next section.

6.3 New Method of Concrete Resistivity Measurement for Concrete in Atmospheric Conditions

This experiment involved the development and testing of an innovative method for quick, accurate and replicable resistivity measurements for concrete in atmospheric conditions. The resistivity testing method is applicable to different concrete types, in saturated or dry conditions, and in high or low concrete resistivities. This testing methodology allows for concrete to be tested in the actual environmental exposure conditions. This method does not require extracting core samples from structures in atmospheric conditions and performing the testing in water saturated conditions as per the current Standard [1].

The new method allows for the elimination of variability of test results due to water saturation. The use of temporary embedded stainless-steel probes drilled into the concrete can provide the necessary contact between a four-point Wenner probe and the concrete. A 15mm probe depth was shown to provide the most consistent readings for water-saturated concrete, recently cast new concrete, and long-term dry concrete.

6.4 Effect of Long-Term Exposure Conditions on Concrete Repair Polymer Modified Repair Grouts

Applicable Standard [2] for cathodic protection provides general guidelines in relation to the resistivity of the concrete repair mortar relative to the parent concrete. The resistivity of the repair mortars used in conjunction with cathodic protection repairs are quoted in saturated conditions over a very short period (28 - 96 days). The aim of the experiment was to verify if the short-term resistivity data for repair mortar (as quoted by manufacturers' TDS) is indicative of the true, long-term mortar resistivity in atmospheric conditions for real structures.

The experiment demonstrated that use of repair mortar based on published short term resistivity data (28 days) and under saturated conditions is misleading. The suitability of polymer-modified repair mortars in conjunction with cathodic protection must be verified based on long-term test data under atmospheric outdoor conditions. Testing in accordance with the

methodology trialed in Experiment 3 provides a solution which can be adopted by the industry to test concrete in representative atmospheric conditions.

The key finding from the experiment include:

- Resistivity trends were found to substantially vary with time and between repair mortars. The resistivity of all four tested repair mortars increased over time under both saturated and outdoor conditions. The experimental data identified a major difference between resistivity values at 28 days and at 564 days for all products in saturated and outdoor exposure conditions. Based on this experiment, the 28-day resistivity data typically reported in manufacturer technical data sheets is not indicative of the resistivity value over a relatively short period of time for the life of a repair (564 days). Resistivity trends may continue to increase beyond the 564-day test period of this experiment.

- Resistivity measurements in outdoor exposure conditions were consistently higher than those in saturated condition. The current resistivity Standard [1] which measure samples in saturated conditions will not be representative of real exposure conditions.

- Australian Standard AS 2832.5 (R2018) [2] relates the resistivity of the repair mortar to the electrical resistivity of the parent concrete. While it could be assumed that the resistivity of the repair mortar and parent concrete can be measured to AASHTO designation: T358-19 [1], a short 28-day resistivity testing period in saturated conditions is commonly used for new repair mortars. Based on the data from this experiment, the 28-day resistivity value under saturated conditions is not indicative of the true mortar resistivity value over time under both saturated and outdoor conditions.

6.5 The Impact of Concrete Resistivity and Spacing Between Anode and Rebar on the Cathodic Protection Current Delivery for Impressed Current Cathodic Protection Applications

The aim of this experiment was to verify the correlation between concrete resistivity, current output and anode-to-rebar spacing in impressed current cathodic protection (ICCP) systems. The

laboratory experimental work resulted in the development of a trend line that can be used for the design of ICCP systems. The key conclusions from this experiment are as follows:

- Regardless of the anode-to-rebar spacing, the circuit voltage increased progressively with the increase of resistivity value for each test. This confirms a correlation between the mortar resistivity value and circuit voltage. The higher the resistivity of the mortar, the higher the circuit voltage required to impress the same amount of current.

- At the same concrete resistivity value, the circuit voltage is lower at a set current output when the anode is located closer to the rebar. While the impact of anode spacing is relatively negligible at low concrete resistivities, the impact is considerable at high concrete resistivity values.

- In the case of high resistivity concrete, this work finds that an increase in current output can be obtained by decreasing the anode-to-rebar spacing. Placing the anodes closer to the rebar may impact on the current distribution of the ICCP system and may necessitate the system design to increase anode current density to achieve corrosion protection.

- In high resistivity concrete, the location of the anode can be adjusted to achieve a lower output voltage and consequently, higher cathodic protection current. For the highest resistivity measurement in this experiment (1320 kΩcm), the installation of the anode at 30mm instead of 60mm resulted in the reduction of operating circuit voltage by 183.73% from 10 volts to 3.5 volts to well below the maximum voltage limit for CP systems operation.

6.6 Effect of Concrete Resistivity on the Ongoing Application of Impressed Current Cathodic Protection and the Effect of Anode Placement

The key conclusions from experiment 6 are as follows:

- The average trend of current density versus resistivity indicates that an impressed current cathodic protection (ICCP) system can operate at 20mA/m² at concrete resistivity up to 117.8 kΩcm for anode-to-rebar spacing of 60mm. ICCP systems can operate at 20mA/m² at concrete resistivity up to 226.8 kΩcm at an anode-to-rebar spacing of 30mm.

- The level of current output decreases with the increase of concrete resistivity in both 30mm and 60mm anode-to-rebar spacing configurations.

- Based on the average trend line developed from the data in this experiment at 60mm anode-to-rebar spacing, the current output decreased to less than 1mA/m² at a resistivity of 408 kΩcm. At 30mm anode-to-rebar spacing, the current output decreased to less than 1mA/m² at a significantly higher resistivity of 1187 kΩcm.

- Based on the developed trend line, ICCP systems can operate at relatively high concrete resistivities by modifying the spacing between the anode and rebar. For high resistivity concrete, the desired current output can be achieved by reducing the spacing between the anode and the rebar.

- The trend line developed in this experiment can be incorporated into the design criteria of ICCP systems Standards. The trend line provides an indication of current output at different levels of concrete resistivity. Based on the current density required for a CP system and the measured concrete resistivity of the subject structure, the anode-to-rebar spacing can be modified to achieve the desired current output for the system operation.

6.7 Performance of Impressed Current Cathodic Protection in an Operational Structure

The aim of this work was to assess the applicability of the trend line developed in the laboratory testing in Chapter 3. A correlation between concrete resistivity, anode-to-rebar spacing and current output of a CP system between the experimental laboratory data and a real operating CP system was carried out.

The key results from this experiment indicate that the data from the operating structure supports the overall correlation trend of resistivity, current output, and anode-to-rebar spacing obtained from the laboratory test.

6.8 Future Work

- This research involved the development of a new method of concrete resistivity testing for atmospheric concrete structures. The current concrete resistivity testing Standards do not provide a methodology for testing in atmospheric conditions, being limited to only saturated conditions which is shown in this research to yield unrepresentative results. Additional verification of the developed method in the research may lead to its adoption into the current AASHTO [1] resistivity Standards.

- This research found that the resistivity data included in manufacturers' technical data sheets for resistivity repair mortars are carried out in short-term, saturated conditions. This research further identified that the current testing procedures are not representative of repair mortar resistivity in long-term and atmospheric conditions. Future work may include further long-term testing of repair mortars under both saturated and atmospheric conditions to confirm the duration required for the resistivity value of these mortars to stabilise.

- A trend line correlating resistivity data, anode-to-rebar spacing, and current output of ICCP systems was developed in this research work. Incorporating guidelines related to concrete resistivity data in the current cathodic protection Standards [2] [3] [4] is essential to optimise the design of cathodic protection systems in high resistivity concrete. Further research in this area is required to further develop this trend line/correlation using larger data sets to allow for incorporation of such design data into the applicable Standards for cathodic protection.

- Concrete resistivity may have in theory, a larger impact on galvanic anode systems than ICCP systems. Future research may include establishing guidelines outlining the correlation between concrete resistivity and current output on the performance of galvanic anode systems.

References

[1] AASHTO American Association of State Highway and Transportation Officials, “T358 Standard method of test for surface resistivity indication of concrete’s ability to resist chloride ion penetration,” 2019.

[2] Standards Australia, “AS 2832.5-2008 Cathodic Protection of Metals, Part 5: Steel in concrete structures,” (R) 2018.

[3] The European International Standard ISO 12696:2016, “Cathodic protection of steel in concrete,” 2016.

[4] NACE International Standard, “SP0290-2007 (formerly RP0290) Impressed current cathodic protection of reinforcing steel in atmospherically exposed concrete structures,” 2007.

[5] Standards Australia, “SA HB 84:2018 Guide to concrete repair and protection,” (R) 2018.

[6] B. Elsener, C. Andrade, J. Gulikers, R. Polder and M. Raupach, “Half-cell potential measurements- Potential mapping on reinforced concrete structures,” *RILEM TC 154-EMC: Electrochemical techniques for measuring metallic corrosion,* vol. 36, pp. 461 - 471, 2003.

[7] L. Lazzari, Engineering tools for corrosion: design and diagnosis, 1st ed., vol. 68, Woodhead Publishing, 2017.

[8] P. Chess and J. Broomfield, Cathodic protection of steel in concrete, 1st ed., London: E & FN Spon, 1998.

[9] C. S. Joint Working Party of the Concrete Society the Corrosion Prevention Association and the Institute of Corrosion, “Technical Report No. 73, cathodic protection of steel in concrete,” 2011.

[10] Proceq Resipod family operating manual, “Operating instructions - concrete durability testing,” [Online]. Available: https://www.proceq.com/uploads/tx_proceqproductcms/import_data/files/Resipod%20Family_Operating%20Instructions_English_high.pdf. [Accessed 1 10 2020].

[11] A. Bentur, N. Berke and S. Diamond, Steel corrosion in concrete: fundamentals and civil engineering practice, 1st ed., CRC Press, 2019.

[12] P. Azarsa and R. Gupta , “Electrical resistivity of concrete for durability evaluation: A review,” *Advances in Materials Science and Engineering,* vol. 2017, pp. 1-30, 2017.

[13] W. Morris, M. Vico, M. V. Marcela and S. R de Sanchez, “Corrosion of reinforcing steel evaluated by means of concrete resistivity measurements,” *Corrosion Science,* vol. 44, no. 1, pp. 81-99, 2002.

[14] V. Sanjeev, B. Sudhir and A. Saleem, “Monitoring corrosion of steel bars in reinforced concrete structures,” *The Scientific World Journal,* pp. 957-904, 2014.

[15] Giatec Scientific SURF operating manual, “Surface resitivity of concrete using wenner four-electrode method,” [Online]. Available: http://www.pcte.com.au/images/pdf/ResipodResistivityMeter/resipod_family_OI_E_2013.01.07_low.pdf. [Accessed 1 8 2018].

[16] R. Polder, “Test methods for on site measurement of resistivity of concrete — a RILEM TC-154 technical recommendation,” *Construction and Building Materials,* vol. 15, no. 2, pp. 125-131, 2001.

[17] Strategic Highway Research Program National Research Council Washington, DC, “Cathodic Protection of Reinforced Concrete Birdge Elements: A State-of-the-Art Report,” 1993. [Online]. Available: https://trid.trb.org/view/368657.

[18] H. Layssi, A. Alizadeh, P. Ghods and M. Salehi, “Electrical resistivity of concrete, concepts, applications, and measurement techniques,” *Concrete International,* vol. 37, no. 5, pp. 41-46, 2015.

[19] R. Spragg, Y. Bu, K. Snyder, D. Bentz and W. Weiss, “Electrical testing of cement-based materials: role of testing techniques, sample conditioning, and accelerated curing,” FHWA/IN/JTRP-2013/28 Joint Transportation Research Program, Indiana Department of Transportation and Purdue University, West Lafayette, Indiana, 2014.

[20] F. Dullien, Porous media fluid transport and pore structure, Acedemic Press , 1979.

[21] M. Newlands, M. Jones, S. Kandasami and T. Harrison , “Sensitivity of electrode contact solutions and contact pressure in assessing electrical resistivity of concrete,” *Materials and Structures,* vol. 41, pp. 621-632, 2007.

[22] K. Gowers and S. Millard, “Measurement of concrete resistivity for assessment of corrosion severity of steel using wenner technique,” *ACI Materials Journal,* vol. 96, no. 5, pp. 536 - 541, 1999.

[23] C. Chen, J. Chang and W. Yeih, “The effects of specimen parameters on the resistivity of concrete,” *Construction and Building Materials,* vol. 71, pp. 35-43, 2014.

[24] R. Spragg, C. Villani, K. Snyder, D. Bentz, J. Bullard and W. Weiss, “Factors that influence electrical resistivity measurements in cementitious systems,” *Transportation research record: Journal of the Transportation Research Board,* vol. 2342, pp. 90-98, 2013.

[25] R. Weydert and C. Gehlen, “Electrolytic resistivity of cover concrete: relevance, measurement and interpretation,” 1999.

[26] M. Salehi, P. Ghods and P. Isgor, “Numerical investigation of the role of embedded reinforcement mesh on electrical resistivity measurements of concrete using the wenner probe technique,” *Materials and Structures,* vol. 49, no. 1-2, pp. 301-316, 2016.

[27] H. Toutanji and T. Korchi, “The influence of silica fume on the compressive strength of cement paste and mortar,” *Cement and Concrete Research,* vol. 25, no. 7, pp. 1591-1602, 1995.

[28] M. Shankar, G. Di and A. Ashraf, “Non-destructive evaluation of carbon nanofibre concrete,” 2013.

[29] America’s Cement Manufacturers, “How cement is made,” [Online]. Available: http://www.cement.org/cement-concrete-applications/how-cement-is-made. [Accessed 5 10 2018].

[30] R. Noort, M. Hunger and P. Spiesz, “Long-term chloride migration coefficient in slag cement-based concrete and resistivity as an alternative test method,” *Construction and Building Materials,* vol. 115, pp. 746-759, 2016.

[31] J. Su, C. Tang, W. Wu and R. Huang, “Effect of moisture content on concrete resistivity measurement,” *Journal of the Chinese Institute of Engineers,* vol. 25, no. 1, pp. 117-122, 2002.

[32] O. Sengul, “Use of electrical resistivity as an indicator for durability,” *Construction and Building Materials,* vol. 73, p. 434–441, 2014.

[33] America’s Cement Manufacturers, “Chemical admixtures,” [Online]. Available: http://www.cement.org/cement-concrete-applications/concrete-materials/chemical-admixtures. [Accessed 15 5 2018].

[34] Cement Australia Data Sheet, “Fly Ash,” [Online]. Available: http://www.cementaustralia.com.au/wps/wcm/connect/website/bulk/Bulk-Home/our-products/fly-ash/. [Accessed 15 02 2018].

[35] Cement Australia Data Sheet, “Slag,” [Online]. Available: http://www.cementaustralia.com.au/wps/wcm/connect/website/bulk/Bulk-Home/our-products/fly-ash/. [Accessed 15 05 2018].

[36] F. Presuel, Y. Wu and Y. Liu, “Effect of curing regime on concrete resistivity and aging factor over time,” *Construction and Building Materials,* vol. 48, pp. 874-882, 2013.

[37] W. Weiss, K. Snyder, J. Bullard and D. Bentz, “Using a saturation function to interpret the electrical properties of partially saturated concrete,” *Journal of Materials in Civil Engineering,* vol. 25, no. 8, pp. 1097-1106, 2013.

[38] E. Guneyisi, T. Ozturan and M. Gesoglu, “A study on reinforcement corrosion and related properties of plain and blended cement concretes under different curing conditions,” *Cement and Concrete Composites,* vol. 27, no. 4, pp. 449-461, 2005.

[39] Y. Lui and F. Presuel, “Normalization of Temperature Effect on Concrete Resistivity by Method Using Arrhenius Law,” *ACI Materials Journal,* pp. 433-442, 2014.

[40] Cement Concrete & Aggregates Australia, “Moisture in concrete and moisture-sensitive finishes and coatings,” 2007. [Online]. Available: http://59.167.233.142/publications/pdf/Moisture.pdf. [Accessed 01 03 2018].

[41] Y. Villagran-Zaccardi, J. Garcia, P. Huelamo and A. Di Maio, “Influence of temperature and humidity on Portland cement mortar resistivity monitored with inner sensors,” *Materials and Corrosion,* vol. 60, pp. 294-299, 2009.

[42] M. Saleem, S. Hussain and M. Maslehuddin, “Effect of moisture, chloride and sulfate contamination on the electrical resistivity of portland cement concrete,” *Construction and Building Materials,* vol. 10, no. 3, pp. 209-214, 1996.

[43] R. Mederios-Junior, J. Hino Junior, G. Bill, A. Monteiro and I. Kawanami, “Accelerated carbonation effect on electrical resistivity and sorptivity of concrete,” *Journal of Building Pathology and Rehabilitation,* vol. 3, no. 1, p. 7, 2018.

[44] I. Yoon, “Influence of carbonation of concrete on electrical resistivity,” *Journal of the Korea Institute for Structural Maintenance and Inspection,* vol. 18, pp. 27-33, 2014.

[45] M. Khadra, J. Lataste, N. Burlion, T. Rougelot and J. Carlier, “Carbonation effect on measurements of electrical resistivity tomography,” in *Conference: 2nd International Conference on Civil, Structural and Transportation Engineering (ICCSTE'16)*, Ottawa, Canada, 2016.

[46] W. Morris, E. Moreno and A. Sagues, “Practical evaluation of resistivity of concrete in test cylinders using a wenner array probe,” *Cement and Concrete Research,* vol. 26, no. 12, pp. 1779-1787, 1996.

[47] M. Paredes, R. Kessler and R. Powers, “Resistivity measurements of water saturated concrete as an indicator of permeability,” in *NACE Corrosion Conference*, Houston, Texas, USA., 2005.

[48] W. Morris, A. Vico and M. Vazquez, “Chloride induced corrosion of reinforcing steel evaluated by concrete resistivity measurements,” *Electrochimica Acta,* vol. 49, no. 25, pp. 4447-4453, 2004.

[49] ASTM International, “ASTM C1876 – 19 Standard test method for bulk electrical resistivity or bulk conductivity of concrete,” 2019.

[50] Standard Main Roads Western Australia, “Test Method WA 622.1 - 2012 Resistivity of Concrete,” Western Australia Government Document.

[51] J. Broomfield, “Acceptable electrical resistvities of concrete repairs for cathodic protection systems,” CPS Corrosion Prevention Association Technical Notes no. 19, 2011.

[52] Sika Australia Pty Limited, “Sika MonoTop®-352 NFG product data sheet,” 2017. [Online]. Available: https://aus.sika.com/en/construction/concrete-repair-

protection/concrete-repair-mortars/cementitious-repairmortars/sika-monotop-352nfg.html. [Accessed 12 02 2019].

[53] BASF Australia Ltd, "MasterEmaco® N 5200CI product data sheet," [Online].

[54] M. Salman, M. Sikandar, H. Nasir, M. Waseem and S. Iqdal, "Protection against reinforcement corrosion using various hydroxy acid-based rust converters: tests in mortar medium," *European journal of environmental and civil engineering,* pp. 1-16.

[55] V. Ortolan, M. Mancio and B. Tutikian, "Evaluation of the influence of the pH of concrete pore solution on the corrosion resistance of steel reinforcement," *Journal of building pathology and rehabilitation,* vol. 1, no. 1, pp. 1-7, 2016.

[56] S. Starck, H. Beushausen, M. Alexander and R. Torrent, "Complementarity of in situ and laboratory-based concrete permeability measurements," *Materials and structures,* vol. 50, no. 3, p. 1, 2017.

[57] L. Bourreau, V. Bouteiller, F. Schoefs, L. Gailet, B. Thauvin, J. Schneider and S. Naar, "Uncertainty assessment of concrete electrical resistivity measurements on a coastal bridge," *Structure and infrastructure engineering,* vol. 15, no. 4, pp. 443-453, 2019.

[58] M. Aguilar, A. Silva, L. Aguiar and D. Leite, "The evolution of electrical resistivity thru the curing in concretes with different W/C ratio," in *International symposium on structural health monitoring and nondestructive testing 4-5 Oct 2018,* , Saarbrücken – Germany (SHM-NDT 2018), 2018.

[59] M. Al-Zahrani, M. Maslehuddin, S. Al-Dulaijan, A. Sharif and S. Alidi, "Performance evaluation of repair materials," in *The 6th Saudi Engineering Conference, KFUPM, Dhahran*, 2002.

[60] S. Cheytani, "Data analysis of the long-term residual effect of cathodic protection on reinforced concrete structures," School of Materials Science and Engineering, Faculty of Science, 2020.

[61] C. Martin, "Grout Acidification of Ribbon Anode in Impressed Current Cathodic Protection Systems in Concrete," University of New South Wales, Masters thesis, 2017.